CHEMICAL REVIEWS

REVIEW

pubs.acs.org/CR

Metal Azolate Frameworks: From Crystal Engineering to Functional Materials

Jie-Peng Zhang,* Yue-Biao Zhang, Jian-Bin Lin, and Xiao-Ming Chen*

MOE Key Laboratory of Bioinorganic and Synthetic Chemistry, State Key Laboratory of Optoelectronic Materials and Technologies, School of Chemistry and Chemical Engineering, Sun Yat-Sen University, Guangzhou 510275, China

CONTENTS

1. INTRODUCTION

Crystal engineering of coordination polymers with structure-based properties is of great current interest.[1] Coordination polymers are a new kind of molecular materials which have infinite metal−ligand backbones connected by coordination bonds. The term coordination polymer first appeared in the 1960s,[2] but the investigations have only become extensive since 1990.[3] Although some inorganic coordination materials such as Prussian blue can be included in coordination polymers, most of the current investigations are focused on those with organic bridges. Considering the diversity of organic molecules, coordination polymers have versatile structures and properties, giving them very good potential in adsorptive, molecular separation/exchange, catalytic, electronic, magnetic, and optical applications, and consequently attract wide attention from chemists around the world nowadays. Although investigations on coordination polymers with other properties are also very active, most of the investigations in the past decade have been focused on those of porous structures, or porous coordination polymers (PCPs).[4] It is noteworthy that the term metal−organic frameworks (MOFs)[5] has been popularly used to describe both porous and nonporous coordination polymers.

As the complicated, diversified structures of coordination polymers are usually assembled in one-step or one-pot reactions, the polymeric structures formed by the assemblies of the metal ions (or clusters) and bridging organic ligands are much more difficult to control, in comparison with a typical organic reaction. Moreover, they are usually quite difficult to describe and understand. Fortunately, many of them may be well described and hence easily understood by simplication of the metal−ligand connectivities into periodic network topologies (nets). Since the breakthrough works of A. F. Wells,[6] the observed and predicted topologies have been hugely expanded, most of which have been deposited in the open-access databases.[7] While the numeric symbols (e.g., the connectivity of the C atoms in diamond has point symbol 6^6 and vertex symbol $6_2.6_2.6_2.6_2.6_2.6_2$) can be used to describe topologies in a mathematic sense,[8] traditional symbols are straightforward and easy for indexing purposes. Hereafter, the zeolite framework type codes (three capital letters, such as SOD for sodalite) are used to describe the zeolitic topologies,[7a] and the RCSR symbols (three lowercase letters in bold, such as **dia** for diamond) are used for other ones.[7b] The EPINET symbol (with format "sqc" + "numeric index", such as sqc6 for diamond)[7c] will be adopted for topologies having neither the zeolite framework code nor the RCSR symbol. Finally, the point and vertex symbols are used for topologies not registered in the above-mentioned databases.[9]

From the view of topology, many coordination polymers can be regarded as one-dimensional (1D) to three-dimensional (3D)

Special Issue: 2012 Metal-Organic Frameworks

Received: April 25, 2011
Published: September 22, 2011

nets being constructed by single metal ions (or metal clusters) as "nodes" and organic ligands as "linkers" through coordination bonds. Of course, higher polytopic (e.g., tritopic and tetratopic) organic ligands can also be regarded as nodes, and metal ions can also serve as 2-connected linkers. Obviously, the topological description not only is very useful for understanding the net structures, but also can be used for the design of them. Although different metal ions may have different charges, electron configurations, and ionic radii, hence exhibiting different coordination geometries, their coordination geometries are basically predictable. Consequently, single metal ions can be used as nodes in linking with bridging ligands to construct specific coordination nets. Therefore, this nodes and linkers molecular design strategy or net-based approach is versatile and was first applied to design new coordination polymer structures by Robson's group.[3,10] Moreover, since many kinds of discrete metal clusters, especially the polygonal and polyhedral ones, are structurally well-defined, they can be more efficiently used as nodes or secondary building units (SBUs), compared to single metal ions.[5d,11] Nevertheless, the topology, or net-based, approach, using either single metal ions or SBUs, has become one of the important molecular design strategies for the design and synthesis of coordination polymers.

The pillared-layer approach is also noteworthy and utilizes serendipitous or deliberately designed two-dimensional (2D) layers that have ligating sites at both sides and that are further linked by ditopic ligands (pillars) into 3D architectures with different interlayer distances depending on the lengths of the pillars. In this approach, the layers are usually dense; thus, interpenetration may be avoided, even when the pillars are quite long. A nice early example was copper(II) pyrazine-2,3-dicarboxylate layers pillared by a series of neutral ditopic N-ligands, which produced isostructural PCPs with different porosities.[4,12] From a broader perspective, the stable coordination layers in the pillared-layer structures can be regarded as 2D SBUs. In this context, there are also some columnlike units serving as 1D SBUs that can be interlinked by ditopic ligands in the other two dimensions into 3D scaffolds. To some extent, the designability of 1D SBUs is between those of the clusters and layers.

Whatever synthetic strategies are employed, organic ligands are the basic components of coordination polymers. The versatility of organic ligands has also been accepted as the major advantage of coordination polymers. Judicious selection/design of organic ligands is the key approach for desired structures and functions. In the past two decades, many types of polytopic organic ligands with different donor groups, such as carboxylate, pyridyl, amine, sulfonate, phosphate, etc., have been used in the generation of coordination polymers.[13] Among them, polypyridyls and polycarboxylates have been very widely used because they generally have good ligating ability to metal ions and readily adjustable length and geometry. Although carboxylate-based SBUs have been very successful, carboxylate groups are actually very versatile in coordination because each single O-donor can bind one, two, and even three metal ions, which induces significant uncertainty in the self-assembly and properties of coordination polymers. Pyridyl-type ligands have simple coordination modes, but their relatively weak coordination ability and charge neutrality are disadvantageous for controlling the compositions (such as the metal/ligand ratios) of coordination polymers. The use of mixed carboxylate/pyridyl-type ligands may be an effective approach to combine the advantages of different types of coordination groups.[14] Recently, metal azolate frameworks (MAFs) have emerged as a new kind of coordination polymers promising for crystal engineering and materials science, because azolate ligands have the advantage of strong and directional coordination ability in bridging metal ions. Some recent reviews have discussed the chemistry of coordination complexes based on different subsets of azoles and/or azolates.[13,15] In this review, we do not intend to provide a comprehensive collection of literature, but to focus on the progress in the molecular design, synthesis, and properties of MAFs with selected examples.

Scheme 1. Structures of Prototypical Azoles and Their Corresponding Azolates

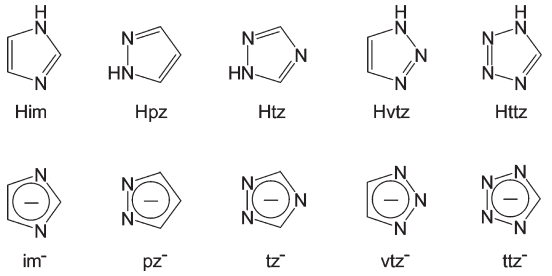

2. CHEMISTRY OF METAL AZOLATE FRAMEWORKS

Azoles, the five-membered aromatic nitrogen heterocycles, are very important building blocks of many important compounds widely used in medicine, agriculture, industry, and coordination chemistry. The coordination behaviors of the sp^2 N-donors in azoles and pyridines are basically identical. Although azoles are mostly known as bases (the protonated form is azolium cation) as pyridines, the all-nitrogen azoles including imidazole (Him), pyrazole (Hpz), 1,2,4-triazole (Htz), 1,2,3-triazole (*v*-trizole, Hvtz), and tetrazole (Httz) can also be deprotonated to form the corresponding azolate (or azolide) anions (Scheme 1). As the N atom has an electron-withdrawing effect, an azolium/azole/azolate ring containing more N atoms has higher acidity (easier to deprotonate) or lower basicity (more difficult to protonate). For example, imidazole has a higher basicity than pyridine, probably because six electrons are delocalized on five atoms, resulting in higher electron density. In contrast, tetrazole has an acidity similar to that of carboxylic acid, while other azoles are generally very weak acids. Basicity is a direct measure of binding ability toward a proton and may also be applied to estimate the bonding strength with transition-metal ions, because coordination bonds between a soft Lewis acid and base are relatively covalent in nature.

Deprotonation not only allows all N atoms to coordinate with metal ions but also further increases the basicity of these donors. Consequently, MAFs have particularly high thermal and chemical stability, which is one of the most important issues for practical applications of coordination polymers. Actually, azoles, especially imidazole, have long been known to have the ability to protect the surface of copper and other metals against corrosion, which has been attributed to the formation of polymeric metal azolates on the metal surfaces.[16] Imidazolate is also an important ligand in many metalloenzymes, such as in the copper/zinc superoxide dismutases.[17] Nevertheless, azolates had not been widely used as bridging ligands for coordination polymers before the past decade. Possible reasons include the very short bridging length and difficulty of deprotonation of the ligand, as well as the ease of forming highly insoluble and intractable products.[15a]

Scheme 2. Comparison of the Typical Coordination Modes of Azolates, Pyridine, and Carboxylate (X = C−H or N)

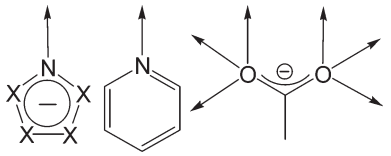

While technical issues have been largely solved by improved synthetic and characterization methods, the theoretical drawbacks are now reconsidered in a different way.

2.1. Framework Design Principles

First, azolates provide bent linkages (ca. 70° or 140°) not easily available for traditional types of ligands composed of six-membered rings (180°, 120°, 60°), which would be useful for generating novel structures. Note that the bond lengths follow the sequence N−N < C−N < C−C; thus, the bending angles of azolates containing *n* N-donors are generally smaller than 72*n*°. Compared to other metal−ligand systems, transition-metal ions and azolate anions have a higher tendency to form highly insoluble, neutral, binary "salts". Similar to that of pyridines, each N-donor of azolate generally coordinates with only one transition-metal ion in the same direction as its lone electron pair. For comparison, an sp^3 O atom, such as those in a carboxylate, usually coordinates variably (typically up to three metal ions) (Scheme 2). Non-directional and/or variable coordination numbers of azolates are commonly observed for oxophilic alkali-, alkaline-earth-, and rare-earth-metal ions,[18] which are well-known as hard Lewis acids with a great tendency to form ionic bonds.

2.1.1. Predictable Local Coordination Geometries. Considering that ligands tend to use all the available ligating sites during self-assembly (lower energy), the coordination geometry and connectivity of binary MAFs can be readily predicted. In a neutral, binary metal−ligand system, the metal-to-ligand ratio is determined by their charges, and the coordination number of the metal ion should be equal to or less than the number of available ligating sites. Because of the short bridging lengths of azolates, low-valence metal ions with low coordination numbers, such as univalent coinage-metal ions Cu(I)/Ag(I) and divalent 4-coordinate Zn(II), are suitable for constructing binary phases. Otherwise, coordination polymers with more complex compositions would be obtained with incorporation of additional counterions and/or secondary ligands, either deliberately or unintentionally, which are very common for other metal−ligand systems. It should be noted that azolate ligands can also be derived to have additional coordinative groups, such as carboxylates and pyridyls. The pyridyl derivatives are still very similar to simple azolates, but the introduction of carboxylate groups generally produces ligands with completely different coordination behaviors.

2.1.2. Low Topology/Framework Density. The low coordination numbers occurring in MAFs render 3- or 4-connected topologies, which are not only the simplest and most viable structural prototypes but also of the lowest framework densities (number of nodes per unit volume), being useful for the construction of porous frameworks (Table 1).[7b,19] Therefore, there are many porous MAFs reported in the literature despite the very short bridging lengths of the azolate rings. The most representative structures include the imidazolate-based zeolitic nets and 1,2,4-triazolate-based, simple 3-connected nets.

Table 1. Characteristics of Selected Simple Topologies

net	coordination	space group	Wyckoff position	volume[a] (Å^3)	node density[a] (Å^{-3})
bcu	8	$Im\bar{3}m$	2a	1.5396	1.2990
pcu	6	$Pm\bar{3}m$	1a	1.0000	1.0000
nbo	4	$Im\bar{3}m$	6b	8.0000	0.7500
lvt	4	$I4_1/amd$	8c	12.3200	0.6494
qtz	4	$P6_222$	3c	4.0001	0.7500
dia	4	$Fd\bar{3}m$	8a	12.3168	0.6495
ANA	4	$Ia\bar{3}d$	48g	84.1486	0.5704
SOD	4	$Im\bar{3}m$	12d	22.6268	0.5303
RHO	4	$Im\bar{3}m$	48i	112.5880	0.4263
LTA	4	$Pm\bar{3}m$	24k	56.1247	0.4276
srs	3	$I4_132$	8a	22.6268	0.3536
lig	3	$I4_1/amd$	16f	45.2544	0.3536
nbo-a	3	$Im\bar{3}m$	24g	112.5670	0.2132
lvt-a	3	$I4_1/amd$	32i	168.6400	0.1898

[a] Cell volume of topology with edge length 1 Å.

Scheme 3. Side Groups Play Different Roles Depending on the Lengths of the Bridging Ligands[a]

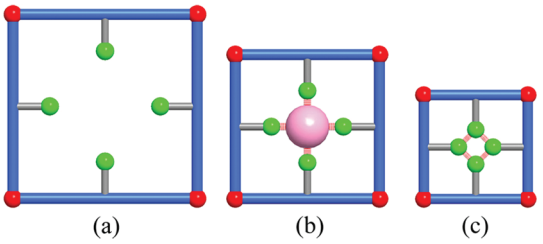

[a] Key: (a) The side groups are innocent for very long bridging lengths. (b) The side groups cooperate to interact with a guest molecule for medium bridging lengths. (c) The side groups interact with each other for very short bridging lengths.

2.1.3. Side Group Directed Superstructures. Compared with other metal−ligand systems, the side (or substituent) group directed approach is characteristic of MAFs. While crystal engineering of polycarboxylate- and polypyridyl-based coordination polymers is usually equal to the design of ligands with suitable linking geometry and/or length between multiple coordination groups, the small azolate rings have fixed bridging geometries and lengths. Combining with the simple coordination modes, these characters reduce the number of potential superstructures, which is beneficial for structure prediction and control. Nevertheless, there are still very rich structural types even when the node geometry is fixed. The short bridging lengths of azolates give rise to short separations between not only the metal ions but also the ligands (Scheme 3). The substituent, or pendant, or side groups on the azolate rings linked to the adjacent metal ions then easily interact with each other or interact with guest molecules cooperatively. Therefore, these groups can be utilized to control the relative orientation of adjacent building blocks, leading to different extended superstructures.

2.2. Synthesis Considerations

While azoles are generally weak acids, their deprotonation can be achieved by the aid of base and/or high temperature. Coordination

Chart 1. Substituted Imidazolates

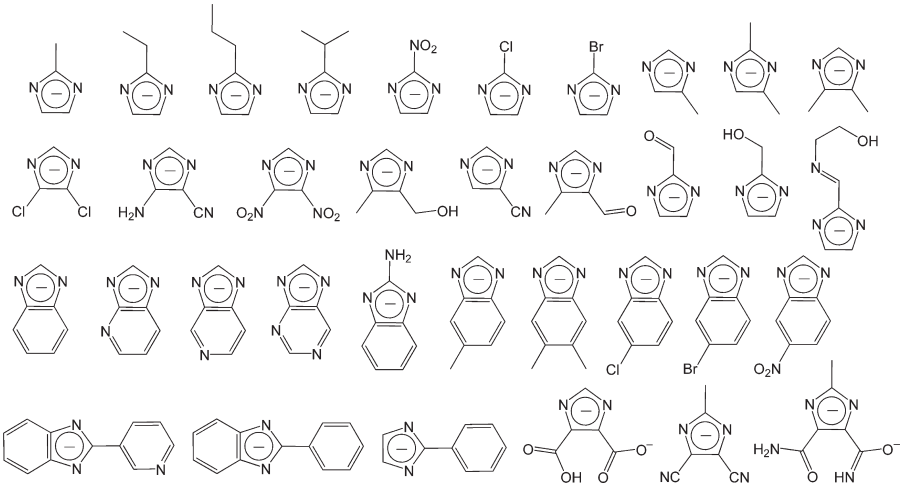

of one or more N-donors of an azole to metal ion(s) (electron-withdrawing) also increases the acidity of the remaining N−H moiety and facilitates its deprotonation. Actually, MAFs usually precipitate rapidly in basic solutions as highly insoluble powders due to their polymeric structures linked by the strong coordination bonds. In this regard, single crystals are usually obtained by slow reactions such as liquid diffusion and solvothermal reaction, as well as by addition of some coordination buffers. In situ ligand formation reactions[20] have played an important role in the generation of MAFs, especially 1,2,4-triazolates and tetrazolates, which reduced difficulties in not only the ligand synthesis but also the crystal growth. Alternatively, bulk microcrystalline powder with good crystallinity may be prepared by rapid solution mixing or solvent-free approaches.

MAF synthesis is relatively insensitive to the reaction conditions because most of the common species presented in the solution, such as anions and solvent molecules, can hardly compete with the targeted metal azolate bonds, which is particularly true for those composed of soft metal ions and diazolates. Nevertheless, the coordination affinity varies among different species, including different azolates. Therefore, additional species presented in the solution can either be innocent or act as a coordination additive/buffer, a template, a counterion, and even a coligand. Taking these into consideration, the reaction outcomes can be more predictable.

2.3. Special Properties

After formation of a coordination bond, the sp^2 electron lone pair is shared between the N-donor and the metal ion acceptor and then becomes coordinatively saturated and cannot be further utilized for any strong interaction with other species. Therefore, in many binary MAFs where all N-donors are involved in coordination, the pore surface becomes quite inert and hydrophobic, which determines the unique host−guest properties of these adsorbents. The most remarkable effect should be the chemical stability because polar species can hardly attack the coordination bond to replace the ligand. As the carboxylate O-donor in most PCPs is coordinatively unsaturated (see above), the metal carboxylate clusters are usually the primary guest binding sites and solvent attracting sites.[21] While most carboxylate-based PCPs are relatively hydrophilic, simple MAFs are usually hydrophobic. On the other hand, active sites can be rationally introduced into an MAF and then demonstrate their functions, because there is no interference from other active groups such as carboxylate O atoms and counterions.

While different types of azolates share many common characteristics, their coordination behaviors are obviously different according to their number and positions of N-donors, which lead to different superstructures and functionalities. We will discuss MAFs based on different types of azolates in the following sections.

3. METAL IMIDAZOLATE FRAMEWORKS

The two N-donors in imidazolate point outward from the five-membered ring with an angle of ca. 140°, which is essential for the generation of novel framework structures. Most reported metal imidazolate frameworks are based on univalent coinage-metal ions and/or divalent first-row transition-metal ions. See Chart 1 for the structures of the substituted imidazolates.

3.1. Chains and Rings

Although univalent coinage-metal ions can adopt a coordination number of 2 (linear), 3 (most trigonal, a few T-shaped), or 4 (tetrahedral), they are usually restricted to be linear 2-coordinated in the binary imidazolate frameworks because each ligand only provides two coordination sites. Univalent coinage-metal imidazolates may be regarded as the simplest type of coordination polymers, because linking pure 2-connected components can only give extended or closed (i.e., ring) chainlike structures. In analogy to other metal−ligand systems with bent ditopic building blocks,[22] univalent coinage-metal imidazolates also possess three typical possible structural types, i.e., a zigzag chain, helical chain, and polygon (Scheme 4). The moderately bent coordination geometry of imidazolate provides very rich structural chemistry different from that of other types of coordination polymers. While the zigzag chains of coinage-metal imidazolates are similar to the linear ones, the helical chains and polygons are of particular interest because the smaller curvature generates larger circuits. For example, coordination polygons composed of common ligands are generally triangles (60°), tetragons (90°), and hexagons (120°), but the univalent coinage-metal imidazolates are suitable for construction of octagons/nonagons/decagons (135°/140°/144°), which are all very difficult to construct by other bent ditopic ligands.

dx.doi.org/10.1021/cr200139g |*Chem. Rev.* 2012, 112, 1001–1033

Scheme 4. Self-Assembly of Univalent Coinage-Metal Imidazolate Frameworks[a]

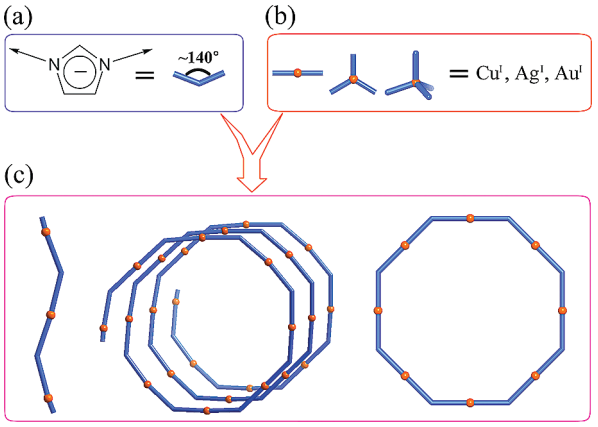

[a] Key: (a) Imidazolate is a bent linker. (b) Univalent coinage-metal ions can adopt linear, trigonal, and tetrahedral coordination geometries. (c) In the resultant metal imidazolate frameworks, univalent coinage-metal ions are restricted to have linear coordination geometry, giving the simplest supramolecular isomerism with zigzag, helical, and ring isomers.

Nevertheless, the unsubstituted imidazolate predominantly forms simple zigzag chain structures. So far, seven crystal structures have been reported for [Cu(im)][23] and [Ag(im)].[23b,24] The main structural difference between the zigzag chain and other structural types (helical chain and polygon) is that in the former all adjacent imidazolate rings adopt the *trans*-conformation but in the latter the *cis*-conformation is dominant. During polymerization of angular building blocks, each segment of the oligomer would rotate between the *cis*- and *trans*-conformations, the relative abundance of which depends on the relative stability of the resultant structures. Since the *trans*-conformation is energetically more stable (electrostatic repulsion), an infinite chain prefers the *all-trans*-conformation without external directing forces. On the other hand, a closed-ring oligomer is more stable than an open-chain one because the former has higher entropy (more species) and the latter has higher enthalpy (dangling coordination sites), which is the thermodynamical basis of selective formation of closed rings. On the other hand, kinetically, the closed ring only forms when all adjacent angular building blocks adopt the *cis*-conformation. The possibility decreases exponentially as the number of angular building blocks increases. Slowing the polymerization speed and addition of a suitable template are reasonable strategies to increase the possibility of forming a polygon, because the former increases the chance for selection and the latter increases the stability of the desired product. Nevertheless, these approaches did not result in structural types other than the zigzag chain for [Cu(im)] or [Ag(im)], though the precipitation speed can be controlled by the concentration of coordination buffering agents. This fact may be ascribed to the lack of a suitable template to interact with these structures (including oligomeric intermediates) based on the unsubstituted imidazolate.

Substitution of the primary imidazolate with alkyl groups has been proven to be very effective even such side groups can only form very weak hydrophobic interactions. Changing the length of the alkyl groups revealed the importance of hydrophobic interaction in directing the superstructure. For [Cu(mim)] and [Ag(mim)] (Hmim = 2-methylimidazole), octagon, decagon, helical, and sinusoidal chains have been found to form with inclusion of hydrophobic templates such as benzene, toluene, cyclohexane, xylene, and mesitylene. Extensive hydrophobic contacts between the methyl group and the template molecules are important and evident in the X-ray structures (Figure 1). In contrast, in the absence of a template, zigzag chains were observed.[25]

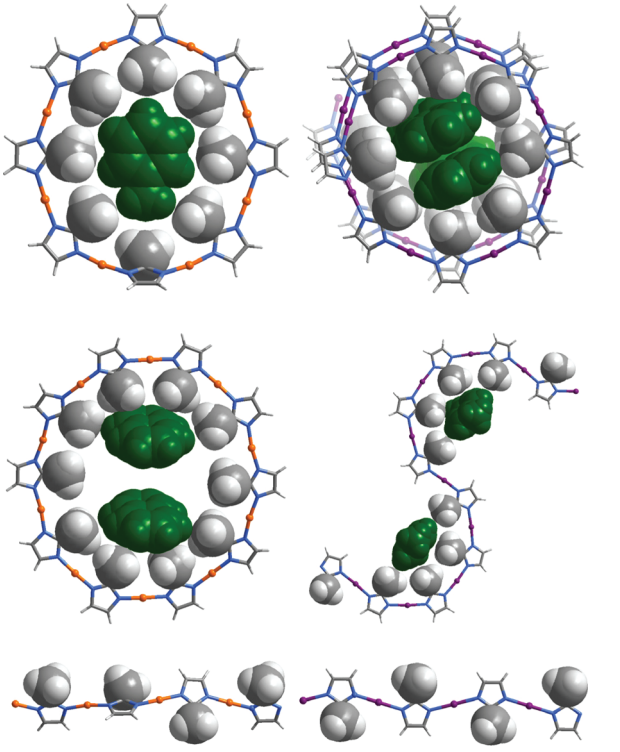

Figure 1. Isomeric univalent coinage-metal 2-methylimidazolates (left, copper(I), right, silver(I)). Methyl groups and templates are shown in space-filling mode; template molecules are highlighted in green.

For the ethyl derivative, the zigzag chain and a triple helix were synthesized in relatively nonpolar and polar media, respectively.[26] No template-including structure has been observed, which may be ascribed to the bulkier side group that reduces the required space. Nevertheless, this character is beneficial for constructing genuine supramolecular isomers.[22b] The interesting structural feature of [Cu(eim)] (Heim = 2-ethylimidazole) is that the ethyl groups show a tendency to gather together, rather than the presence of attractive interaction with a hydrophobic template. Comparing the structures of the methyl and ethyl derivatives shows that ethyl is long enough to interact with its neighbors in the same chain while methyl is much shorter/smaller. Nevertheless, the interaction between ethyl groups should be weak. Therefore, their aggregation requires a polar environment; otherwise, the ethyl groups are randomly oriented in opposite directions, resulting in the zigzag chain (Figure 2).[26]

Further increasing the size of the side group also increases alkyl···alkyl interactions. A comprehensive enumeration of supramolecular isomers has been performed for the silver isopropylimidazolate [Ag(ipim)] by extensively varied synthetic conditions, but the simple zigzag chain has not been discovered. Alternatively, three genuine interweaving isomers including a sinusoidal chain, a quintuple helix, and a chicken wire were obtained (Figure 3).[27] While the quintuple helix has the highest

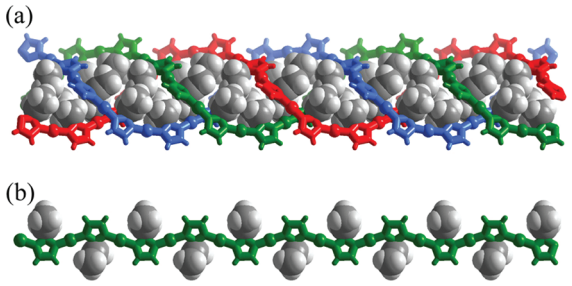

Figure 2. Triple helix (a) and zigzag chain (a) supramolecular isomers of [Cu(eim)] (ethyl groups are shown in space-filling mode).

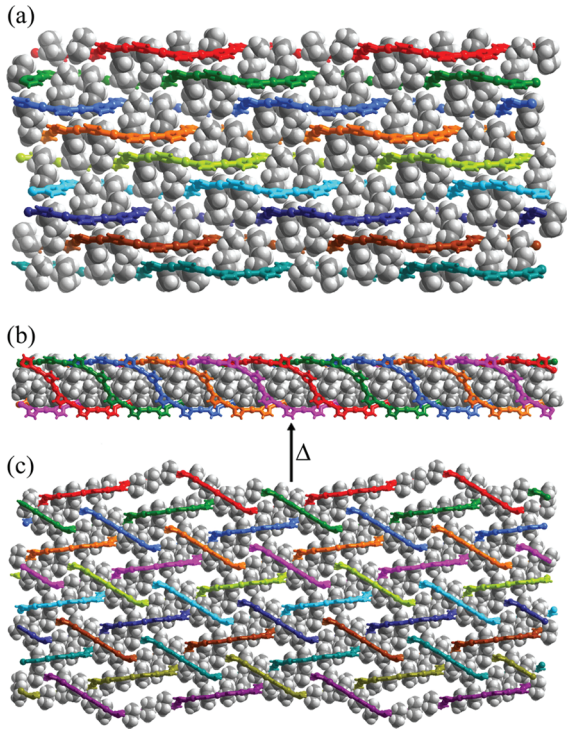

Figure 3. Interweaving isomerism and isomerization of [Ag(ipim)]: (a) sinusoidal chains; (b) quintuple helix; (c) chicken-wire-like mesh (alkyl groups are shown in space-filling mode).

strand number among known multiple helices of 1D coordination polymers,[28] the chicken-wire interweaving pattern is new for molecular structures. In these isomers, every three or four adjacent isopropyl groups gather to form arc-shaped fragments, which interconnect with each other into curved chains. Comparing the sinusoidal chains between [Ag(mim)] and [Ag(ipim)] revealed that steric hindrance or alkyl···alkyl interactions between the side groups are only present in the latter structure. Such side group interactions produce a strong self-aggregation effect to direct adjacent units to be arranged in the *cis*-conformation. Therefore, the simple zigzag chain structure (*all-trans*-conformation) can be hardly formed. On the other hand, the large steric hindrance reduces the arc curvature, which not only prevents the formation of closed rings but also increases the length of the helical pitch, being helpful for the formation of novel types of entanglements such as multiple helices with high strand numbers. Interestingly, on heating, the chicken wire transforms to the quintuple helix via a two-step mechanism as

Scheme 5. Controlling the Conformation of Molecular Chains[a]

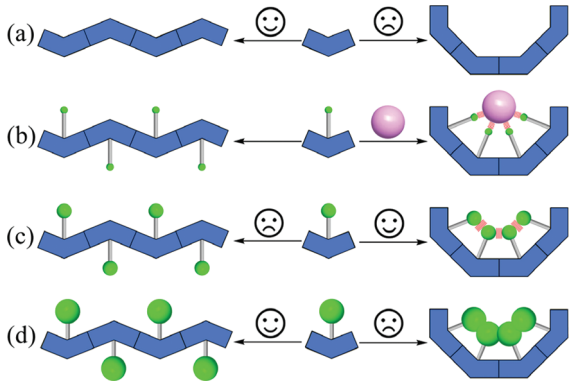

[a] Key: (a) Without a side arm, the nontwisted chain dominates. (b) Small side arms aggregate around a template and twist the chain. (c) Suitable side arms self-aggregate to twist the chain. (d) Bulky side arms induce steric hindrance for a twisted chain.

evident by differential scanning calorimetry (DSC) and variable temperature powder X-ray diffraction (VTPXRD) studies. This crystal-to-crystal structural transformation is unique because there is not only a change of entanglement topology[29] but also the absence of guest uptake/release. While the change in topology requires extensive, cooperative bond cleavage/reformation even more complicated than those found in the few known examples of changing interpenetration numbers,[30] the absence of guest uptake/release avoids mixing of the energy effect from the guest component, hence enabling the mechanism elucidation from simple thermodynamic data.

A further increase in the size of the side group may not produce more interesting structures because too much steric hindrance between the side groups leads to the *trans*-conformation again. Such zigzag chain type structures have been reported for univalent coinage-metal 2-aminobenzimidazolate and 2-(3-pyridyl)benzimidazolate.[31] Obviously, alteration of the side groups of imidazolates seems to be the most basic measure, via tuning the supramolecular interactions with the environment, in controlling the formation of the low-dimensional polymeric superstructures (Scheme 5).

3.2. Zeolitic and Zeolite-like Frameworks

While octahedral coordination geometry is more common for bivalent transition-metal ions, they adopt square-planar or tetrahedral coordination geometry in the binary metal imidazolate frameworks. The similarity of coordination geometries between tetrahedral metal imidazolates and aluminosilicates has been recognized for a long time. Linking tetrahedral metal centers by linear bridging ligands gives the common **dia** topology in most cases, because the symmetries of the building blocks and network topology fit well with each other. In principle, using a bent linker breaks the perfect tetrahedral T_d symmetry (arises from the metal center) for **dia** and introduces structural diversity for other 4-connected topologies (Scheme 6). The binary cobalt(II) and zinc(II) imidazolates **coi**-$[Co(im)_2]$[32] and **zni**-$[Zn(im)_2]$[33] have been synthesized for more than 30 years. A quartzlike framework, **qtz**-$[Fe(mim)_2]$, was also reported in 1983.[34] However, these 4-connected frameworks neither are porous nor belong to the registered zeolite types.[7a] The first zeolitic metal imidazolate

Scheme 6. Using a Bent Linker To Break the Ideal T_d Symmetry of the Tetrahedral Metal Center for Construction of Diverse 4-Connected Topologies Other Than dia

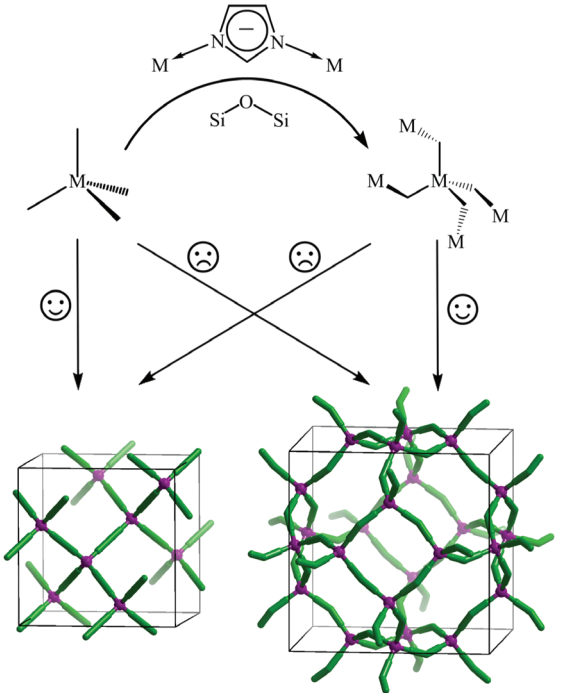

framework may be BCT-$[Fe(mim)_2]\cdot 0.13$ferrocene, which was synthesized by reacting ferrocene with molten Hmim. However, the included ferrocene cannot be removed without decomposition of the framework.[35]

These promising candidates for metal−organic zeolites gained attention at the beginning of this century. By virtue of template inclusion, You and co-workers synthesized a zeolite-like **nog**-$[Co(im)_2]\cdot 0.4$MB (MB = 3-methyl-1-butanol) in 2002.[36] The robustness of the porous framework was proven by exchanging the included template with EtOH and removing it later by vacuum treatment, in which the single-crystal structure of **nog**-$[Co(im)_2]\cdot 0.1$EtOH was determined. Later, they extended $[Co(im)_2]$ to other isomeric zeolite-like and zeolitic (**neb**, **zni**, **cag**, BCT) frameworks by varying the template and/or structure-directing agent in solvothermal reaction using alcohols as the main solvent. Although most of these compounds are virtually nonporous or collapse after guest removal, they exhibit interesting and superstructure-dependent magnetic properties because the spin-canting behaviors, arising from uncompensated antiferromegnetic couplings, are sensitive to magnetic exchange topologies.[37]

The first porous metal imidazolate framework with topology mathematically identical to those of zeolites is the zinc(II) benzimidazolate SOD-$[Zn(bim)_2]$ (MAF-3), being reported by us in 2003,[38] which was synthesized by the liquid diffusion method using aqueous ammonia as a coordination buffering agent. The SOD framework of MAF-3 (also known as ZIF-7[39]) is highly distorted, as can be obviously judged from its lower crystal symmetry ($R\bar{3}m$) than that of the hypothetical SOD zeolite ($Im\bar{3}m$). The bulky phenyl side group also significantly reduces the porosity and aperture size (Figure 4). However, these features are beneficial when the material is used as supported microporous membranes for gas separation.[40] After removal of the included guest, the framework shrinks to a narrow-pore phase,[41] and such a gate-opening effect was utilized for separation of ethane and ethene.[41a]

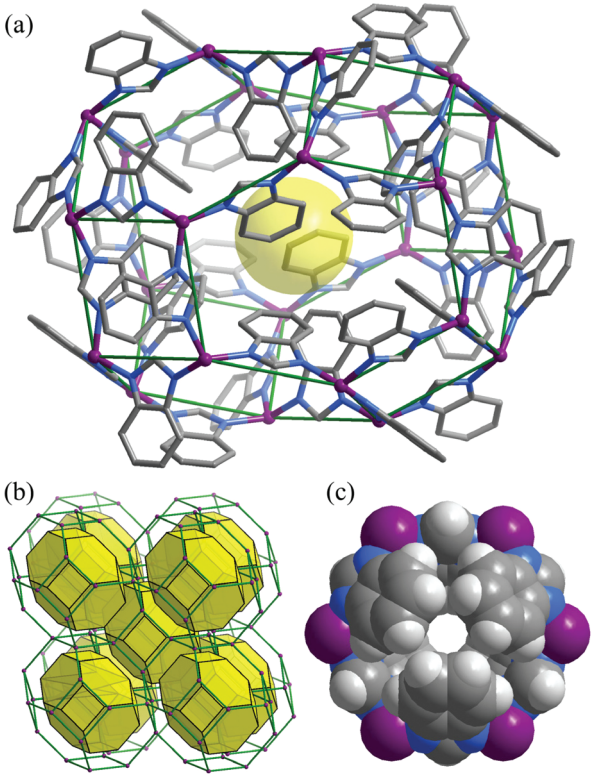

Figure 4. Distorted β-cage (a), distorted SOD topology, (b) and aperture (c) of SOD-$[Zn(bim)_2]$.

We further discovered, soon after the finding of MAF-3, that, by changing the side group to a smaller one and using the mixed-ligand strategy, more porous metal−organic zeolites, SOD-$[Zn(mim)_2]$ (MAF-4), ANA-$[Zn(eim)_2]$ (MAF-5), and RHO-$[Zn(eim/mim)_2]$ (MAF-6), with regular zeolitic topologies can be obtained (Figure 5).[42]

3.2.1. SOD-Type Zinc(II) 2-Methylimidazolate. MAF-4 (also known as ZIF-8[39]) has been extensively studied as a new prototypical PCP, due to its exceptional stability and high porosity, as well as the facile and diversified preparation methods. It is also one of the few commercialized PCPs.[43] The material contains a large 3D intersecting channel system (void 50%, **bcu** topology) composed of large cavities (d = 11.4 Å, 8-connected nodes, Figure 6a) and small apertures (d = 3.2 Å, link between nodes, Figure 6b). As completely lined with methyl groups and aromatic rings, its pore surface is highly hydrophobic and inert, which is scarce in known adsorbents with high porosity. As shown in Figure 6c, each of the four triangular faces of the ZnN_4 coordination sphere is covered by a methyl group, which nicely protects the metal ion from attack by guest species. The strongest adsorption sites for H_2 and CH_4 were determined by neutron powder diffraction experiments and grand canonical Monte Carlo (GCMC) simulations to be located above the C═C bond of the ligand.[44]

So far, many synthetic methods have been developed for SOD-$[Zn(mim)_2]$. The single crystals can be prepared by room temperature liquid-phase diffusion between an aqueous ammonia solution of $Zn(OH)_2$ and a methanol solution of Hmim[42b] or

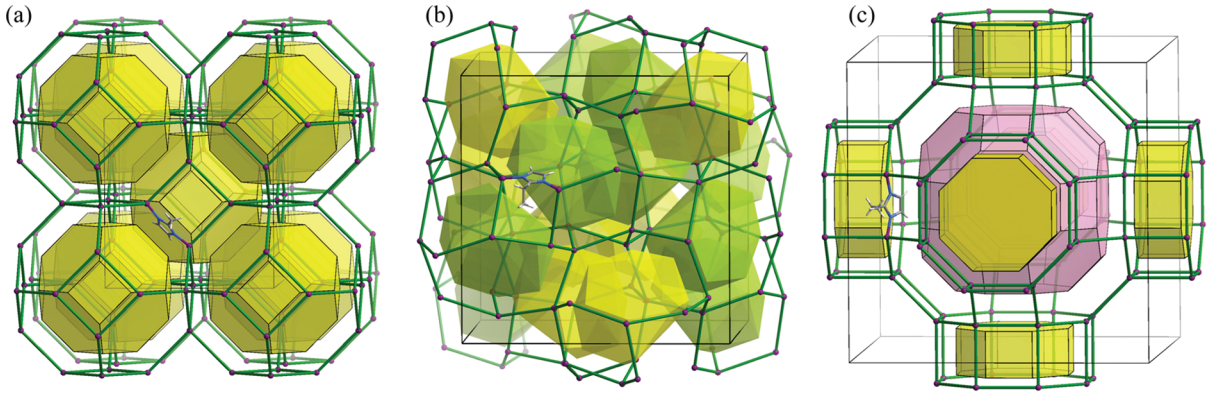

Figure 5. Regular zeolitic framework structures of SOD-[$Zn(mim)_2$] (a), ANA-[$Zn(eim)_2$] (b), and RHO-[$Zn(eim/mim)_2$] (c).

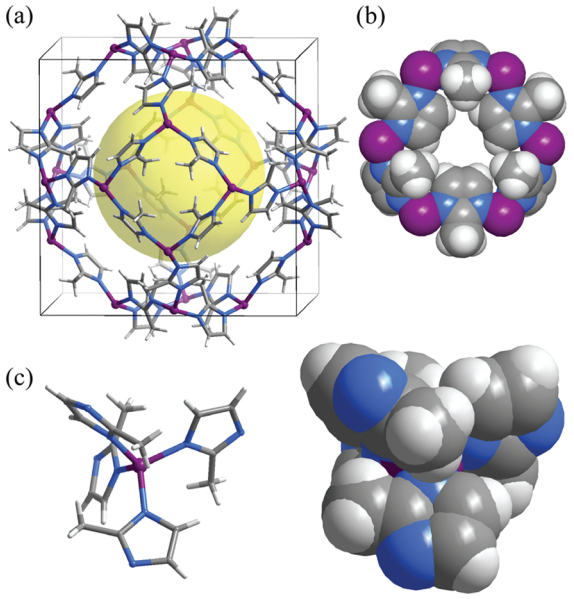

Figure 6. Crystal structure of SOD-[$Zn(mim)_2$]: (a) β-cage with inner cavity highlighted in yellow; (b) space-filling view of the six-ring aperture; (c) ball-and-stick (left) and space-filling (right) viewing of the coordination environment of the metal center.

solvothermal reaction of $Zn(NO_3)_2$ and Hmim in DMF at 413 K.[39] Nanocrystals can be rapidly synthesized at room temperature with largely excessive Hmim using methanol or water as the solvent.[45] A stoichiometric mixture of $Zn(NO_3)_2$ and Hmim in MeOH generates a colloidal solution, which can be utilized to fabricate nanocrystal-based thin films useful as selective sensors for vapors and gases such as detection of propane concentration and ethanol or 2-propanol vapors from water/alcohol mixtures.[46] Microcrystalline powder was synthesized by steam-assisted reaction using largely excess Hmim.[47] Microcrystalline powders can also be rapidly synthesized in high yield at room temperature without excess starting material such as Hmim, using aqueous ammonia as a readily recyclable base.[48] While excess base or high temperature seems to be necessary for deprotonation of the ligand with low acidity, microcrystalline powder can be synthesized at room temperature by solvent/additive-assisted mechanochemical reaction between stoichiometric ZnO and Hmim.[49] Actually, without addition of any solvent or additive, a microcrystalline powder and even a shaped sample on a large scale can be efficiently obtained by heating a mixture of $ZnO/Zn(OH)_2$ and Hmim at 180 °C.[50]

Many data, albeit being slightly different, have been reported to demonstrate the exceptional thermal/chemical stability and high porosity of SOD-[$Zn(mim)_2$]. Nanocrystals with diameters of 40−70 nm are stable up to ca. 200−400 °C in air.[45a,b] Decomposition temperatures for larger crystals were reported in the range from 420 °C in air[42b] to 550 °C in N_2.[39,45c] Yaghi et al. showed that it is chemically stable for at least 7 days in boiling benzene, methanol, and water or 1 day in aqueous NaOH.[39] Willis et al. showed that its hydrothermal stability (50% steam at 350 °C) and activation energy (58.5 kJ mol^{-1}) of ligand displacement are higher than those of other typical PCPs.[51] Nevertheless, the water stability may also depend on the crystal size or preparation method. Matzger et al. showed that additional powder X-ray diffraction (PXRD) peaks appeared after three months, when the activated sample was immersed in water at room temperature, being much more stable than typical PCPs except MIL-100.[52] Kaskel et al. showed additional PXRD peaks appear just after one day when the commercial sample is stored in water at 323 K.[53] The measured pore volume and Brunauer−Emmett−Teller (BET) and Langmuir specific surface areas were reported to be 0.31−0.69 cm^3 g^{-1} and 1000−1700 and 1200−1900 m^2 g^{-1}, respectively,[39,42b,45] indicating the crucial role of preparation methods for the samples' quality.

The small aperture size in MAF-4 is useful for molecular sieving applications. Theoretical calculations showed that the diffusion correlations of gas molecules in this material are negligibly small, and the narrow aperture results in high separation ratios for small gas molecules.[54] Nano/microcrystalline membranes seeded and grown on porous titania[55] or alumina[40d,56] via solvothermal reaction have shown potential application for energy-efficient separation of H_2 from other gases. Nano/microcrystals were used as additives in mixed matrix polymer membranes[57] or electrospun with carrier polymers,[58] which combine the processability of organic polymers and the gas separation properties of the PCP, and were used as filters for gas separation[57a,b] and solvent-resistant nanofiltration.[57c] Nanocrystals were used to coat capillaries for gas chromatography, which is useful for sieving C6−C8 linear and branched alkanes.[59] The linear isomer exhibits a longer retention time, because the bulky branched isomers are not able to pass the narrow pore apertures.[60] Microcrystals also demonstrated good performance for kinetic separation of propane and propene.[61]

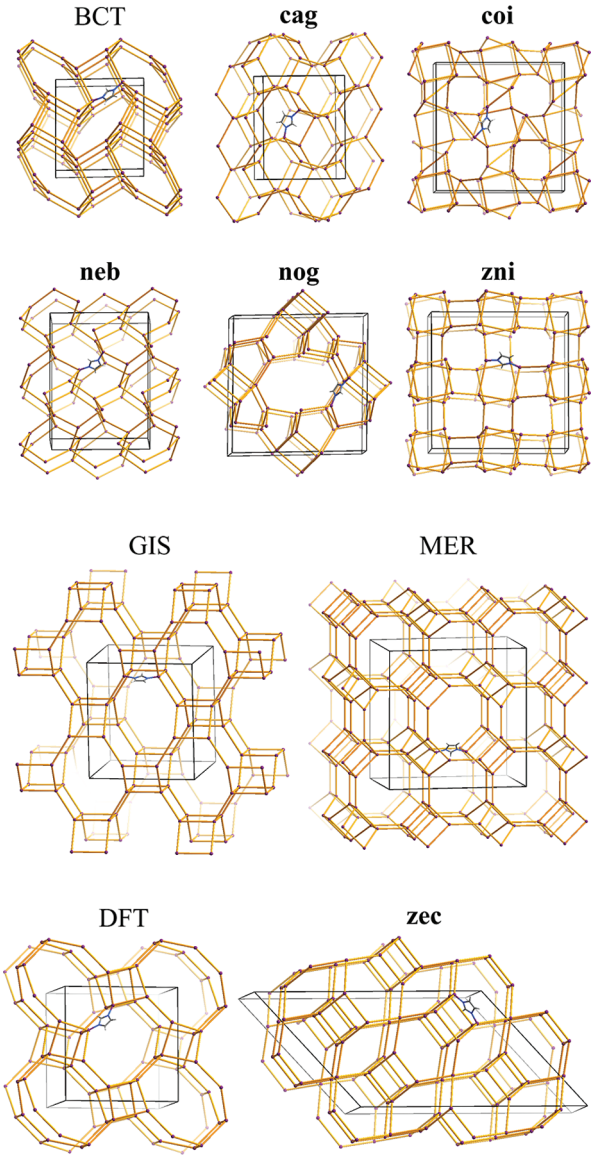

Figure 7. Zeolitic and zeolite-like topologies observed for $[Co(im)_2]$ and $[Zn(im)_2]$.

Although the aperture size of SOD-$[Zn(mim)_2]$ is very small, it has been studied in the context of catalysis. Nevertheless, experiments and ab initio calculations confirmed that the catalytic sites are located on the external surface or at defects of the crystal, being consistent with its small aperture size and inert pore surface.[62] On the other hand, it can be used as the porous medium for other catalysts. Gold nanoparticles supported on the microcrystals have been studied as a catalyst for CO and benzyl alcohol oxidation, which has achieved good conversion and high selectivity to methyl benzoate rather than to benzaldehyde with 10 wt % gold loading.[63] It can also be loaded into Pt/TiO_2 nanotubes, giving better photocatalytic performance than that of pure Pt/TiO_2 nanotubes because of its large surface area and adsorbent properties that reduce charge recombination of Pt/TiO_2 nanotubes.[64]

While studies were mainly focused on its robustness, SOD-$[Zn(mim)_2]$ also illustrates a certain degree of framework flexibility. The sorption behaviors of organic vapors on microcrystals have been investigated using an inverse gas chromatography methodology. The pore aperture diameter could be expanded

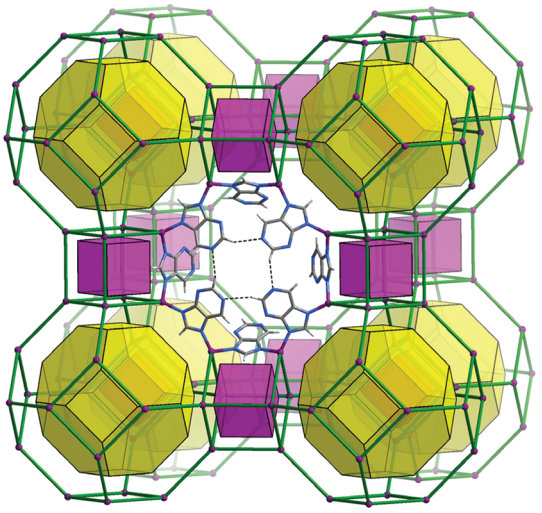

Figure 8. Framework structure of the LTA-type zinc(II) purinate (ligands on an eight-membered ring are shown to highlight the aperture size and their interactions: C···N, 3.44 Å; H···N, 2.57 Å).

to ca. 5 Å for passing linear alkanes and isobutane.[60] Moggach et al. reported that the framework distorts to accommodate more guest at 1.47 GPa in a 4:1 (v/v) mixture of methanol and ethanol as a hydrostatic medium.[65] On the other hand, Chapman et al. reported an irreversible pressure-induced amorphization after compression beyond 0.34 GPa using a nonpenetrating fluid (Fluorinert) as the hydrostatic medium, which generates a less porous phase. The total uptake of N_2 at 77 K and BET surface areas systematically decrease as the compression pressure increases, however, which indicated the amorphous phase still having nanoporosity.[66]

Yaghi et al. have done rather extensive work for this new type of novel porous materials, which were termed zeolitic imidazolate frameworks (ZIFs). In a recent review, they summarized comprehensively the zeolitic frameworks that have been accessible from different azolate ligands.[15d] In their first report,[39] solvothermal reaction using amide as the solvent with varying temperature and time was employed, which enabled the discovery of several new structural types for $[Zn(im)_2]$ (**cag**, BCT, DFT, GIS, MER). By using imidazolate ligands with different substituent groups, a series of new zeolite frameworks, including SOD-$[Co(bim)_2]$, SOD-$[Co(mim)_2]$, RHO-$[Zn(bim)_2]$, and RHO-$[Co(bim)_2]$, were also synthesized. They also showed high porosity for MAF-4 and RHO-$[Zn(bim)_2]$ through gas sorption analyses, as well as exceptionally high stability for MAF-4. Tian et al. also used the liquid diffusion method with different structure-directing agents to construct $[Zn(im)_2]$ isomers with **nog**, **cag**, **zec**, BCT, DFT, and GIS topologies (Figure 7). However, only the **nog** phase can retain the framework integrity after guest removal,[67] which is similar to their earlier reports about the $[Co(im)_2]$ isomeric frameworks,[36,37] implying that network topology can play an important role in determining the framework stability.[68]

Yaghi et al. have synthesized a variety of novel imidazolate-based metal−organic zeolites. LTA-type frameworks were constructed by purinate and 5-azabenzimidazolate, while another similar ligand, 4-azabenzimidazolate, resulted in the nonporous **dia** structure.[69] As shown in Figure 8, the presence of at least one N atom on the 5- or 6-position is necessary to avoid steric hindrance between the C−H moieties of adjacent purinate ligands. Actually, the intermolecular contacts between these moieties are

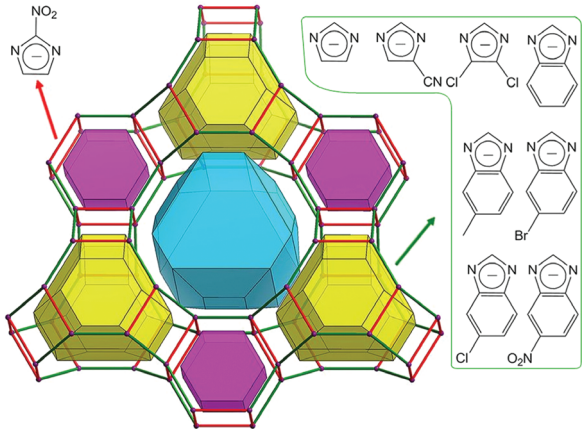

Figure 9. Series of GME-type zinc(II) imidazolate frameworks constructed by mixing 2-nitroimidazolate with other imidazolates.

representative of formal C−H···N hydrogen bonds. The purinate-based LTA framework showed adsorption of Ar rather than N_2 at 77 K, being consistent with its very small aperture size. While this material possesses a moderate surface area and hydrogen uptake, single-component sorption isotherms and breakthrough experiments suggested it as a potential adsorbent for CO_2/CH_4 separation. Employing imidazolates with bulkier substituent groups, two zeolite-like frameworks (**poz** and **moz**) containing colossal cages were also constructed, which display selective CO_2 sorption properties.[70]

Yaghi et al. introduced the high-throughput screening method to investigate the impact of the metal-to-ligand molar ratio, solution concentration, temperature, reaction time, substituent group, solvent, and especially using different mixtures of imidazole derivatives on the topological structures of imidazolate-based frameworks. More than 10 new materials showing a variety of topologies (**zni**, **cag**, **lcs**, **frl**, MER, SOD, GME, RHO, GIS, LTA) were disclosed, most of which contain mixed imidazolate ligands.[71]

It is also worth noting that Yaghi et al. further synthesized a series of isoreticular GME frameworks by combining 2-nitroimidazolate with other imidazolate derivatives (Figure 9)[72] and also isoreticular RHO frameworks composed of different imidazolate derivatives.[73] Comparison of the sorption properties of these isoreticular materials enabled the authors to reveal the influence of the polarizability and/or symmetry of the substituent group on CO_2 sorption properties.

The SOD topology appears to be the most stable porous zeolitic structure for binary metal imidazolate frameworks reported so far.[68,74] Besides zinc(II) and cobalt(II) 2-methylimidazolates, several SOD-type metal imidazolate frameworks are also known. Li et al. synthesized SOD-type zinc(II) 2-chloroimidazolate and 2-bromoimidazolate and compared their kinetic separation properties for propane and propene with those of the 2-methylimidazolate analogue MAF-4. They showed that MAF-4, with the smallest aperture size which controls the diffusion rates, has the best performance among the three tested materials.[61] Yaghi et al. demonstrated that the aldehyde group in the SOD-type zinc(II) 2-formylimidazolate can be reduced to hydroxymethyl or condensed with organic amine to ((2-hydroxyethyl)imino)methyl in a postsynthetic manner.[75] Examination of the SOD-type metal imidazolate frameworks shows that the tetrahedral ZnN_4 coordination geometry and bent imidazolate linker nicely compensate the distorted tetrahedral node geometry in the regular SOD topology. For example, the Zn(II) ions adopt nearly perfect tetrahedral coordination geometry in the crystal structure of SOD-[Zn(mim)$_2$] (N−Zn−N = 109.5°).[42] The crystal structure of the nonporous **dia**-[Zn(mim)$_2$] isomer was recently reported, in which the Zn(II) ions possess severely distorted tetrahedral geometry (N−Zn−N = 101-121°).[47]

Cd(II) can also serve as a tetrahedral node, and substitutent groups of imidazolates also play important roles in directing the framework structures. The 2-fold interpenetrated **dia**-[Cd(im)$_2$] was reported early.[76] Using alkyl-, nitro-, and phenyl-substituted imidazolates, Tian et al.[77] synthesized a series of cadmium(II) imidazolates with SOD, MER, ANA, RHO, **ict**, and **yqt1** topologies. Remarkably, the RHO-type cadmium(II) imidazolate frameworks are more porous (Langmuir surface area 3000 $m^2\ g^{-1}$) than the Zn(II) analogues, owing to the longer node-to-node distance arising from the relatively long Cd−N bonds. As shown in Table 2, a small variation of the coordination bond length results in a very large change of the framework density, because the volume of a net is proportional to the cube of the edge length.

Besides the discovery of several new zeolitic zinc(II)/cobalt(II) imidazolate frameworks using different imidazolate derivatives,[78] Feng et al. used combinations of Li(I)/Cu(I) and B(III) to function as bivalent tetrahedral metal centers, in analogy to the evolution from SiO_2 to $AlPO_4$. Although these frameworks are constructed by tetrakisimidazolylborate rather than an imidazolate anion and a B^{3+} cation, the structural chemistry is similar to that of the above-discussed examples. When the imidazolyl moieties are nonsubstituted, nonporous **zni** networks are obtained. Introduction of methyl groups to the imidazolyl groups produced porous SOD- and RHO-type frameworks depending on the substituted positions,[79] illustrating again the structure-directing effect of substituent groups. Even though the Li/B compound possesses the lightest elements for metal−organic zeolites, these materials exhibit lower pore volumes and surface areas than their Zn/Co/Cd analogues, because the very short B−N bonds significantly reduce the node-to-node separations (Table 2). When the steric hindrance is increased on the 4- and 5-positions of the imidazolyl moiety, a 2D **sql**-**a**-type framework is obtained.[79b]

When the imidazolate is substituted with coordinative functional groups, the resultant coordination structures are usually completely different from those constructed by simple imidazolates, except in a few cases. Eddaoudi et al. employed 8-coordinated In(III) as tetrahedral nodes and partially deprotonated 4,5-imidazoledicarboxylic acid as bent linkers to construct several types of anionic zeolitic frameworks, some of which are capable of cation exchange, being similar to aluminosilicates.[80] Holdt el al. reported that, under solvothermal conditions in the presence of $Zn(NO_3)_2$, 4,5-dicyano-2-methylimidazole can be partially hydrolyzed and deprotonated to form imidazolate-4-amide-5-imidate, giving a microporous framework with 3-connected topology, in which each Zn(II) is 5-coordinated by three ligands and each ligand also bridges three Zn(II) ions.[81]

3.3. Nonporous 4-Connected Networks

Bivalent tetrahedral metal ions and imidazolates can also form nonporous 4-connected networks. Reported examples include **qtz**-[Zn(eim)$_2$] found in the rapid room temperature mechanochemistry synthesis,[49] **dia**-[Zn(mim)$_2$] and **dia**-[Co(mim)$_2$] obtained by hydrothermal synthesis of Hmim and $Zn(OAc)_2$ or $Co(OAc)_2$,[47] and the layered structure **sql**-[Zn(bim)$_2$] synthesized

Table 2. Framework Density Variation of Zeolitic Structures[a]

structure type	T−O (Å)	T···T (Å)	cell volume (nm^3)	density (T/nm^3)	ref
zeolite[b]	Si−O, 1.6	3.1	720	16.7	7a
$[Zn(mim)_2]$	Zn−N, 2.0	6.0	4923	2.4	42
$[Co(mim)_2]$	Co−N, 2.0	6.0	4878	2.5	39
$[Cd(mim)_2]$	Cd−N, 2.2	6.4	5950	2.0	77
$[Li(B(im)_4)]$	B−N, 1.6; Li−N, 2.0	5.7	4120	2.9	79a
$[Cu(B(im)_4)]$	B−N, 1.6; Cu−N, 2.0	5.7	4110	2.9	79a

[a] Using the zeolitic topology SOD for comparison. [b] Using hypothetical SiO_2 for calculation.

via solvothermal in situ ligand formation from *o*-phenylenediamine and oxalic acid.[82]

Compared to the tetrahedral counterparts, square-planar metal imidazolate frameworks are rare. Only one simple 2D square grid (**sql**) structure was structurally characterized for $[Ni(im)_2]$.[83] $[Cu(im)_2]$ crystallizes as four isomeric forms, including 3D **pts**,[84] SOD, **mog**, and a complexed binodal 2D net with point symbol $(5^2.6^4)(5^4.6^2)_4$,[85] in which Cu(II) atoms adopt distorted square-planar to flatten tetrahedral coordination geometries.

The 4-connected topologies can also be constructed by mixed univalent coinage-metal and divalent metal ions, in which the im−M(I)−im linkages represent long 2-connected metalloligands. For example, we constructed 4-connnected networks $[Cu^ICu^{II}(im)_3]$ and $[Cu^I{}_2Cu^{II}(im)_4]$ with 4.8^5 and **sql** topologies, respectively, by controlled reduction of Cu(II) at different reaction temperatures under solvothermal reactions.[86] It should be noted that the simple uninodal 4-connected topology for $[Cu^ICu^{II}(im)_3]$ (point symbol 4.8^5, vertex symbol $4.8_4.8_4.8_6.8_4.8_6$) has not been observed or theoretically predicted.[7] Such structures may also be constructed by mixed metal ions, such as **sql**-$[Cu^I{}_2Co^{II}(im)_4]$[87] and **sql**-$[Cu^I{}_2Zn^{II}(im)_4]$.[88] A neutral 4,6-connected **gar** net, $[In_2Zn_3(im)_{12}]$, was reported by Yaghi et al.[39]

3.4. Polyimidazolates

Although attention has been mainly focused on simple imidazolates, several investigations on metal polyimidazolates have recently been documented. For example, Liu et al. reported a nonporous framework, $[Cu_2(bbimb)]$ (H_2bbimb = 1,3-bis(2-benzimidazolyl)benzene), with ABW topology, in which Cu(I) is linearly coordinated and $bbimb^{2-}$ possesses the μ_4-coordination mode.[89] A coordination polymer composed of trisimidazolate was observed in $[Ag_{17}(tbimb)_5(Htbimb)(H_2O)_5]\cdot H_2O$ (H_3tbimb =1,3,5-tris(2-benzimidazolyl)benzene) as reported by Su et al.[90] Recently, Sun et al. reported a microporous framework, $[Cu(dimb)]$ (H_2dimb = 1,4-bis(1*H*-imidazol-4-yl)benzene), with binodal 4-connected topology and 1D channels, which shows exceptional chemical stability in boiling water, benzene, methanol and even 1 M aqueous sodium hydroxide.[91] They further employed a trisimidazole ligand, 1,3,5-tris(1*H*-imidazol-4-yl)benzene (H_3timb), to construct two isomeric porous $[Co(Htimb)]$ frameworks with 4-connected **ecl** and BCT topologies, in which two of the three imidazole moieties are deprotonated and four N-donors are involved in coordination (metal also 4-coordinated). The BCT isomer shows interesting stepwise adsorption of CO_2 with pronounced hysteresis.[92] See Chart 2 for the structures of polyimidazolates.

Metal imidazolate frameworks have been widely investigated in many aspects. Some rational crystal engineering approaches, such as the introduction and alteration of side groups on the imidazolate ring, adding coordination buffering and/or structure-directing agents, and using mixed ligands, have been developed for controlling the superstructures and/or isomerism of simple chainlike and porous zeolitic structures. Particularly, porous metal imidazolates have become one of the most important classes of PCPs for their unique porous structures and interesting properties, such as high stability and selective adsorption to different gas or organic molecules.

Chart 2. Polyimidazolates

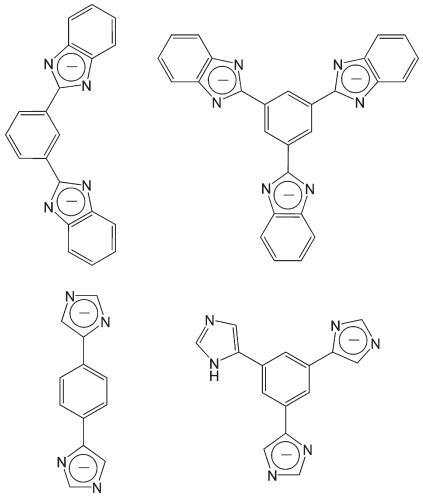

4. METAL PYRAZOLATE FRAMEWORKS

Compared with the isomer imidazolate, pyrazolate possesses a rather small bridging angle (ca. 70°), which fixes two metal ions in a short distance (ca. 3.5−4.7 Å depending on the ion radius).[15g] Actually, pyrazolate derivatives are well explored as ligands for the construction of discrete, polynuclear complexes rather than coordination polymers.[15c] On the other hand, the coordination geometry of pyrazolate is somewhat similar to the *syn,syn*-μ-η^1,η^1-bidentate mode of carboxylate, which is the basis of paddle-wheel $M_2(RCOO)_4$, trigonal-prismatic $M_3O(RCOO)_6$, and octahedral $M_4O(RCOO)_6$ SBUs commonly used in porous metal carboxylate frameworks. Therefore, linking multiple pyrazolate rings with different lengths and geometries would be a reasonable strategy for generating cluster-based polymeric networks.

4.1. Clusters and Chains

The small bridging angle of pyrazolate makes it suitable for the construction of low-dimensional structures (Figure 10), especially combining linear 2-coordinate univalent coinage-metal ions to form triangles.[15f] A great variety of such trigonal-planar

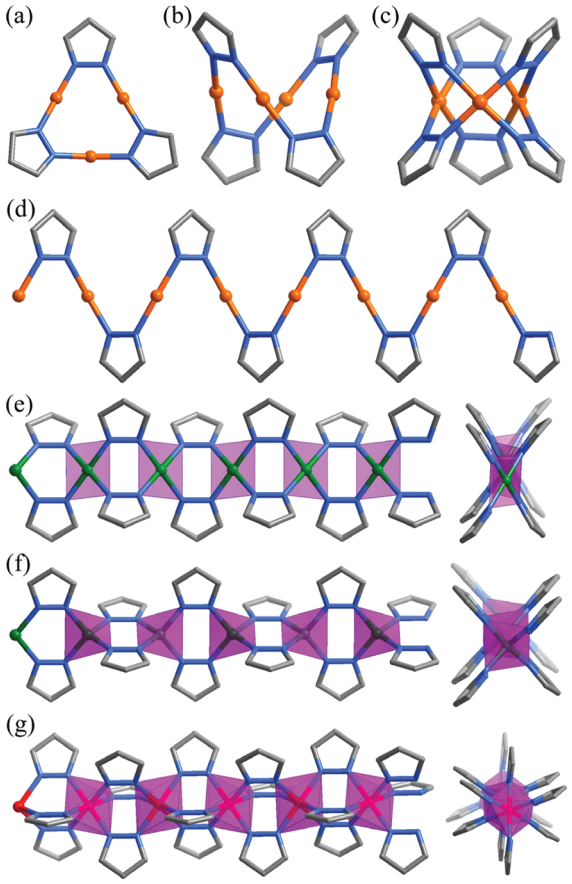

Figure 10. Several typical cluster/chain structures composed of simple pyrazolate ligands: (a) planar triangle; (b) saddlelike four-membered ring; (c) trigonal-prismatic triangle; (d) simple zigzag chain; (e) double zigzag chain with square-planar metal ions; (f) double zigzag chain with tetrahedral metal ions; (g) triple zigzag chain with octahedral metal ions.

$[M_3(pz)_3]$ clusters (M = Cu^I, Ag^I, Au^I) have been constructed by pyrazolate derivatives bearing different substitutent groups.[93] Besides strong photoluminescence, these complexes also demonstrated interesting host−guest properties due to the close arrangement of three coordinatively unsaturated coinage-metal ions, which may interact with each other via metallophilicity or with other molecules via π coordination or Lewis acid−base pairing. With bulky substituents, univalent coinage metal pyrazolates can also form larger, distorted rings such as tetranuclear saddle-shaped cycles.[94] Alternatively, infinite zigzag chains can be obtained when steric hindrance from the substituent groups is eliminated.[95]

Divalent 4-coordinate metal ions such as Fe(II), Co(II), Ni(II), Cu(II), Zn(II), and Cd(II) can assemble with simple pyrazolate to form 1D chains composed of vertex-sharing $M_2(pz)_2$ rings.[95,96] The $M_2(pz)_2$ rings are planar for tetrahedral metal ions and bent for square-planar metal ions. Cu(II) can adopt both square-planar and flattened tetrahedral geometries to form the two types of isomeric $[Cu(pz)_2]$ chains. The square-planar one contains interchain cavities capable of accommodating small molecules, which interact with the Cu(II) centers to show vaporchromic effects.[96e] Cyclic trimers $[M_3(pz)_6]$ composed of square-planar divalent metal ions have only been observed for Pd(II).[97]

It is noteworthy that, by introduction of some simple anions, many high-symmetry polynuclear clusters can be produced

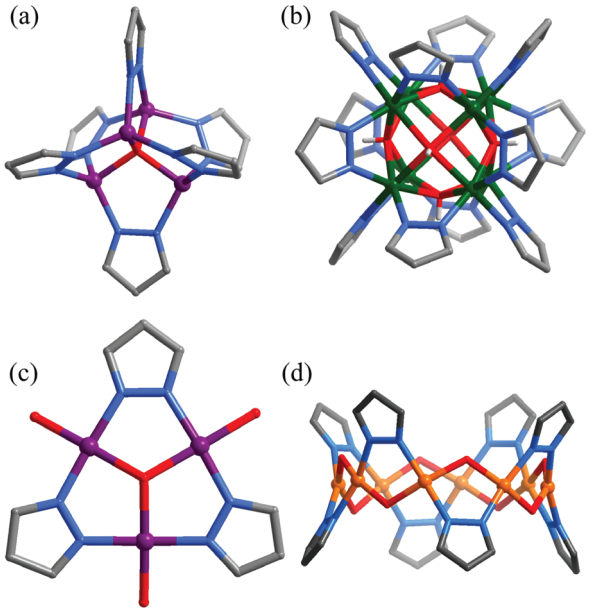

Figure 11. Typical polynuclear clusters bridged by pyrazolates and oxide/hydroxide: (a) octahedral $[Co_4(\mu_4\text{-}O)(\mu\text{-}pz)_6]$; (b) cubic $[Ni_8(\mu_4\text{-}OH)_6(\mu\text{-}pz)_{12}]$; (c) triangular $[Cu_3(\mu_3\text{-}O)(\mu\text{-}pz)_3(H_2O)_3]^+$; (d) crown ether-like $[Cu(\mu\text{-}OH)(\mu\text{-}pz)]_8$.

(Figure 11). A few reported structures, such as $[Co_4(\mu_4\text{-}O)(\mu\text{-}dmpz)_6]$,[98] are structurally similar to those constructed by carboxylate ligands. Meanwhile, many structural types of such pyrazolate-bridged clusters have not been observed in other metal−ligand systems. For example, Xu reported an octanuclear $[Ni_8(\mu_4\text{-}OH)_6(pz)_{12}]^{2-}$ cluster with a cubic arrangement of eight metal ions and a cuboctahedral arrangement of twelve pyrazolates.[99] Reactions of Cu(II) salts with pyrazolates in the presence of secondary ligands usually generate trinuclear $[Cu_3(\mu_3\text{-}X)(\mu\text{-}pz)_3]^{n+}$ (X = OH^-, O^{2-}, halide, etc.) clusters.[15e] A series of cyclic crown ether analogues, $[Cu_n(\mu\text{-}OH)_n(\mu\text{-}pz)_n]$, have also been constructed,[100] some of which can encapsulate anions in their inner cavities.

4.2. 3D Networks Based on Polypyrazolates

Similar to the relation between traditional coordination compounds and coordination polymers, many of the clusters and chains discussed above may serve as SBUs, which can be connected into higher dimensional networks using polypyrazolate ligands to replace the monopyrazolates. See Chart 3 for the structures of polypyrazolates.

The simple bispyrazole 3,3′,5,5′-tetramethyl-4,4′-bipyrazole (H_2bpz) has received considerable attention as a neutral bipyridyl-type ligand.[101] Due to the steric hindrance between the methyl groups, the two five-membered rings have a dihedral angle φ = 50−90°, mostly 70°, which is coincident with that in the famous (10,3)-a (**srs**) topology. In other words, the $[M_3(pz)_3]$ triangles may be connected by covalent bonds to form highly porous 3-connected networks, using bpz^{2-} to replace the ordinary monopyrazolates (Figure 12a). Yin et al. reported the crystal structure and photoluminescence of the 8-fold interpenetrated **nof**-$[Cu_2(bpz)]$, which was synthesized by solvothermal reaction of $Cu(NO_3)_2$ and H_2bpz in aqueous ammonia (Figure 12b).[102]

By liquid diffusion between an aqueous ammonia solution of Ag_2O and a MeOH solution of H_2bpz, Kitagawa et al. synthesized the 4-fold interpenetrated **srs**-$[Ag_2(bpz)]$ with considerable

dx.doi.org/10.1021/cr200139g |*Chem. Rev.* 2012, 112, 1001–1033

Chart 3. Polypyrazolates

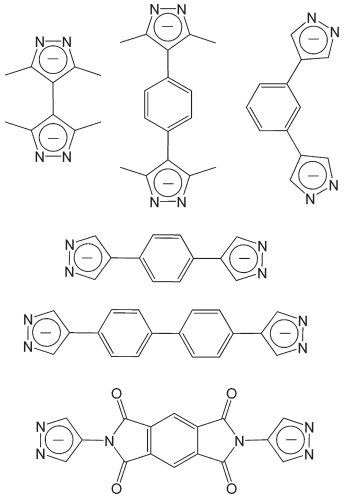

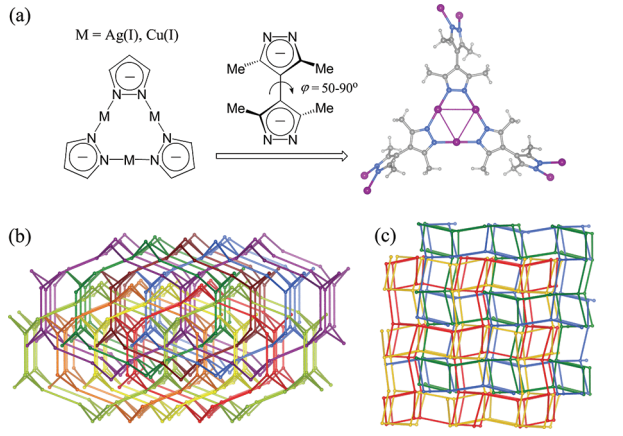

Figure 12. Construction principle of flexible 3D 3-connected networks (a) and observed 8-fold interpenetrated **nof** (b) and 4-fold interpenetrated **srs** (c) topologies for $[M_2(bpz)]$.

porosity (Figure 12c).[103] They showed that **srs**-$[Ag_2(bpz)]$ can readily adsorb small aromatic molecules in a single-crystal to single-crystal manner. The adsorbed aromatic molecules are sandwiched between two Ag_3 planes as monomers, dimers, or trimers arranged in a complicated sequence. Weak Ag···π and C−H···Ag interactions were observed between the framework and the guest. Interestingly, during the adsorption/desorption process or at different guest-loading levels, the single crystal exhibits a variety of single-crystalline, twined or polycrystalline, and even amorphous-like phases. The single-crystal structure of an intermediate phase has been solved, which revealed various stacking conformations between the Ag_3 triangles (Figure 13). The crystal structures of guest-free, intermediate, and guest-saturated states contain 1, 9, and 15 independent $Ag_2(bpz)$ units. The dpz^{2-} ligands adopt very diversified conformations even in the same crystal structure.

Kitagawa et al. subsequently studied the syntheses, supramolecular isomerism, and properties of the full series of four isomorphous/isomeric **nof**- and **srs**-$[M_2(bpz)]$ (M = Cu or Ag) frameworks. Although $[M_2(bpz)]$ had a tendency to crystallize as the less porous 8-fold interpenetrated **nof** structure, the more porous 4-fold interpenetrated **srs** one can be obtained as a pure phase by using a suitable template with a rapid solution mixing method. Comparison of C_2H_2 and CO_2 sorption behaviors of the isomorphous/isomeric materials showed that the more porous **srs** frameworks, with exposed metal centers, have higher affinity for C_2H_2. With the aid of the strong coordination bonds and multiple interpenetration, these materials have exceptionally high thermal and chemical stabilities. For example, **srs**-$[Cu_2(bpz)]$ can be stable up to 500 °C, and oxidation of the Cu(I) ions only occurs on the crystal surface after the sample is exposed in air for one month.[104]

The pyrazolate-bridged chains have been used as 1D SBUs in the construction of porous 3D frameworks. Long et al. constructed a highly porous framework, $[Co(bdp14)]$ (H_2bdp14 = 1,4-benzenedipyrazole), which can be viewed as an extension of $Co(pz)_2$ chains by the long, coplanar ligand (Figure 14). This material shows very unusual five-step N_2 sorption and broadly hysteretic H_2 sorption at 77 K, which were ascribed to the scissorlike breathing of the framework.[105] Similar porous frameworks composed of Zn(II) and/or 1,3-benzenedipyrazolate have also been prepared. The Zn(II) compounds have excellent stability in boiling solvents including water and remarkably less flexibility than $[Co(bdp14)]$,[106] which has been assigned to the stereochemical rigidity of the ZnN_4 tetrahedron.[107] The N_2 adsorption induced five-step phase transtion of $[Co(bdp14)]$ has been elucidated by a variety of spectroscopic techniques combined with in situ pressure-controlled PXRD and molecular simulations, which revealed the structural transformations on the ligand conformation and coordination sphere, as well as energetic details of each of the five transitions.[108]

The square-planar form of $M(pz)_2$ chains can also be connected to a 3D porous framework. Galli et al. reported the synthesis, ab initio PXRD structural determination, and sorption property of $[Ni(bdp14)]$, which showed remarkable framework flexibility similar to that of $[Co(bdp14)]$ and very good capability of removing harmful organic vapors even in the presence of humidity (Figure 15).[107]

Coordination similarity between pyrazolate and carboxylate has been used to construct classic framework types so far found in carboxylate-based PCPs. We found that the benzenedicarboxylate in the prototype $[Zn_4O(bdc)_3]$ (MOF-5, H_2bdc =1,4-benzenedicarboxylic acid) can be partially replaced by bpz^{2-} to construct an isoreticular framework, $[Zn_4O(bpz)_2(bdc)]$.[109] The Zn_4O cores are connected by bpz^{2-} to form square-grid layers, which are further pillared by bdc^{2-} into a **pcu** network with tetragonal symmetry (Figure 16). This material showed high porosity with a Langmuir surface area over 1900 $m^2\ g^{-1}$ and a pore volume of 0.58 $cm^3\ g^{-1}$, as well as guest-dependent luminescent properties. It was also shown that a hypothetical isoreticular framework, $[Zn_4O(bpz)_3]$, cannot be prepared albeit different reaction conditions had been tried.

Complete substitution of all dicarboxylates with bipyrazolates in the prototype $[Zn_4O(bdc)_3]$ was realized by Tonigold et al. using a long ligand, 1,4-bis[(3,5-dimethyl)-pyrazol-4-yl]benzene.[110] While the single crystals were grown by solvothermal reactions in several days, bulk synthesis of the phase-pure sample was achieved in a few minutes by microwave irradiation. The highly porous material was found to have a large BET surface area of ca. 1500 $m^2\ g^{-1}$, strong resistance toward moisture, and good catalytic performance for oxidation of cyclohexene. They found that Co(II), rather than Zn(II), is necessary for the construction of an oxo-centered, pyrazolate-capped tetranuclear $[M_4O(pz)_6]$.[98] This fact may be associated with the fact that the coordination

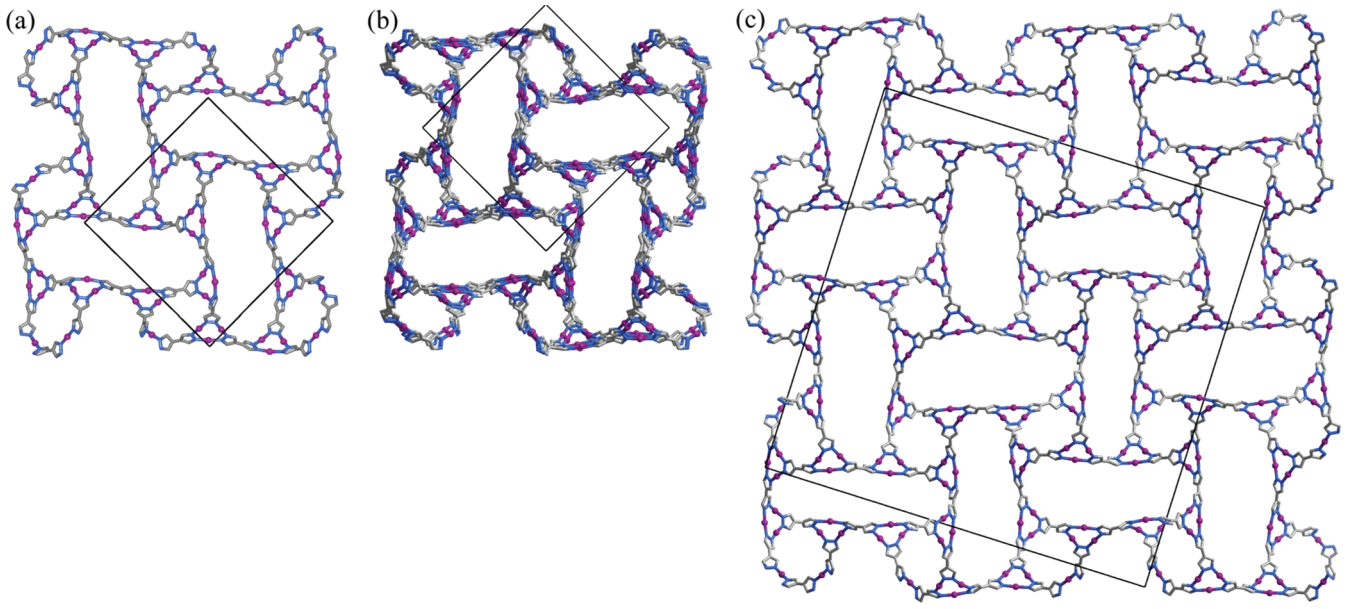

Figure 13. Parallel projections of the single-crystal structures of the guest-free state (a), one of the several intermediate states (b), and the saturated state of **srs**-[Ag_2(bpz)] along the crystallographic 4-fold axes (substituent groups and guest molecules are omitted for clarity).

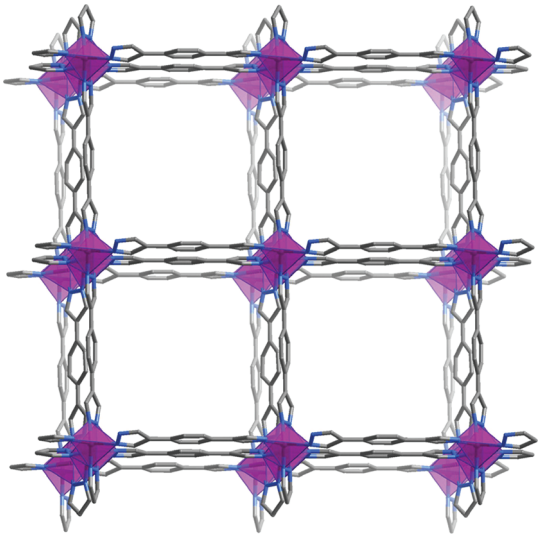

Figure 14. Structure of [Co(bdp14)] in its most expanded configuration.

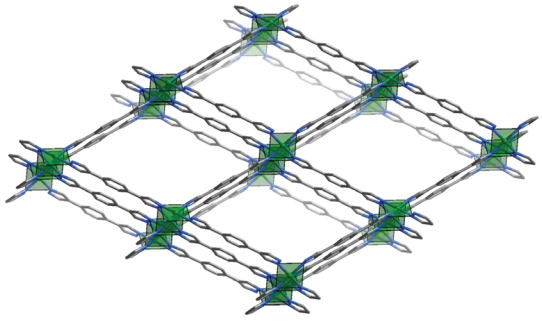

Figure 15. Structure of [Ni(bdp14)] in its contracted configuration.

sphere of the Co(II) ions is significantly distorted from the regular tetrahedra, which may be difficult for Zn(II) bearing four identical donors (Figure 17).[107]

With very long linear bipyrazolate ligands, Masciocchi et al. also constructed two highly porous frameworks, **fcc**-[$Ni_8(\mu_4\text{-}OH)_4(\mu_4\text{-}OH_2)_2(pbp)_6$] ($H_2$pdp = 4,4′-bis(1*H*-pyrazol-4-yl)-biphenyl) and **fcc**-[$Ni_8(\mu_4\text{-}OH)_4(\mu_4\text{-}OH_2)_2(tet)_6$] ($H_2$tet = 2,6-bis(1*H*-pyrazol-4-yl)pyrrolo[3,4-*f*]isoindole-1,3,5,7(2*H*,6*H*)-tetrone), with Langmuir surface areas over 1700 $m^2\ g^{-1}$ (Figure 18),[111] in which the octanuclear SBUs are structurally similar to the discrete complex $[Ni_8(\mu_4\text{-}OH)_6(pz)_{12}]^{2-}$.[99]

Owing to the simple coordination mode, small bridging angle, and short bridging distances of pyrazolates, their coordination polymers have quite limited structure types. Meanwhile, polypyrazolates adopt the advantages of the adjustable length and geometry of the donor groups, just as polycarboxylates and polypyridyls. Therefore, they are beneficial for the rational design of targeted coordination frameworks. While the coordination mode of pyrazolate is very similar to that of the bidentate bridging carboxylate groups, there are still differences between them. Actually, polypyrazolates can be utilized not only to replace polycarboxylates in a few cases but also to generate novel frameworks that have not been observed for polycarboxylates. More importantly, pyrazolates have very strong coordination ability (similar to that of imidazolates) to common transition-metal ions. Consequently, metal pyrazolate frameworks are generally more stable than metal carboxylate frameworks.

5. METAL 1,2,4-TRIAZOLATE FRAMEWORKS

Neutral triazole derivatives are exobidentate bridging ligands similar to either imidazolate or pyrazolate and have gained numerous attention for constructing coordination complexes with interesting functions such as spin crossover behavior.[15i,112] On the other hand, except for rare cases, simple 1,2,4-triazolates usually behave as 3-connected nodes with all three N-donors involved in coordination. Although 1,2,4-triazoles can be readily prepared by condensation reactions using hydrazine derivatives

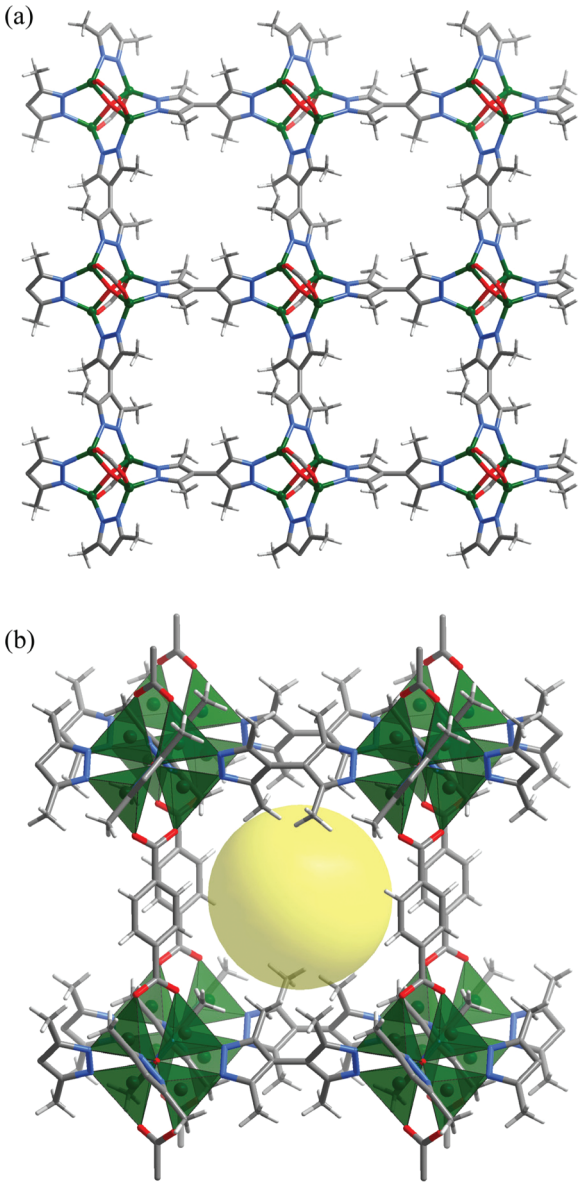

Figure 16. Framework structure of $[Zn_4O(bpz)_2(bdc)]$: (a) Zn_4O clusters bridged by bpz^{2-} to form a 2D layer (b) and further linked by bdc^{2-} to form a **pcu**-type 3D network.

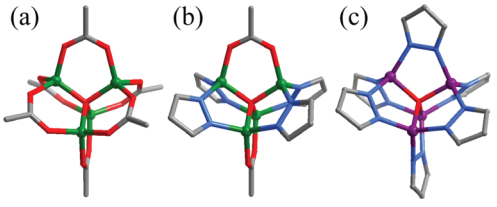

Figure 17. Comparison of $[M_4(\mu_4\text{-O})(RCOO/pz)_6]$ structures showing that the distortion of the tetrahedral coordination environment of the metal ion increases with more pyrazolate ligands because N−N < O···O in length: (a) $[Zn_4(\mu_4\text{-O})(RCOO)_6]$; (b) $[Zn_4(\mu_4\text{-O})(pz)_4(RCOO)_2]$; (c) $[Co_4(\mu_4\text{-O})(pz)_6]$.

as the main starting materials (Scheme 7),[113] metal 1,2,4-triazolate coordination polymers remained rarely explored before the discovery of a new solvothermal in situ ligand formation

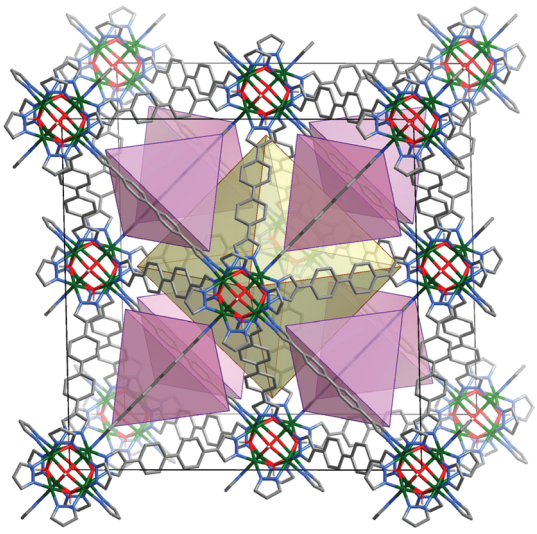

Figure 18. Structure of **fcc**-$[Ni_8(\mu_4\text{-OH})_4(\mu_4\text{-OH}_2)_2(pbp)_6]$.

Scheme 7. Typical Synthetic Methods for 1,2,4-Triazoles

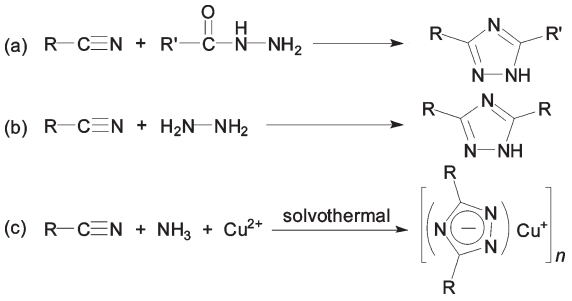

reaction, in which triazolates are generated by the oxidative cyclization between organonitriles and ammonia.[114]

5.1. Simple 3-Connected Networks

Binary univalent coinage-metal 1,2,4-triazolate is a straightforward metal−ligand system for the construction of 3-connected networks. Because the Y-shaped coordination geometry of 1,2,4-triazolate significantly deviates from a regular triangle, the resultant topologies are usually different from the commonly encountered topologies. Due to the low topology density of 3-connected nets, 3D univalent coinage-metal triazolates are relatively "porous" despite the fact that the node-to-node separations, ca. 3.1 Å for Cu(I) and 3.4 Å for Ag(I), are the shortest ones among all types of coordination polymers. See Chart 4 for the structures of substituted 1,2,4-triazolates.

Similar to the pyrazolates, 1,2,4-triazolates also have a preference of forming $M_2(tz)_2$ planar dinuclear structures, which gives rise to four-membered rings in the topologies of metal 1,2,4-triazolate frameworks. The simplest univalent coinage-metal 1,2,4-triazolates, [Cu(tz)] and [Ag(tz)], are isostructural 2D layers with the **sql-a** topology, which is decorated from the common **sql** net by replacing the square-planar node with a square (a group of four Y-shaped nodes). The known types of topologies based on square-planar nodes (typical ones include 2D **sql**, 3D **lvt**, and 3D **nbo**) are much rarer than those based on tetrahedral ones. Molecular materials possessing the 3D **lvt** and **nbo** nets are very rare because the less porous 2D **sql** structures

dx.doi.org/10.1021/cr200139g |*Chem. Rev.* 2012, 112, 1001–1033

Chart 4. Substituted 1,2,4-Triazolates

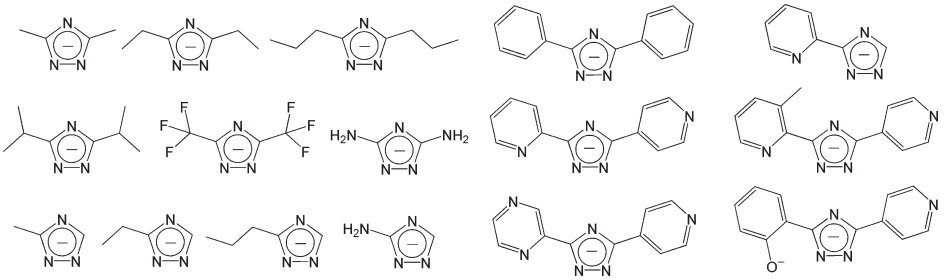

are more stable. Nevertheless, 3D **lvt** and **nbo** structures can also be rationally constructed if one can control the dihedral angles between adjacent square-planar nodes.[115] The short bridging distance of 1,2,4-triazolate facilitates control over the dihedral angle between adjacent $M_2(tz)_2$ SBUs. Small side groups at the 3,5-positions of the ligand are enough to introduce steric hindrance between adjacent $M_2(tz)_2$ SBUs, leading to the initial discovery of the 2-fold interpenetrated **lvt-a**-[Cu(dmtz)] (H_2dmtz = 3,5-dimethyl-1,2,4-triazole) and noninterpenetrated **nbo-a**-[Cu(dptz)] (H_2dptz = 3,5-dipropyl-1,2,4-triazole). Two adjacent $M_2(tz)_2$ SBUs are parallel, slanting, or perpendicular to each other in **sql-a**-[Cu(tz)], **lvt-a**-[Cu(dmtz)], and **nbo-a**-[Cu(dptz)], respectively (Figure 19).[114] Later, Yao et al. also reported a 2-fold interpenetrated **lvt-a** structure for [Cu(datz)] (H_2datz = 3,5-diamino-1,2,4-triazole),[116] in which the amino group is similar to a methyl group in size.

While these porous metal triazolate scaffolds are filled by 2-fold interpenetration and/or side groups, [Cu(detz)] (H_2detz = 3,5-diethyl-1,2,4-triazole) can be expected to have a truly porous structure because ethyl is longer than methyl to prevent 2-fold interpenetration of the **lvt-a** net and is shorter than propyl to save some space inside the **nbo-a** framework. The hypothetical structure was realized as **nbo-a**-[Cu(detz)] (MAF-2), which was first synthesized as a cubic phase by solvothermal in situ metal/ligand reaction.[117]

It should be noted that other 3-connected networks without $M_2(tz)_2$ SBUs are also possible. For example, though **lvt-a**-[Cu(dmtz)] preferentially crystallizes at most conditions, two structural isomers possessing two different 3D 3-connected topologies (uninodal **lig** and binodal 6.10^2) were also discovered by introduction of coordination buffering additives in the solvothermal reaction systems. In contrast, only the **lig** topology has been reported for [Ag(dmtz)] so far.[118]

The crystal structure of MAF-2 suggests the flexible ethyl groups may control the passage between the large cavities via rotation along the C−C single bond, which may lead to unique dynamic sorption behaviors (Scheme 8).[119] However, the low yield and purity, as well as the crystallographic symmetry-imposed disorder of the ethyl groups, prevent further characterization and deduction.[117] Alternatively, the trigonal phase of MAF-2 was synthesized in high yield by a direct reaction between $[Cu(NH_3)_2]OH$ and Hdetz in MeOH at room temperature.[119] The trigonal and cubic phases represent contracted and expanded forms of the framework with the dihedral angle between adjacent $Cu_2(tz)_2$ SBUs of 79° and 90°, respectively, which can be reversibly converted by uptake/release of benzene. More importantly, the ethyl groups are completely ordered and block the apertures in the trigonal phase. Sorption experiments using identical equilibrium criteria showed that the material could

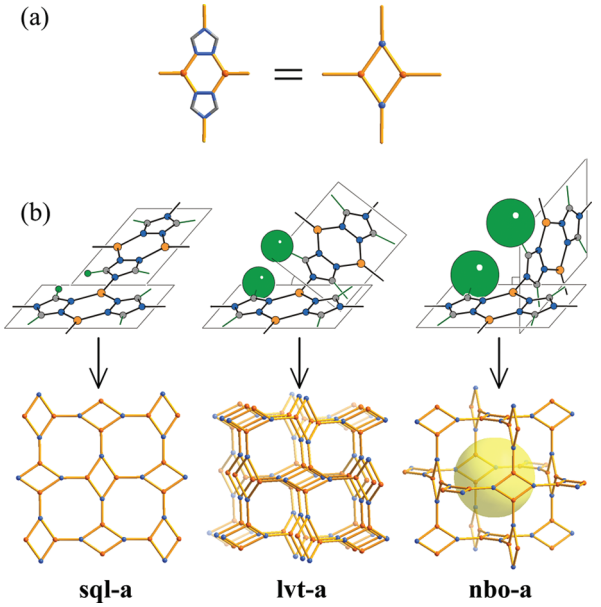

Figure 19. Topologies of copper(I) 1,2,4-triazolate frameworks can be controlled by the sizes of the ligand side groups: (a) topology simplification from a dinuclear $Cu_2(tz)_2$ unit to four 3-connected nodes or a square-planar node; (b) the size of the side group controls the dihedral angle between adjacent square-planar nodes, giving 2D and 3D topologies.

adsorb N_2 at 195 K rather than 77 K, which cannot be explained by the difference in diffusion speeds because there is no sorption hysteresis observed (Figure 20).

The single-crystal structure of the guest-free and N_2-loaded phases of MAF-2 measured at 90 K confirmed that the host framework has no change neither at low temperature nor after guest adsorption. Therefore, guest diffusion must be allowed (adjusted) by momentary (thermal) motions of the ethyl groups, whose magnitude is controlled by the temperature. This kind of framework flexibility (only one equilibrium framework structure at different sorption states) has been denoted as *kinetically controlled flexibility* (KCF) because the structure change is controlled by kinetic factors rather than the existence of multiple thermodynamically stable states (Scheme 9). For comparison, common types of framework flexibility (at least two different equilibrium framework structures at different adsorption states) is termed *thermodynamically controlled flexibility* (TCF).

MAF-2 also shows TCF, in which the framework contracts, expands, or distorts upon adsorption of different solvent molecules including MeOH, EtOH, MeCN, and benzene. However, it cannot adsorb larger molecules such as cyclohexane, showing

Scheme 8. Temporary Gate-Opening Mechanism for Guest Adsorption[a]

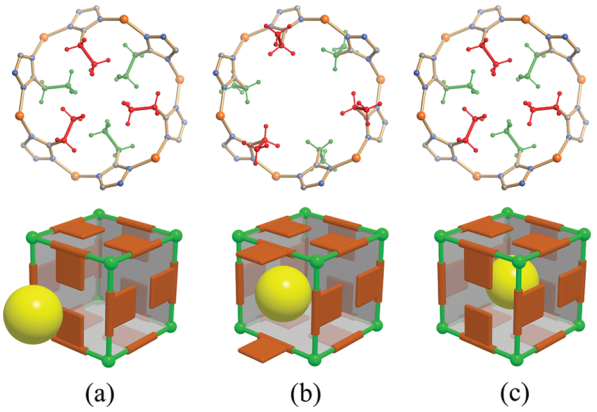

[a] Key: (a) gate closed before adsorption; (b) gate open during guest diffusion; (c) gate closed again after adsorption.[119]

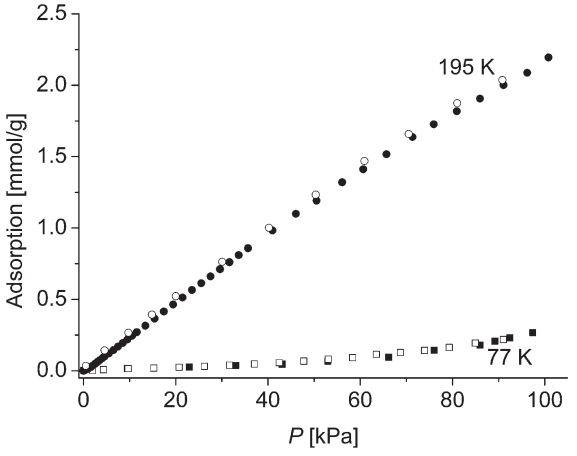

Figure 20. N_2 sorption isotherms of MAF-2 at 77 and 195 K (solid and open symbols denote adsorption and desorption, respectively).

very high benzene/cyclohexane selectivity. The hydrophobic, *kinetically controlled* gates of MAF-2 also facilitate adsorption of relatively large organic molecules over smaller H_2O molecules even at very high humidity, which can be hardly realized by common hydrophobic adsorbents due to capillary condensation or by size-selective adsorbents because H_2O molecules are smaller than organic molecules (Figure 21). Such hydrophobic character may be responsible for its ultrahigh chemical stability in air, despite the fact that the porous framework is composed of exposed Cu(I) ions.

The unique framework flexibility of MAF-2 gives rise to S-shaped isotherms for C_2H_2 and CO_2, which results in not only a high C_2H_2/CO_2 uptake ratio (3.7) at room temperature and 1 atm (Figure 22) but also a very high usable storage capacity (USC) for C_2H_2 (Figure 23),[120] because the compression pressure for pure C_2H_2 must be lower than 2 atm (in practice, 1.5 atm for safety).[121] While gas storage performances of PCPs reported in most publications are evaluated just simply by the uptake at a certain given temperature and pressure, the USC considers a full charge−discharge cycle between two given temperature/pressure sets, which represents the practical performance of an

Scheme 9. Typical Energy Profiles for Different Types/Degrees of Framework Flexibility[a]

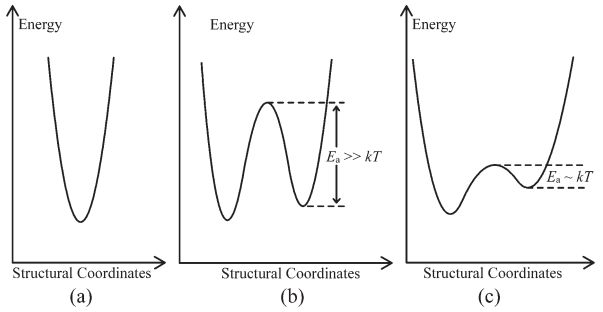

[a] Key: (a) A rigid framework possesses only one deep potential well. (b) A framework with thermodynamically controlled flexibility possesses two potential wells separated by an energy barrier much higher than the thermal energy. (c) A framework with kinetically controlled flexibility possesses two potential wells separated by an energy barrier comparable to the thermal energy.

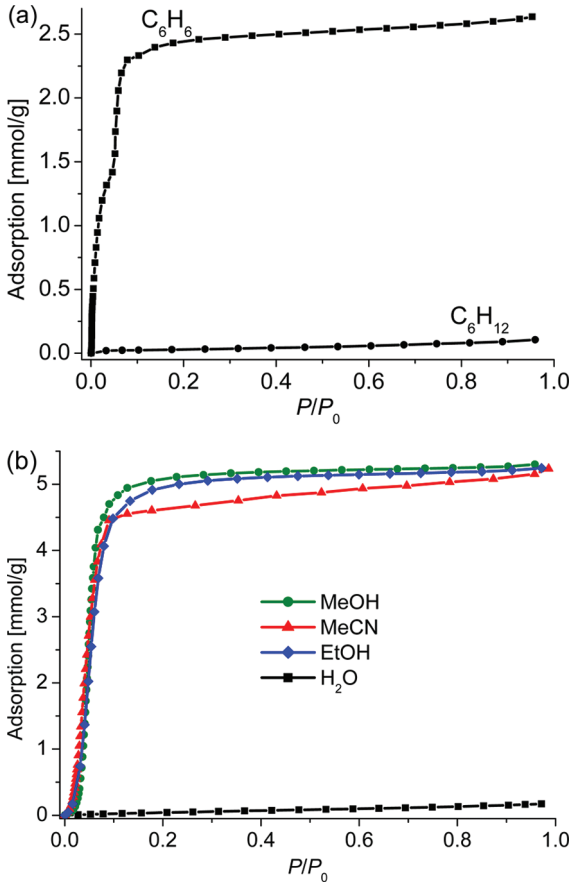

Figure 21. Size-selective adsorption of benzene over cyclohexane (a) and anti-size-selective sorption of organic molecules over H_2O (b) of MAF-2.

adsorbent. Actually, for a gas storage porous material, the USC should be considered to be the uptake difference between a lower limit pressure (1 atm or higher for autodischarging and preventing contamination from the atmospheric environment) and a higher feasible pressure (depending on the strength of the container

dx.doi.org/10.1021/cr200139g |*Chem. Rev.* 2012, 112, 1001–1033

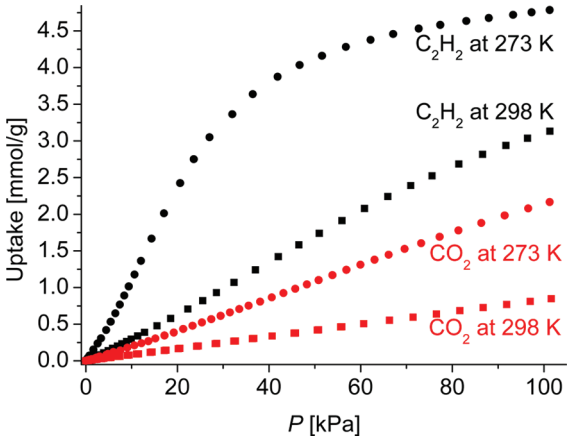

Figure 22. C_2H_2 and CO_2 adsorption isotherms of MAF-2.

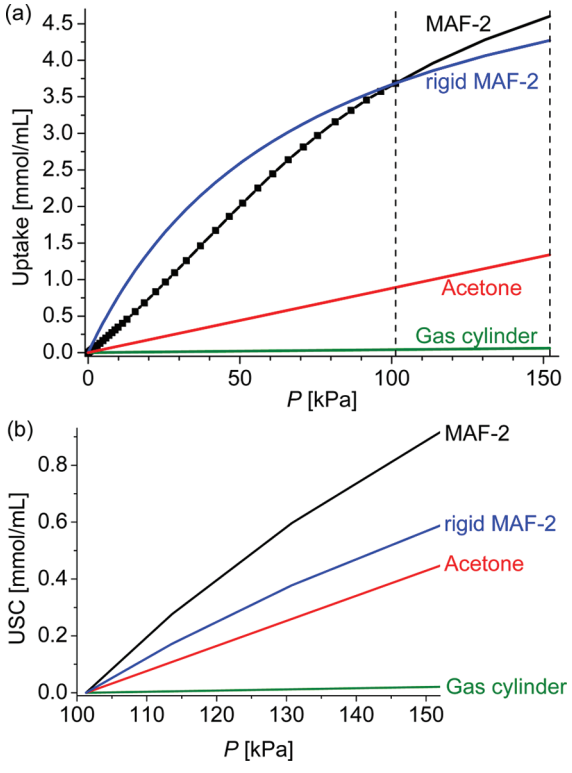

Figure 23. Comparison of the volumetric uptake (a) and usable storage capacity (b) of C_2H_2 for MAF-2, rigid MAF-2 (a hypothetical rigid microporous adsorbent with the same pore volume and C_2H_2 uptake at 1 atm as MAF-2), and other typical materials at 298 K.

and gas properties). As shown in Figure 23, the S-shaped C_2H_2 isotherm renders a higher USC than a normal Langmuir isotherm. The crystal structures of C_2H_2- and CO_2-loaded phases of MAF-2 were determined by the laboratory X-ray single-crystal diffraction technique at ordinary temperatures, giving very accurate structures of the C_2H_2 and CO_2 molecules trapped in the framework.

The steric hindrance effect may be adjusted more precisely using only one substituent group. The copper(I) 3-amino-1,2,4-triazolate, [Cu(atz)], also adopts the 2D **sql-a** topology as for [Cu(tz)], because a single amino group is not large enough to distort the adjacent dinuclear SBUs for a 3D **lvt-a** or **nbo-a**

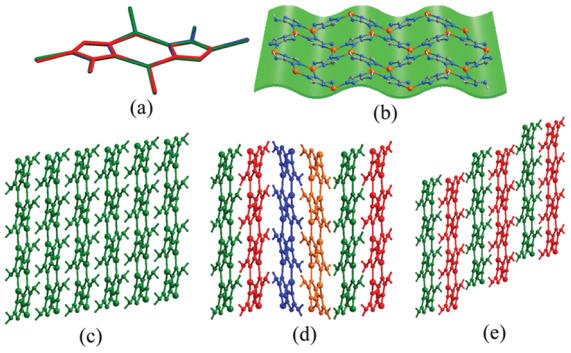

Figure 24. Identical local coordination geometries (a), undulated **sql-a** layer (b), and packing fashions of α (c), β (d), and γ (e) packing polymorphs of [Cu(atz)].

structure. However, the amino group already destroys the planarity of the 2D layer, which may be crucial for the observation of three different genuine packing polymorphs, which have essentially identical local coordination geometries and 2D expanded structures (Figure 24).[122]

Adjusting the alkyl length resulted in four silver(I) 3-alkyl-1,2,4-triazolates, **utp**-[Ag(mtz)], **utp**-[Ag(etz)], sqc5603-[Ag(etz)], and sqc5603-[Ag(ptz)], with 3D 3-connected topologies not observed in other MAFs. The two **utp** structures with methyl and ethyl groups have the same topology but different coordination structures. The isostructural sqc5603 networks are porous for the ethyl derivative, because the longer propyl groups occupy too much void space (Figure 25). The porous material sqc5603-[Ag(etz)] displays near-white photoluminescence, which changes in response with solvents such as H_2O, CH_2Cl_2, and MeCN.[19]

Some binary univalent coinage-metal 1,2,4-triazolates cannot be straightforwardly simplified as 3-connected topologies, because the metal ions and/or the ligand show "abnormal" coordination modes, for example, when the substituent groups are too bulky[117] or have coordination ability competing with that of the triazolate ring (see below). Using silver(I) 3,5-bis(trifluoromethyl)-1,2,4-triazolate, Omary et al. constructed a porous framework with a large porosity and fluoro-lined pore surface.[123] Interestingly, it undergoes remarkable breathing at different N_2 sorption states. The sequential N_2 sorption sites were determined by single-crystal structures in N_2 flow at different temperatures.[124] In the crystal structure of this material (Figure 26), there are not only normal trigonal-planar metal ions and μ_3-η^1,η^1,η^1 ligands but also seesaw (4-coordination) and μ_5-η^2,η^2,η^1 ones, respectively, probably because the highly acidic perfluorinated triazolate behaves more like an ionic species. The coordination behavior of Ag(I) is also more versatile than that of Cu(I). Another case of similar coordination modes was observed in [Ag(dphtz)] (Hdphtz = 3,5-diphenyl-1,2,4-triazole) among a series of binary silver(I) 3,5-disubstituted 1,2,4-triazolate frameworks synthesized by Yang et al. with the aid of aqueous ammonia buffering.[125]

5.2. Quasi-Imidazolates

It is difficult to simultaneously fulfill the 6- and 3-coordination for the divalent metal ions and 1,2,4-triazolate ligands, respectively, in the binary metal triazolate framework $[M(tz)_2]$. Alternatively, one of the three N-donors may remain uncoordinated, and the metal ion adopts 4-coordination. More practically, additional anions and/or ligands may be incorporated to furnish the charge and coordination number requirement.

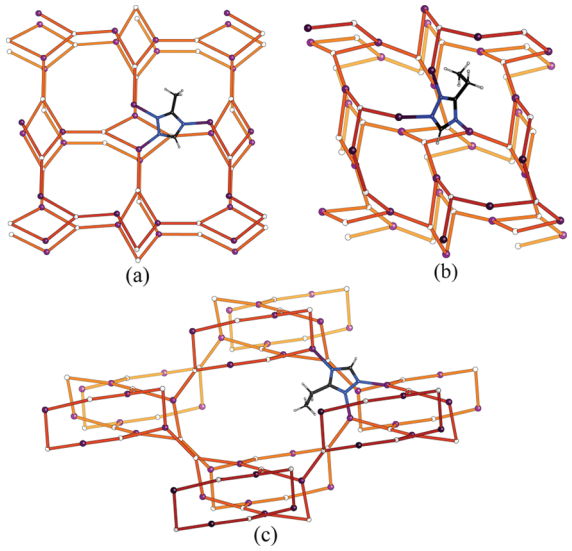

Figure 25. Framework topologies of **utp**-[Ag(mtz)] (a), **utp**-[Ag(etz)] (b), and sqc5603-[Ag(etz)] (c).

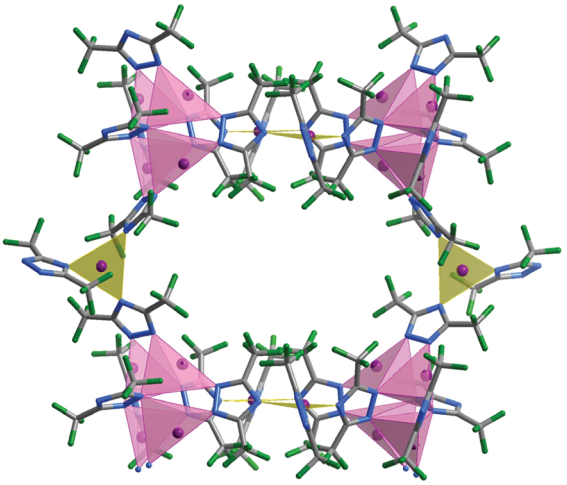

Figure 26. Portion of the framework structure of silver(I) 3,5-bis-(trifluoromethyl)-1,2,4-triazolate.

A few binary bivalent metal 1,2,4-triazolate frameworks have been reported so far. The simple zinc(II) 1,2,4-triazolate $[Zn(tz)_2]$ has a 2-fold interpenetrated **dia** network structure,[126] which is isostructural with $[Cd(im)_2]$ and $[Hg(im)_2]$.[76a] It should be noted that the 2-fold interpenetrated **dia**-$[Zn(im)_2]$ has not been reported albeit many isomers are known (see section 3.2). This fact may be attributed to the very small size difference between the N atom and C−H moiety on the azolate rings.

Using 3-methyl-1,2,4-triazolate (mtz^-) to replace 2-methylimidazolate, we recently constructed the SOD-$[Zn(mtz)_2]$ (MAF-7) that is isostructural with MAF-4 (Scheme 10). The isoelectronic C−H to N substitution increases the pore size or volume negligibly, but significantly enhances the sorption affinity for various guest molecules, especially those with higher polarity. While H_2 sorption is only slightly improved, the uncoordinated N-donors double the C_2H_2 and CO_2 adsorption amounts at room temperature and 1 atm. More dramatically, the H_2O adsorption ability of MAF-7 is more than 100 times higher than that of the highly hydrophobic

Scheme 10. Construction Principles of Inorganic Zeolites and Metal−Organic Zeolites

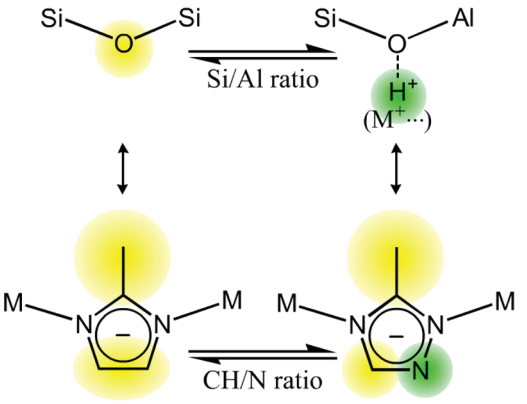

MAF-4. The stepped H_2O sorption isotherm of MAF-7, with steep uptake change occurring in moderate humidities, indicates potential application in adsorptive heating/cooling applications. Interestingly, solid solution frameworks $[Zn(mtz)_{2-x}(mim)_{2x}]$ (MAF-47-x, $0 < x < 1$) can also be facilely prepared with different Hmtz/Hmim feeding molar ratios, which allow fine adjustment of the step pressure over a wide range, being beneficial for utilization of different types of low-grade heats (Figure 27).[48]

5.3. With Coordinative Substituents

Pyridyl-substituted 1,2,4-triazolates might be regarded as size-expanded azolates (Scheme 11), but the structure-building principle is changed. The position of the pyridyl donor has a crucial role. Particularly, a 2-pyridyl group can cooperate with a triazolate N atom to function as a typical chelating group similar to 2,2′-bipyridines, which is the predominant bonding site during self-assembly with metal ions. Therefore, the coordination mode of 3,5-bis(2-pyridyl)-1,2,4-triazolate ($dpt22^-$) is predictable because there are two bidentate chelating sites, which is suitable for formation of neutral binary complexes with univalent tetrahedral metals such as Cu(I). The predictable local coordination geometry in [Cu(dpt22)] and conformation flexibility of $dpt22^-$ have been utilized for a systematic enumeration of the first full series of polygon, zigzag chain, helical chain, and additional zipper-like double chain genuine supramolecular isomers (Figure 28).[127] Symmetric substitution of 1,2,4-triazolate with two 3- or 4-pyridyl groups results in exopentadentate ligands with five potential independent monodentate sites, whose coordination modes can be hardly predicted.[128]

The coordination modes of asymmetric dipyridyl-1,2,4-triazolates containing one 2-pyridyl group and one 3-/4-pyridyl group are also somewhat predictable. For example, 2,4-bis(2-pyridyl)-1,2,4-triazolate ($dpt24^-$) would exhibit a bidentate chelating site and then three monodentate sites. When a divalent metal ion is used, the metal ion should be chelated by two $dpt24^-$ ligands to give a neutral $M(dpt24)_2$ unit. Because a common divalent metal ion prefers an octahedral coordination mode, the two remaining sites can be occupied by auxiliary terminal ligands to give a discrete mononuclear complex or by the N-donors from two other $M(dpt24)_2$ units to give a 4-connected coordination polymer, even when the metal ion is highly oxophilic. Due to steric hindrance effects, the pyridyl N-donor would have a priority in coordination over the remaining azolate N-donors, which is useful for the construction of open frameworks based on

dx.doi.org/10.1021/cr200139g |*Chem. Rev.* 2012, 112, 1001–1033

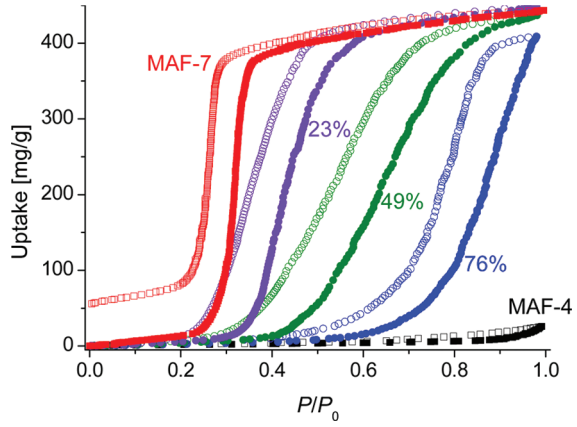

Figure 27. Water sorption isotherms of MAF-4, MAF-7, and the solid solution frameworks $[Zn(mtz)_{2-x}(mim)_{2x}]$ with different molar ratios of mim^-.

Scheme 11. Comparison of the Coordination Behaviors of Dipyridyl-1,2,4-triazolate Isomers[a]

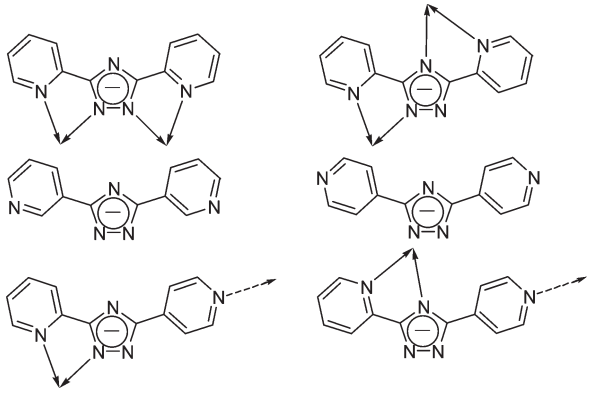

[a] The most preferential chelating and secondary coordination sites are highlighted by solid and dashed dative bonds, respectively.

4-connected nodes such as **sql** and **nbo** nets. The remaining uncoordinated N-donors can be utilized to interact with guest molecules, if they are exposed on the pore surface.

Interestingly, $[Mn(dpt24)_2]$ (MAF-24) crystallizes as three structural isomers (MAF-24α, MAF-24β, and MAF-24γ), although the coordination networks possess the same **sql** layer topology. In MAF-24α, MAF-24β, and MAF-24γ, Mn(II) centers adopt *all-trans-*, *all-cis-*, and *half-trans-* plus *half-cis-*configurations. The 2D layers also pack differently in the three isomers, giving distinct porous properties. Two mononuclear complexes, *cis*-$[Mn(dpt24)_2(H_2O)_2]$ and *trans*-$[Mn(dpt24)_2(MeOH)_2]$, were also isolated from different reaction solvents as the intermediates in forming **sql**-$[Mn(dpt24)_2]$ isomers (Figure 29).[129] Similar layer structures containing other metal ions were also reported later. An isostructural Co(II) analogue of α-$[Mn(dpt24)_2]$ was reported by Wang et al.[130] Two isomeric 2D frameworks, $[Fe(dpt24)_2]$ isostructural with α- and β-$[Mn(dpt24)_2]$, were also synthesized by Tong et al., who also investigated the influence of Co(II) doping on spin crossover magnetic properties on the α-phase.[131]

A series of porous 2-fold interpenetrated **nbo** frameworks $[M(L)_2]$ (M = divalent metal ions, L = $dpt24^-$ analogues) have been reported, most of which are isostructural (Figure 30).[129−132] Using isostructural $[Co(dpt24)_2]$ (MAF-25) and $[Co(mdpt24)_2]$ (MAF-26; Hmdpt24 = 3-(3-methyl-2-pyridyl)-5-(4-pyridyl)-1,2,4-triazole), in which the former has uncoordinated triazolate N-donors partially exposed on the pore surface and the additional methyl groups cover the N-donors of the latter, we demonstrated that even partially exposed uncoordinated N-donors can also effectively enhance the gas binding affinity. While the crystal structure of the gas-loaded phase could not be obtained,[133] the primary CO_2 adsorption sites were confirmed by GCMC simulations (Figure 31).[134] Interestingly, $[Co(dpt24)_2]$[130] and $[Fe(dpt24)_2]$[131a] can both crystallize as isomeric contracted and expanded forms, depending on the solvent used in the syntheses. Tong et al. also reported the noninterpenetrated **nbo** network $[Fe(dpt24)_2]$ synthesized by solvothermal reaction using dioxane as the solvent.[131a]

Moreover, these complexes show interesting crystal-to-crystal transformations (Figure 32). We reported reversible structural transformation on coordination configurations between the mononuclear complexes *cis*-$[Mn(dpt24)_2(H_2O)_2]$ and *trans*-$[Mn(dpt24)_2(MeOH)_2]$.[129] Li et al. reported reversible

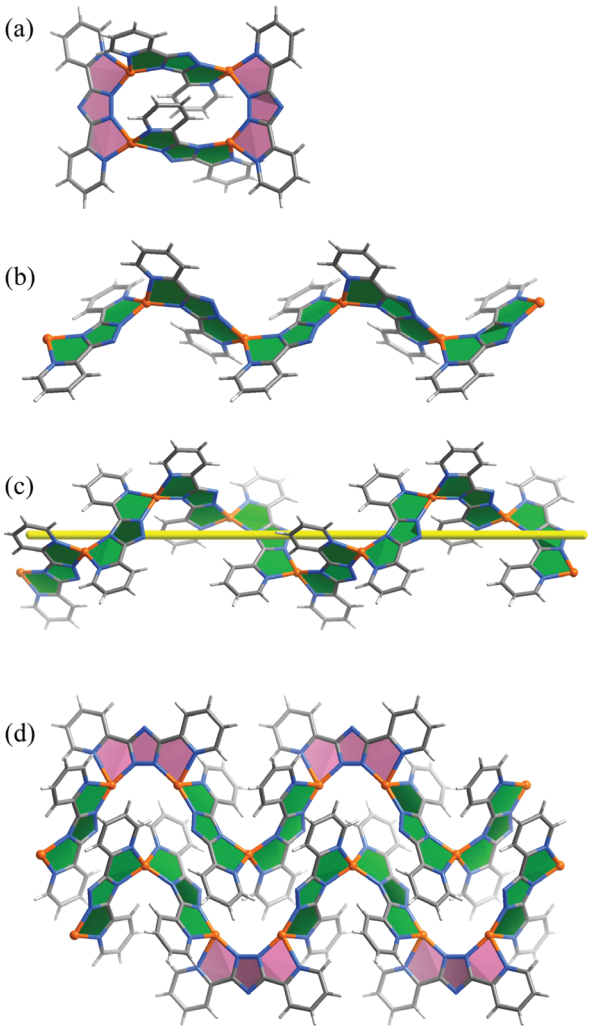

Figure 28. Four-membered ring (a), zigzag chain (b), 4_1-helical chain (c), and zipperlike double chain (d) supramolecular isomers of [Cu(dpt22)] (*cis-* and *trans*-bridging ligands are highlighted in different colors).

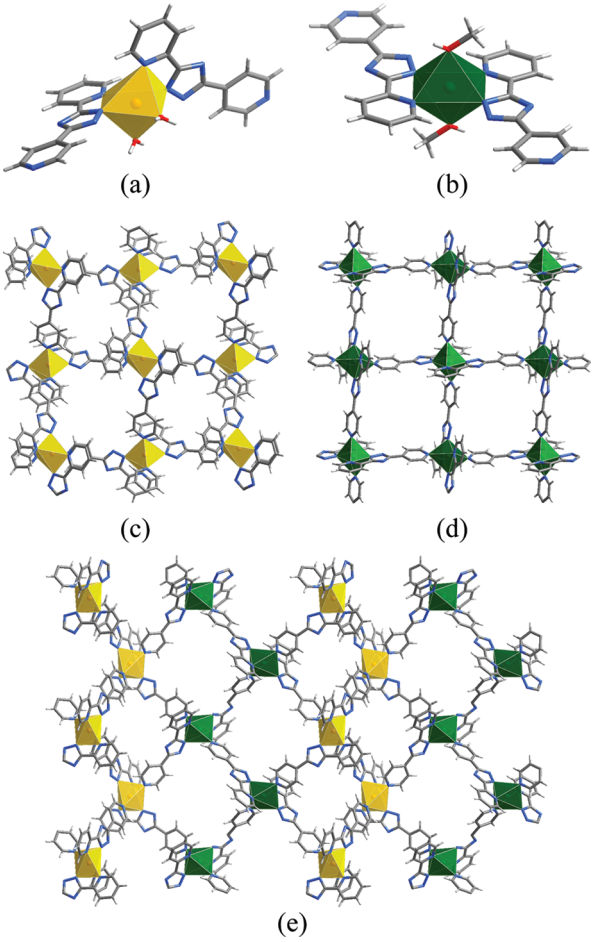

Figure 29. Stereochemical diversity of mononuclear complexes and isomeric networks composed of $Mn(dpt24)_2$ (*cis*- and *trans*-geometries of the Mn(II) centers are highlighted as yellow and green polyhedra, respectively).

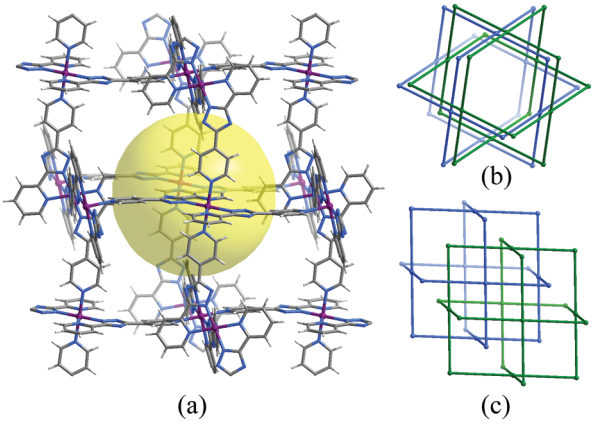

Figure 30. Portion of **nbo**-$[M(L)_2]$ (a) and the 2-fold interpenetration topology viewed along the 3-fold (b) and 4-fold (c) axes.

transformations between a zero-dimensional (0D) mononuclear complex, $[Cu(pzpt)_2(H_2O)]$ (Hpzpt = 3-(pyridin-4-yl)-5-(pyrazin-2-yl)-1,2,4-triazole), and a 3D porous framework, $[Cu(pzpt)_2]$, with 2-fold interpenetrated **nbo** topology.[132] Tong et al. reported irreversible isomerization from β-$[Fe(dpt24)_2]$ to α-$[Fe(dpt24)_2]$, corresponding to a *cis*- to *trans*-configuration change.[131b]

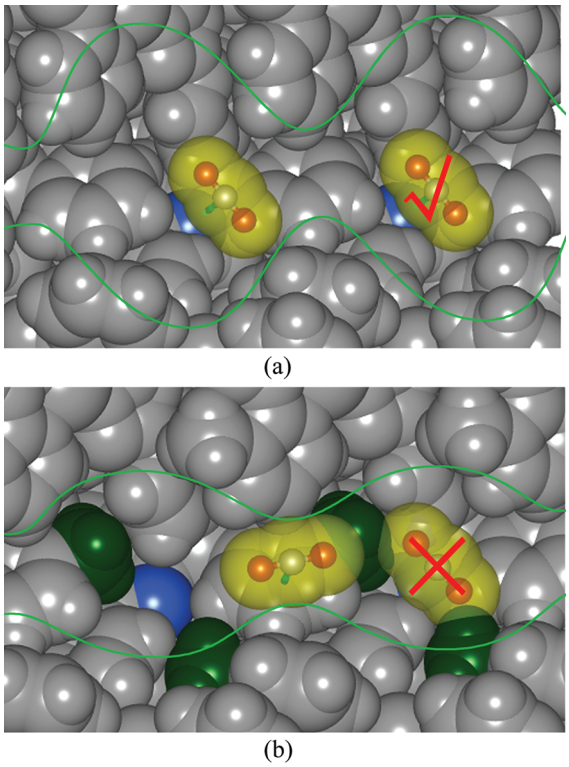

Figure 31. Role of partially exposed uncoordinated N-donors (blue; methyl groups are highlighted in green) and the pore size (the green line represents the shape of the 1D channels) in determining the primary CO_2 adsorption sites in MAF-25 (a) and MAF-26 (b).

A few MAFs composed of monopyridyl-substituted 1,2,4-triazolate ligands have also been reported.[135] Du et al. reported a 2-fold interpenetrating **lig** network, $[Zn(dptt)]\cdot 2H_2O$ (H_2dptt = bis(5-(4-pyridyl)-1,2,4-triazol-3-yl) disulfide), in which the bis-triazolate ligand was generated by in situ S−S coupling of 5-(4-pyridyl)-1,2,4-triazole-3-thiol (Hptt) in solvothermal conditions. Each Zn(II) ion is coordinated by two pyridyl groups from two ligands and two triazolate N-donors from two triazolate rings of one ligand. Using conventional room temperature synthesis without in situ ligand reaction, $[Zn(ptt)_2]\cdot 4.5H_2O$ was obtained, in which only the thiolate and pyridyl groups are involved in coordination with Zn(II) (Scheme 12).[136]

5.4. With Secondary Counterions and/or Ligands

The coordination geometries of the metal ions and triazolate ligands become more diverse when additional components are introduced into the metal−ligand system, either as counterions or as ligands. Raptis et al. showed that different anions can be incorporated into the 3D porous cationic silver(I) triazolate framework $[Ag_4(dphtz)_3]^+$, in which Ag(I) ions adopt linear and trigonal coordination geometries and the ligands are all μ_3-*N*,*N*′,*N*″.[137]

We have reported a flexible porous framework, $[Ag_6Cl(atz)_4]$-$OH\cdot xH_2O$, composed of 5-fold interpenetrating cationic **dia-f**-$[Ag_3(atz)_2]$ coordination networks, in which Ag(I) ions and triazolate ligands are 2- and 3-coordinated, respectively.[30b] Chloride anions are embedded between the four-membered rings of adjacent **dia-f**-$[Ag_3(atz)_2]$ networks, while the hydroxide and H_2O reside in the 1D channels. Depending on the amount of loaded guest H_2O molecules, the interpenetration number of the

dx.doi.org/10.1021/cr200139g |*Chem. Rev.* 2012, 112, 1001–1033

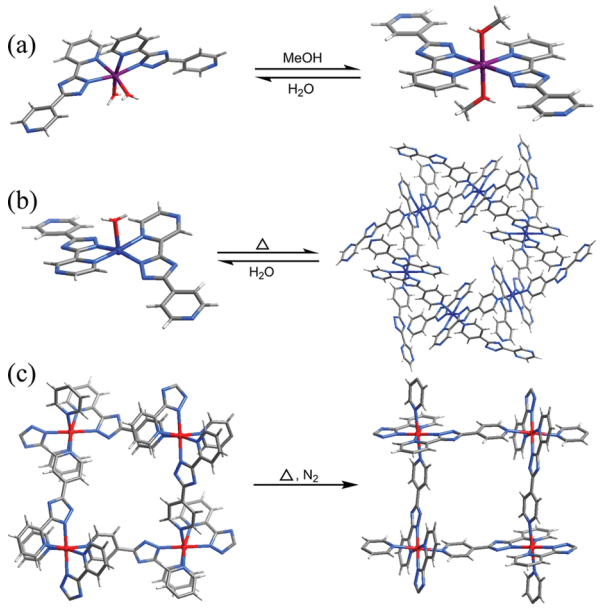

Figure 32. Solid-state transformations of $[M(dpt24)_2(L)_x]$ ($x = 0, 1, 2$) species: (a) reversible *cis*−*trans* coordination geometry transformation of 0D complexes mediated by solvent exchange; (b) reversible 0D to 3D transformation mediated by removal and addition of H_2O; (c) irreversible transformation of the coordination geometry from *cis* to *trans* in 2D frameworks.

Scheme 12. Temperature-Dependent Self-Assembly of 5-(4-Pyridyl)-1,2,4-triazole-3-thiol with Metal Ions

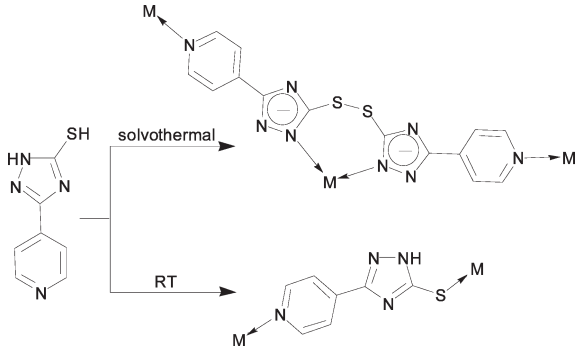

silver(I) triazolate framework can be reversibly switched between 5 and 6 in a single-crystal to single-crystal manner. A similar 2-fold interpenetrated **dia-f** structure was observed in $[Cu_6Br(tz)_4]Cu_4Br_4(OH)$ as reported by Zubieta et al.[138] It can be seen that the interpenetration number of **dia-f** is determined by the distortion degree of the networks (Figure 33).

With polyoxometalates as counteranions, Lu et al. have constructed a series of cationic coinage-metal triazolate frameworks showing structure types ranging from discrete clusters to 3D networks[139] and even an interesting 2-fold interpenetrated **pcu** type polycatenation structure composed of discrete polyhedral nanocages (Figure 34).[140]

By introduction of a series of simple inorganic anions as secondary ligands and/or counteranions, Zubieta et al. have constructed a great variety of M/triazolate/X ternary metal triazolate frameworks (M = Cu(I,II), Zn(II), and Cd(II); X = F^-, Cl^-, Br^-, I^-, OH^-, SO_4^{2-}, and NO_3^-), in which the metal ions show various types of common coordination geometries.[126,138] The most remarkable structures may be $[Cu^{II}_3(OH)_3(tz)_3(H_2O)_4]\cdot 4.5H_2O$ and $[Cu^{II}_3(\mu_3\text{-}OH)(\mu_3\text{-}tz)_3][Cu^{I}Br_2]_2$,[141] in which $Cu_3(\mu_3\text{-}OH)(\mu\text{-}tz)_3$ triangles, bridged by triazolate in the pyrazolate mode, interconnect with each other through the N^4-donors into a uninodal 6-connected **hxg** topology. Charge balance is fulfilled by hydroxide anions directly coordinated on the framework or by interpenetration of two anionic $[CuBr_2]^-$ networks with **dia-a** topology (Figure 35). Similar compounds with slightly different compositions were also reported by other groups.[142]

A series of isostructural porous frameworks [Zn(Rtz)F] (Rtz = triazolate derivatives with different substituents) with different pore sizes/properties have gained considerable interest. The zinc(II) triazolate coordination network in these materials defines an **etb** topology, meaning that each Zn(II) coordinates with three different triazolate ligands and vice versa. The μ-F^- anions furnish charge balance and trigonal-bipyramidal coordination geometry of the Zn(II) ions (Figure 36a). zur Loye et al. first obtained **etb**-[Zn(atz)F] and showed its high thermal stability (380 °C) and application for preparation of ZnO nanorods.[143] They further synthesized isostructural frameworks **etb**-[Zn(tz)F] and **etb**-[Zn(datz)F] with expanded and contracted channel sizes, respectively, both of which have high thermal stability up to 335 °C.[144] Using 3,5-dimethyl-1,2,4-triazolate, we also synthesized isostructural **etb**-[Zn(dmtz)F] with a hydrophobic pore surface and high thermal stability (400 °C), as well as a nonporous isomer, **lig**-[Zn(dmtz)F].[145] Gas adsorption isotherms have been reported for **etb**-[Zn(tz)F][126] and **etb**-[Zn(dmtz)F],[145] which showed less N_2 uptake than expected, probably due to the very small channel sizes. The combination of a larger metal ion and a halide gives a similar framework structure, **eta**-[Cd(tz)Cl], with large, chiral channels (Figure 36b).[146]

Framework diversity will be hugely extended when other ligands such as carboxylates are used as coligands, most of which are out of the scope of this review. Nevertheless, structural robustness of MAF motifs can be seen in a few examples. For instance, [Zn(dmtz)(HCOO)] crystallizes as two isomers depending on the reaction conditions. The cationic Zn(dmtz) framework mimics those of univalent coinage-metal triazolates, showing **sql-a** and **nbo-a** topologies as each Zn(II) is coordinated by three dmtz goups and vice versa. The formate anion acting as a terminal ligand furnishes the tetrahedral coordination geometry of Zn(II) (Figure 37).[145]

Actually, the **sql-a** metal triazolate layers have been observed extensively in the literature. A rich family of pillared-layer structures have been constructed by the **sql-a**-$[Zn_2(atz)_2]^{2+}$ or **sql-a**-$[Zn_2(tz)_2]^{2+}$ cationic layers pillared by different dicarboxylates and even carbonate,[147] some of which have shown interesting porous properties (Figure 38).[147b,148] Many single layers of **sql-a**-$[Zn_2(atz)_2]^{2+}$ and **sql-a**-$[Zn_2(tz)_2]^{2+}$ terminated by monoanions such as Cl^-, Br^-, SCN^-, NO_3^-, acetate, and 4-chlorobenzoate have also been isolated.[126,149] Some similar **sql-a** networks based on "expanded triazolates" are also known.[150]

Bearing one more N-donor, 1,2,4-triazolates have much more diversified coordination modes than the diazolates. On one hand, 1,2,4-triazolates can mimic imidazolates and pyrazolates to form similar structural units and even isostructural 3D frameworks. On the other hand, the unique 3-coordination mode of 1,2,4-triazolates endows novel structure types not easily available from either the diazolates or other types of ligands. Particularly, the 3-connected 1,2,4-triazolate frameworks represent a unique class of low-density structures. Compared with the diazolates, triazolates have weaker coordination ability toward transition-metal ions. Consequently, introduction of coordinative side groups, counterions, and even other types of coligands becomes an

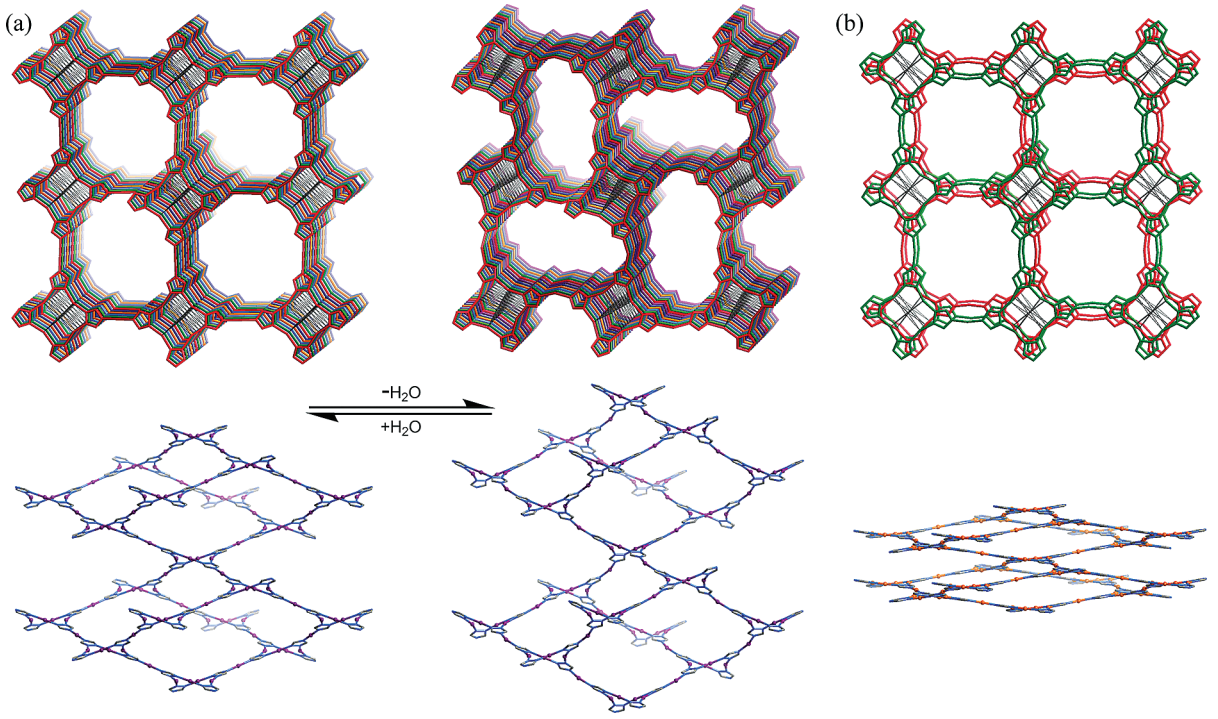

Figure 33. Reversible transformation between the 5-fold (left) and 6-fold (right) interpenetrated $[Ag_6Cl(atz)_4]OH \cdot xH_2O$ (a) and structure of the 2-fold interpenetrated $[Cu_6Br(tz)_4]Cu_4Br_4(OH)$ (b) viewed along the 1D channels (top) and their single $[Ag_3(atz)_2]^+$ and $[Cu_3(tz)_2]^+$ networks viewed perpendicular to the 1D channels (bottom). Substituent groups, hydrogen, and counteranions in the large channels are omitted for clarity.

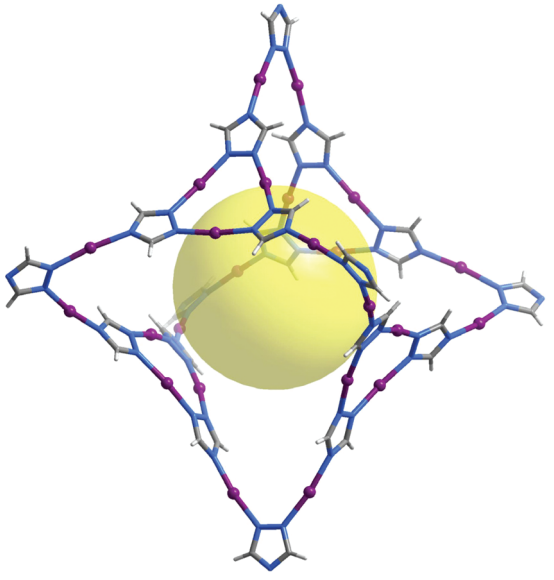

Figure 34. Structure of the $[Ag_{24}(tz)_{18}]^{6+}$ nanocage.

important approach for generating triazolate-based coordination polymers. Nevertheless, univalent coinage-metal ions still have a tendency to form binary metal 1,2,4-triazolate frameworks.

6. METAL 1,2,3-TRIAZOLATE FRAMEWORKS

The coordination difference between the triazolate isomers is similar to that between pyrazolate and imidazolate. The three N-donors of 1,2,3-triazolate locate at the same side of the five-membered ring (Scheme 1). Consequently, 1,2,3-triazolate derivatives are usually used in the construction of discrete polynuclear complexes.

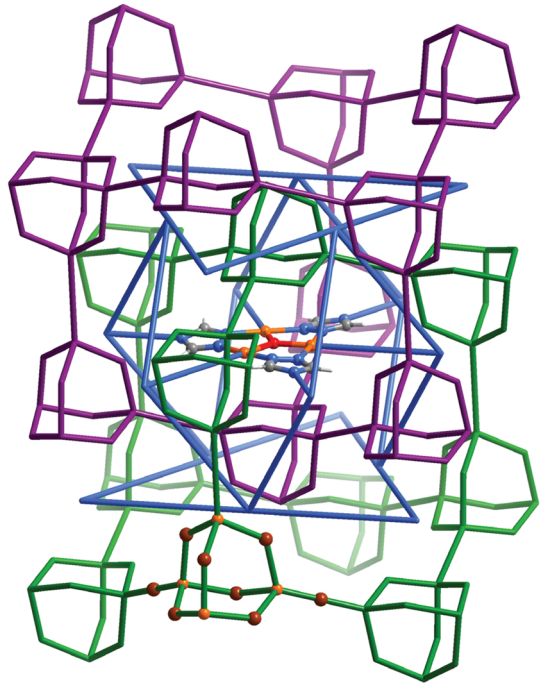

Figure 35. Heterointerpenetration between one $[Cu^{II}_3(OH)(tz)_3]^{2+}$ **hxg** network (blue) and two $[Cu^{I}Br_2]^-$ **dia-a** networks (green and purple).

dx.doi.org/10.1021/cr200139g |*Chem. Rev.* 2012, 112, 1001–1033

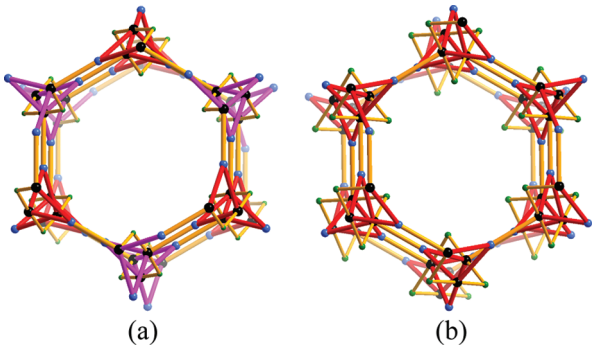

Figure 36. Simplified structures of (a) **etb**-[Zn(tz)F] and (b) **eta**-[Cd(tz)Cl] (metal, black; triazolate, blue; halide, green; left and right helices are highlighted in purple and red, respectively).

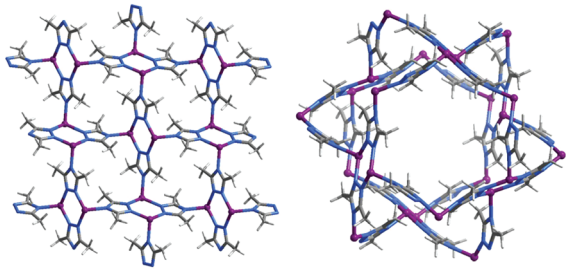

Figure 37. Isomeric $[Zn(dmtz)]^+$ networks with **sql-a** (left) and **nbo-a** (right) topologies.

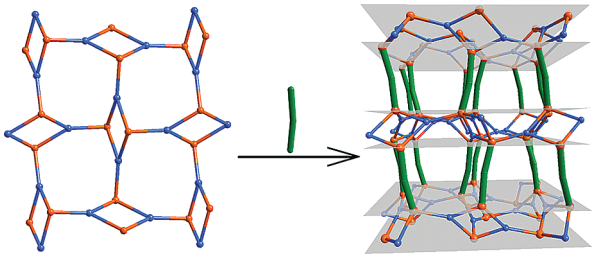

Figure 38. Pillaring **sql-a** layers into a 3D framework.

Two crystal structures have been reported for univalent coinage-metal 1,2,3-triazolates. The simple copper(I) 1,2,3-triazolate, [Cu(vtz)], is a flat ladder-type ribbon, in which the trigonal metal ions and μ_3-vtz$^-$ aromatic rings reside alternately on the ribbon plane (Figure 39a).[151] The coordination modes of the metal ion and ligand in the silver(I) benzotriazolate [Ag(bvtz)] are similar to those in [Cu(vtz)], but the substituent groups (phenyl rings) of adjacent ligands become too close to each other to be aligned in a parallel manner. Rotating adjacent benzotriazolates in opposite directions avoids the steric hindrance and results in a 2D brick-wall-type layer with **hcb** topology (Figure 39b).[152]

For divalent metal ions, the most commonly observed prototype is the T_d-symmetric pentanuclear $[M_5(vtz)_6]^{4+}$ cluster, in which a central octahedral metal ion is coordinated by six N^2-donors and four outer metal ions are each coordinated by three $N^{1,3}$-donors in a *fac*-fashion. The remaining coordination sites of the outer metal ions can further coordinate with secondary ligands, giving discrete complexes or polymeric networks

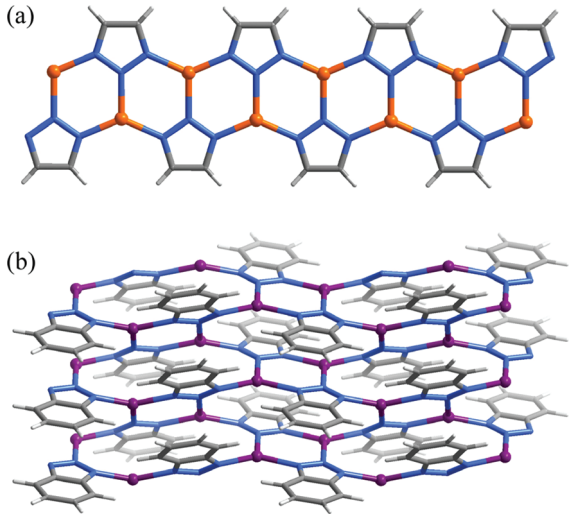

Figure 39. Structures of (a) [Cu(vtz)] and (b) [Ag(bvtz)].

(Scheme 13). For example, a series of neutral 3D porous networks have been rationally constructed by linking the pentanuclear clusters by long, dianionic bridging ligands such as $TCNQ^{2-}$ and dicarboxylates.[153] The pentanuclear cluster can also expand to larger clusters such as $[M_9(bvtz)_{12}]^{6+}$ by sharing the tetrahedral corners.[154] They can also share all of four tetrahedral corners to expand into a neutral diamondoid network with small channels, as observed in $[Cd(vtz)_2]$.[155] Obviously, this structure is not suitable for 1,2,3-triazolate derivatives with large substituent groups. Alternatively, the divalent metal ions adopt 4-coordination, and the ligands behave as imidazolates or pyrazolates. The zinc(II) benzotriazolate crystallizes as three nonporous isomers with ABW,[156] BIK,[157] and **hcb**[158] topologies.

The $[M_5(vtz)_6]^{4+}$ cluster can also be expanded in another way. Volkmer et al. first used benzobistriazolate to construct a porous framework with **pcu** topology with the pentanuclear clusters as the octahedral nodes and the organic ligands as the ditopic linkers. The chloride ions saturate the outer four Zn(II) ions and balance the charge. While this material is highly porous and contains large cavities (d = 11.94 Å), its aperture size is very small (d = 2.52 Å), giving it highly selective sorption for H_2 over N_2 and argon at 77 K (Figure 40a).[159] They further expanded this prototype to an isoreticular framework with higher porosity using an elongated bistriazolate ligand, bis(1,2,3-triazolate[4,5-*b*][4′,5′-*i*])dibenzo[1,4]dioxin, in which the cavity (d = 18.56 Å) and aperture (d = 9.13 Å) sizes are both significantly enlarged; thus, both H_2 and Ar can be adsorbed (Figure 40b).[160]

The click reaction, or Huisgen [2 + 3] cycloaddition between alkyne and azide catalyzed by Cu(I), can give 1,2,3-trizole in very high efficiency,[161] which is particularly useful for producing complicated molecules. This reaction has also been used to construct coordination polymers via in situ generation of the 1,2,3-triazolate ligand.[162] Nevertheless, coordination polymers based on 1,2,3-triazolate derivatives are still relatively few. Long et al. have constructed several interesting PCPs based on poly(1,2,3-triazolate-4-yl)benzene derivatives (Chart 5).[163] It should be noted that, in these PCPs, the polytriazolates coordinate as the corresponding polypyrazolate analogues, but the structural chemistry and materials' properties are somewhat different, which is the same case for many polytetrazolates (see the next section).

Scheme 13. Structural Evolution from $[M_5(vtz)_6]^{4+}$

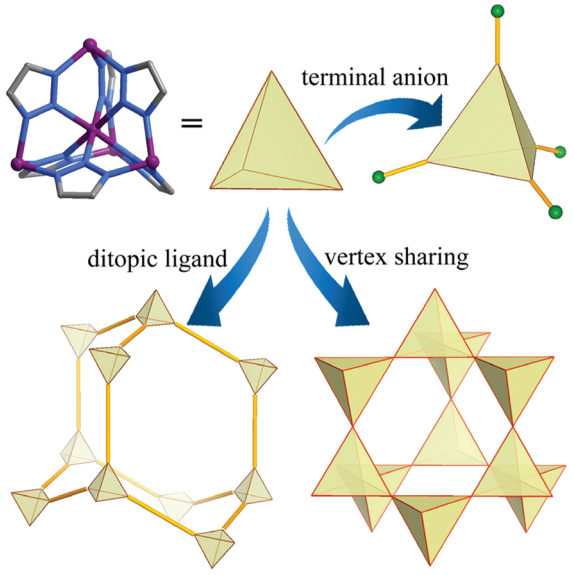

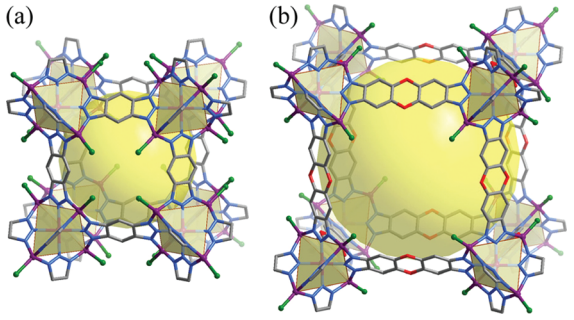

Figure 40. Porous frameworks based on the pentanuclear SBUs linked by short (a) and long (b) bistriazolates.

7. METAL TETRAZOLATE FRAMEWORKS

Tetrazole derivatives are well-known for their instability, decomposing with release of energy. As potential energetic materials, various alkali-metal tetrazolate salts have been synthesized and structurally characterized. The bonding modes in these ionic compounds are significantly different from those of traditional coordination complexes and will not be discussed here. See Chart 6 for the structures of substituted tetrazolates.

Compared to other azolates with fewer N-donors, tetrazolates do not just have the highest number of N-donors and versatile coordination modes; they also have much lower basicity (similar to that of carboxylates) and relatively weak coordination ability. In some coordination complexes, metal ions are coordinated with the pyridyl moieties of the ligand or even with aqua ligands, keeping the tetrazolate anions bare.[164] As a consequence, tetrazolate-based frameworks are thermally and chemically less stable than other types of MAFs. Nevertheless, tetrazolates still possess some common characteristics of azolates, and they can mimic the coordination modes of all other types of azolates.

Tetrazolate-based frameworks have been extensively studied, probably because tetrazoles can be prepared very conveniently by the [2 + 3] cycloaddition between organonitriles and azides in mild conditions, where the most famous one is carried out in water using Zn(II) salt as a catalyst.[165] Actually, many metal tetrazolate frameworks were discovered by solvothermal reactions using organonitriles as the solvents with Zn(II) and other metal ions as both catalysts and building blocks.[166]

Chart 5. Poly(1,2,3-triazolate-4-yl)benzenes

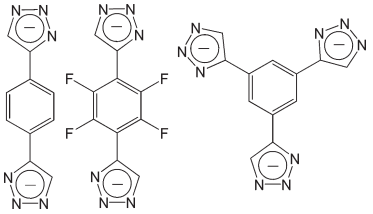

Chart 6. Substituted Tetrazolates

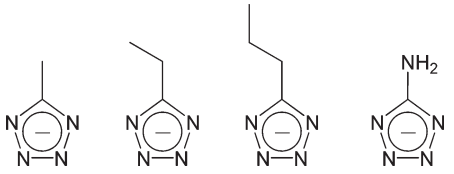

7.1. Univalent Coinage-Metal Tetrazolate Frameworks

The tetradentate coordination mode can be expected to occur in binary univalent coinage-metal tetrazolates. The first examples of the μ_4-η^1:η^1:η^1:η^1 bonding mode for tetrazolate were observed in $[Ag_2(N,N',N''',N'''\text{-}\mu_3\text{-ttz})(\mu_4\text{-ttz})]$ and $[Ag_{1.5}(\mu_4\text{-ttz})](NO_3)_{0.5}$ as reported by Ciani et al., which can be prepared by reacting $AgNO_3$ with Httz in different molar ratios.[167] The ideal stoichiometry and coordination geometries were observed in $[Cu(\mu_4\text{-mttz})]$ (Hmttz = 5-methyltetrazole)[168] and $[Ag(\mu_4\text{-ettz})]$ (Hettz = 5-ethyltetrazole) as reported by Li et al.[169] and $[Cu(\mu_4\text{-ttz})]$ as reported by Zhang et al.[170] These structures can be simplified as typical 4-connected topologies, such as **ptr** and **pts**, regarding the metal ions and ligands as tetrahedral and square-planar nodes, respectively (Figure 41). They also reported a series of binary silver(I) and copper(I) alkyltriazolates synthesized through Ag/Cu ion catalyzed [2 + 3] cycloaddition between oganonitriles and azides under solvothermal conditions. The 1,2,4-triazolate coordination modes were observed in several compounds, such as $[Cu_{10}(N,N',N''',N'''\text{-}\mu_3\text{-mttz})_3(\mu_4\text{-mttz})_7]\cdot 2H_2O$, **sql-a**-$[Ag(N,N',N''',N'''\text{-}\mu_3\text{-mttz})]$, and $[Ag_3(N,N',N''',N'''\text{-}\mu_3\text{-pttz})_2(\mu_4\text{-pttz})]$ (Hpttz = 5-propyltetrazole).[170,171]

7.2. Bivalent Metal Tetrazolate Frameworks

While the bivalent metal ion and tetrazolate in the binary $[M(ttz)_2]$ system cannot simultaneously fulfill the 8- and 4-coordinations, respectively, the combination of 6- and 3-coordinations is also extremely difficult as discussed for the triazolates (see section 5.2). Nevertheless, the decorated **dia** network of vertex-sharing $[M_5(vtz)_6]^{2+}$ clusters was first observed in $[Zn(N,N',N''\text{-}\mu_3\text{-mttz})_2]$ as reported by Xiong et al.,[172] in which Zn(II) adopts an octahedral coordination geometry and the tetrazolate behaves asa tridentate 1,2,3-triazolate.

The imidazolate coordination modes were observed in several binary zinc(II) tetrazolates, because Zn(II) ions prefer tetrahedral coordination geometries. $[Zn(N,N'''\text{-}\mu\text{-ttz})_2]$[172] has a 2-fold interpenetrated **dia** structure isostructural with $[Zn(tz)_2]$,[126] being consistent with the above discussion about steric hindrance

dx.doi.org/10.1021/cr200139g |*Chem. Rev.* 2012, 112, 1001–1033

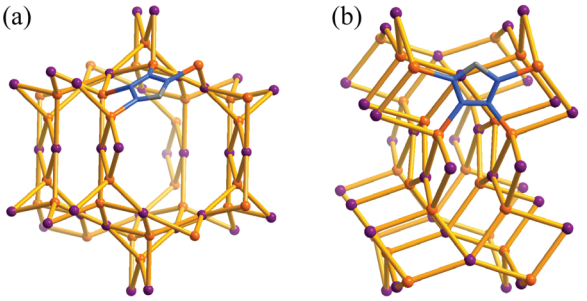

Figure 41. Univalent coinage-metal tetrazolates with **ptr** (a) and **pts** (b) topologies.

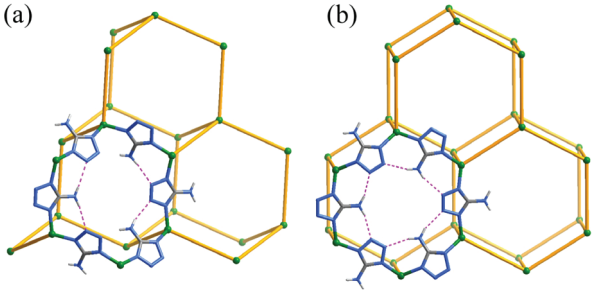

Figure 42. Isomeric $[Zn(ttz)_2]$ frameworks with **dia** (a) and $4^3.6^3$ (b) topologies.

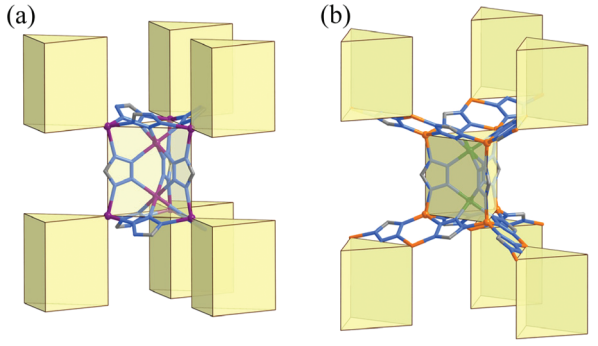

Figure 43. Sharing six corner metal ions of $[M_8(Rttz)_9]^{7+}$ clusters (a) or interlinking six edges of $[Cu^I_6Cu^{II}_2(\mu_4\text{-mttz})_9]^+$ clusters by Cu−N coordination bonds (b) to form **acs** networks (substituent groups and hydrogen atoms are omitted for clarity).

effects of C−H to N substitution; i.e., the molecular sizes follow the order imidazolate > triazolate > tetrazolate. With a bulky side group, butyl, the noninterpenetrated **dia** structure was obtained.[173] By introduction of a smaller amino group, $[Zn(N,N'''\text{-}\mu\text{-attz})_2]$ represents a noninterpenetrated **dia** network with considerable porosity, which was reported recently by Benerjee et al.[174] They also observed high CO_2 uptake at room temperature and 1 atm attributed to the presence of free amino groups and uncoordinated tetrazolate N-donors on the pore surface, although N−H···N hydrogen bonds between these complementary functional groups reduce their activities. An isomer of $[Zn(N,N'''\text{-}\mu\text{-attz})_2]$ with a honeycomb-like bilayer structure (uninodal 4-connected topology with point symbol $4^3.6^3$ and vertex symbol 4.6.4.6.4.6) was also reported by Wang et al., in which all uncoordinated tetrazolate N-donors are involved in N−H···N hydrogen bonds.[175] While the structure-directing roles of the side groups are mainly attributed to the steric hindrance effect, $[Zn(N,N'''\text{-}\mu\text{-attz})_2]$ illustrated the effectiveness of attractive interactions (Figure 42).

It should be noted that the bridging angles of tetrazolates in the above-mentioned examples are mostly around 160°, being significantly larger than those of the imidazolates (ca. 140°) and also the molecular geometry of tetrazolate (slightly larger than 144° because bond lengths involving N atoms are shorter than those involving C atoms), which may be ascribed to the weak bonding interactions from the $N^{2,3}$-donors. The more pronounced ionic bonding character of tetrazolate may also be responsible for the deviation from directional coordination. Some Zn−ttz−Zn moieties in the two $[Zn(ttz)_2]$ isomers significantly deviate from the planar configuration.[174,175] One may also notice that the **dia** and $4^3.6^3$ topologies are suitable for linear bridging ligands rather than bent ones.

Compared with Zn(II), the larger Cd(II) preferred octahedral coordination geometries. Therefore, cadmium(II) tetrazolate frameworks tend to incorporate other counterions and/or coligands, in which the tetrazolate usually acts in the μ_3- and μ_4-modes. A series of cationic frameworks with the general formula $[M_5(\mu_4\text{-Rttz})_3(N,N',N''\text{-}\mu_3\text{-Rttz})_6]X\cdot nH_2O$ (M = Cd^{II} or Cu^{II}; Rttz = tetrazolate or 5-aminotetrazolate; X = NO_3^-, Cl^-, or $0.5SO_4^{2-}$) have been reported,[176] in which the metal ions are all in octahedral coordination. This structure is constructed by trigonal-prismatic $[M_8(Rttz)_9]^{7+}$ clusters (interconnecting with each other by sharing the corner metal ions to form an **acs** net) and contains hexagonal channels, which can be retained after the removal of guest molecules (Figure 43a). Lu et al. showed distinctly different N_2 and H_2 sorption behaviors for isostructural frameworks $[M_5(\mu_4\text{-ttz})_3(N,N',N''\text{-}\mu_3\text{-ttz})_6]NO_3\cdot 8H_2O$ (M = Cd^{II} or Cu^{II}), which was ascribed to the smaller atom radius of Cu resulting in the smaller pore size.[176c,d] It should be noted that the preparation of $[Cd_5(\mu_4\text{-ttz})_3(N,N',N''\text{-}\mu_3\text{-ttz})_6]NO_3\cdot 8H_2O$ involved in situ decarboxylation of ethyl tetrazolate-5-carboxylate. Direct employment of Htta as the reactant produced another porous cadmium tetrazolate framework, $[Cd_5(N,N'''\text{-}\mu\text{-ttz})_{3/4}(N,N',N''\text{-}\mu_3\text{-ttz})_3(N,N',N'''\text{-}\mu_3\text{-ttz})_3(\mu_4\text{-ttz})_{9/4}(OH)(H_2O)]\cdot 5H_2O$, with a completely different structure, in which the triazolate ligands possess four different types of coordination modes.[176a]

Using simple anions as the coligand sometimes produces simple coordination and high-symmetry networks. Chang et al. reported an SOD-like microporous framework, $[Cd(\mu\text{-}N_3)(\mu_4\text{-mttz})]$, synthesized by reaction of $Cd(ClO_4)_2$ and sodium azide in acetonirile/ethanol/water under solvothermal conditions. All the Cd(II) ions are octahedrally coordinated by four N-donors from the μ_4-mttz and two more N-donors from the $\mu\text{-}N_3^-$.[177] With $CdCl_2$ as the starting material, Deng and Zeller et al. also synthesized an isostructural framework, $[Cd(\mu\text{-Cl})(\mu_4\text{-mttz})]$, which exhibits high sensitivity to nitrite in both DMF and water.[178] Using $CuCl_2$ as the metal source, Zhang et al. obtained a copper(I,II) tetrazolate framework, $[Cu^I_6Cu^{II}_2(\mu_4\text{-mttz})_9]N_3\cdot xH_2O$, composed of mixed-valence trigonal-prismatic $[Cu^I_6Cu^{II}_2(\mu_4\text{-mttz})_9]^+$ clusters (interconnecting with each other through two Cu−N bonds at each edge to form an **acs** net) with considerable guest-accessible volume, in which all the metal ions and ligands adopt maximum coordination numbers (Figure 43b).[170]

7.3. Polytetrazolates

The ease of ligand preparation also promoted studies of polytetrazolate-based coordination polymers. Interestingly, not

Chart 7. Polytetrazolates

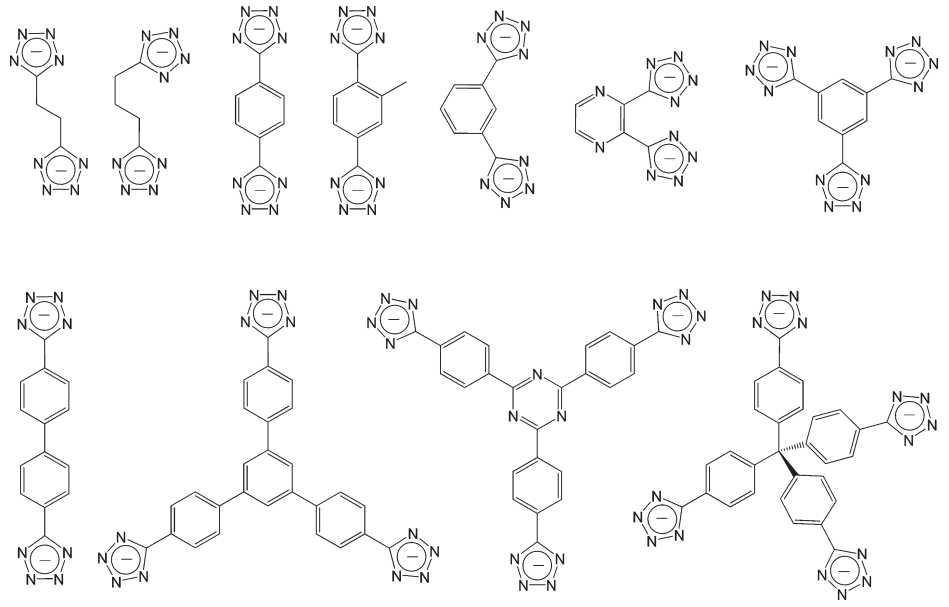

only do the tetrazole moieties have acidity similar to that of carboxylic acid, in most examples the tetrazolate groups also coordinate using the $N^{2,3}$-donors, just similar to the pyrazolates and carboxylates. The first example of such structures is **pcu**-$[Cd_3(bdt)_3(DMF)_4(H_2O)_2]\cdot 4DMF\cdot 4H_2O$ (H_2bdt = 1,4-bis(tetrazol-5-yl)benzene) reported by Tao et al., which is constructed by linear trinuclear clusters with octahedral extended sites and contains 1D channels with a 35% void volume.[179] See Chart 7 for the structures of polytetrazolates.

Long et al. have constructed a series of PCPs by rigid polytetrazolates, most of which possess pyrazolate coordination modes.[180] They also systematically constructed a series of highly porous 3,8-connected frameworks by linking cubic $M_4Cl(ttz)_8(H_2O)_4$ clusters (M = Mn^{2+}, Cu^{2+}, Fe^{2+}) with different triangular polytetrazolate ligands. The chloride-centered tetranuclear clusters are structurally similar to other carboxylate-bridged clusters.[181] For example, $[Mn(DMF)_6]_3[(Mn_4Cl(H_2O)_4)_3(btt)_8]_2$ (H_3btt = 1,3,5-tris(tetrazol-5-yl)benzene) is an anionic porous framework with the **the** topology constructed by 8-connected $Mn_4Cl(\mu\text{-}N', N''\text{-}ttz)_8(H_2O)_4$ clusters and trigonal benzenetritetrazolate ligands, which can also be simplified as fused truncated octahedral cages similar to the SOD net (Figure 44). The coordinated aqua ligand can be partially removed to generate a coordinatively unsaturated Mn^{2+} center, giving a high initial H_2 adsorption heat of 10.1 kJ/mol.[182] They also demonstrated that the Lewis acid Mn(II) exposed on the internal surface can catalyze both the cyanosilylation of aromatic aldehydes and the Mukaiyama aldol reaction in a size-selective fashion.[183] In this material, the cationic guest Mn^{2+} can be exchanged with Li^+, Cu^+, Fe^{2+}, Co^{2+}, Ni^{2+}, Cu^{2+}, and Zn^{2+} to systematically tune the H_2 adsorption affinity, in which the Co^{2+}-containing compound has the highest enthalpy of adsorption of 10.5 kJ/mol.[184] Replacing all Mn^{2+} ions by Cu^{2+} or Fe^{2+} gave isostructural frameworks that can be fully desolvated to give a higher density of coordinatively unsaturated metal centers, which have initial H_2 adsorption heats of 9.5 and 11.9 kJ/mol, respectively.[185] Noninterpenetrated and 2-fold interpenetrated, expanded analogues were also constructed by larger ligands.[186]

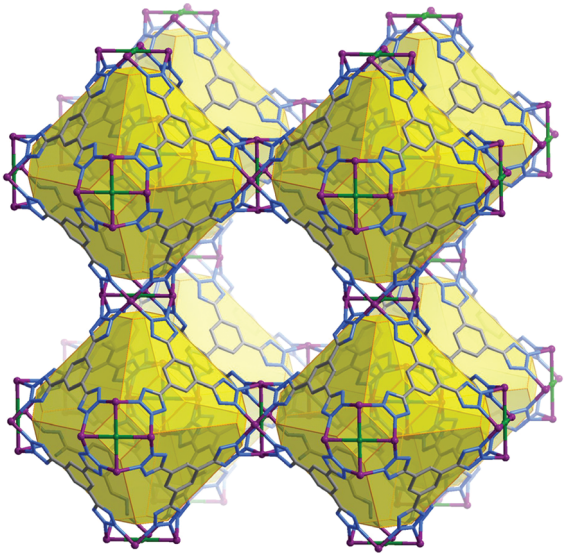

Figure 44. Framework structure of $[(Mn_4Cl(H_2O)_4)_3(btt)_8]^-$.

Long et al. showed that replacing the tetrazolate groups by 1,2,3-triazolate groups can efficiently improve the framework stability toward water and even acidic solution (tested in a solution of HCl with pH 3), which enabled the introduction of ethane-1,2-diamine into the pores for a high adsorption affinity of CO_2 without destroying the framework.[163a] They also observed the same trend in an isostructural series of copper(II) bistetrazolate/bis(1,2,3-triazolate) frameworks, in which the one based on bis(1,2,3-triazolate) exhibits remarkably improved thermal stability.[163b] These phenomena can be rationalized by the relatively low coordination abilities of tetrazolates (indicated by their low pK_a).

Long et al. have also synthesized PCPs based on a tetrakistetrazolate ligand with tetrahedral geometry. The reaction with $CuCl_2$ gave a 4,8-connected anionic **flu** framework $Cu[Cu_4Cl(ttpm)_2]_2\cdot CuCl_2\cdot 5DMF\cdot 11H_2O$ (H_4ttpm = tetrakis(4-tetrazolylphenyl)methane) based on the chloride-centered tetranuclear

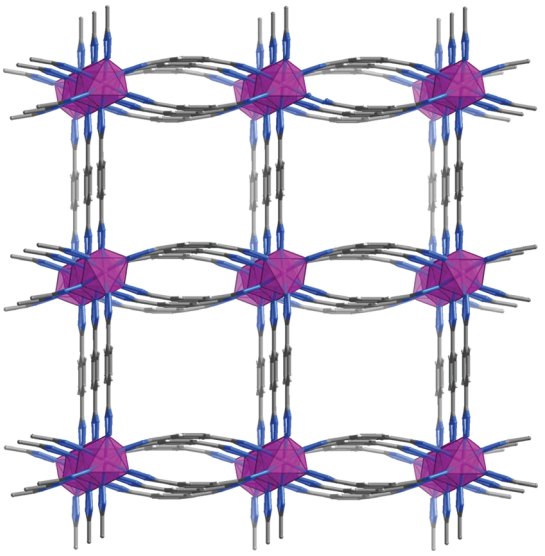

Figure 45. Framework structure of $[Co_2(H_{0.67}bdt)_3]$.

SBUs, in which an extraframework countercation Cu^{2+} is chelated by a pair of N-donors on adjacent tetrazolate rings of the SBU. Notably, not only the guests but also coordinated $CuCl_2$ can be removed by methanol exchange, which produces chloride-deficient Cu_4 squares that could serve as strong binding sites for small molecules. They also constructed a 4,6-connected **gar** framework, $[Mn_6(ttpm)_3]\cdot 5DMF\cdot 3H_2O$, composed of linear trinuclear $Mn_3(ttz)_6$ SBUs, which collapse after removal of guest molecules.[187]

Zubieta et al. reported a thermally and hydrolytically stable microporous framework, $[Co_2(N^{1\prime},N^{1\prime\prime},N^{2\prime},N^{2\prime\prime}\text{-}\mu_4\text{-}H_{0.67}bdt)_3]\cdot 20H_2O$, exhibiting single-chain magnet properties (Figure 45).[188] The columnlike 1D SBUs are very similar to the chain structure composed of trivalent octahedral metal ions and pyrazolates (Figure 10g). It should be noted that most of the reported structural types of polytetrazolate-based frameworks, albeit the tetrazolate groups coordinate in the pyrazolate mode (with the $N^{2,3}$-donors), have not been observed for pyrazolate-based ligands.

Polytetrazolates can also show other expected coordination modes. For example, Bu et al. constructed a microporous framework, [Zn(tdp)] (H_2tdp = 2,3-di-1*H*-tetrazol-5-ylpyrazine), in which each Zn(II) ion is chelated by three tdp^{2-} ligands and each ligand bridges three Zn(II) ions, giving a chiral 3-connected **etd** network (Figure 46). Although the tetrazolate groups coordinate as imidazolates and leave the uncoordinated $N^{2,3}$-donors exposed on the pore surface, C_2H_2 and MeOH adsorption measurements showed no N···H hydrogen-bonding effect between the guest molecules and the N-donor-rich pore surface,[189] which may be ascribed to the low basicity of the tetrazolate groups. They also observed similar imidazolate coordination modes in other nonporous Zn(II) coordination polymers based on flexible bistetrazolate ligands.[190]

The μ_8-coordination mode of a bistetrazolate was observed in $[Ag_2(bdt)]$ as reported by Galli et al., who also showed that $[Cu^{II}_2(OH)_2(N^{1\prime},N^{1\prime\prime},N^{2\prime},N^{2\prime\prime}\text{-}\mu_4\text{-bdt})]$ transforms to $[Cu^{I}_2(bdt)]$ at high temperature as suggested from thermogravimetric analysis,[191] which is accordant with the oxidation ability of Cu(II) at high temperature.[93d]

As shown above, tetrazolate-based coordination polymers have gained intense attention. Although this type of MAF has a relatively low stability compared with other azolates with fewer N-donors, tetrazolates are unique for their very flexible coordination behaviors and have been utilized to generate a large variety of novel framework structures.

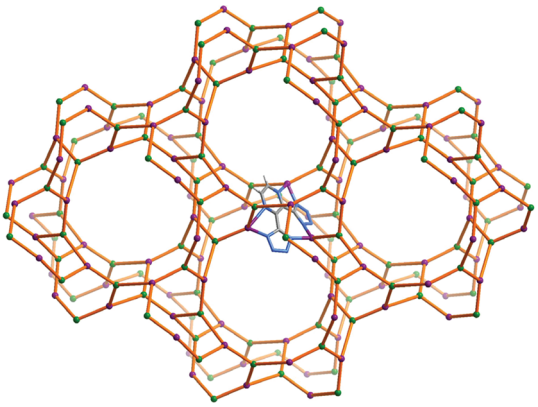

Figure 46. Coordination mode of the ligand and network topology in **etd**-[Zn(tdp)].

8. SUMMARY

With a series of selected examples, the recent progress in the chemistry of MAFs has been discussed. As we can see in the previous sections, MAFs indeed represent a unique and interesting class of coordination polymers and the investigations have been very active in recent years. Some important advances in this multifaceted field are summarized and highlighted here.

The well-defined coordination geometries of azolates have largely simplified the difficulty of design and synthesis. Compared to other metal−ligand systems, many MAFs possess highly predictable coordination geometries and connectivities. Nevertheless, some rational molecular design and synthetic strategies have been developed. A particularly interesting and unique one is the use of uncoordinated side groups to direct the relative orientations of adjacent building blocks and extended framework structures, which has led to a series of novel structures not easily obtained from other metal−ligand systems.

Besides intriguing structures, MAFs also exhibit very interesting properties. As a result of their unique bonding characters, MAFs, especially those based on the diazolates, usually have very high thermal and chemical stability, which is remarkable because stability is a very important issue for practical applications. On the other hand, framework flexibility is also widely observed, particularly in those with simple connectivity (e.g., single metal ions and single bonds) and/or flexible, uncoordinated side groups.

So far, MAFs have been mostly explored as porous materials, while other properties have also been topics of some investigations. Highly stable porous MAFs usually possess weak adsorption affinity due to their inert pore surface. Another structural feature of many porous MAFs is the combination of large nanometer-sized cages and very small apertures with diameter similar to or smaller than those of the common gas molecules, which is useful for molecular sieving. Therefore, porous MAFs are useful for separation applications. Nevertheless, porous MAFs can also have good storage and delivery performance when their pore surface, pore shape, and/or framework flexibility are properly engineered and the application condition is well

selected. For example, the sorption affinity can be improved/tuned by judicious introduction of active sites on the pore surface.

While crystal engineering on azolate-based coordination frameworks has been very fruitful, future research will certainly focus more on developing new applications and improving the performance of either already documented or newly designed MAFs. Some intriguing approaches such as the use of mixed ligands and polyazolates deserve further attention. As we anticipated a few years ago,[15b] research on MAFs has been largely expanded. Nevertheless, further exploration on MAFs will certainly contribute to the chemistry of coordination polymers in the development of functional materials for practical applications.

AUTHOR INFORMATION

Corresponding Author

*E-mail: zhangjp7@mail.sysu.edu.cn (J.-P.Z.); cxm@mail.sysu.edu.cn (X.-M.C.).

BIOGRAPHIES

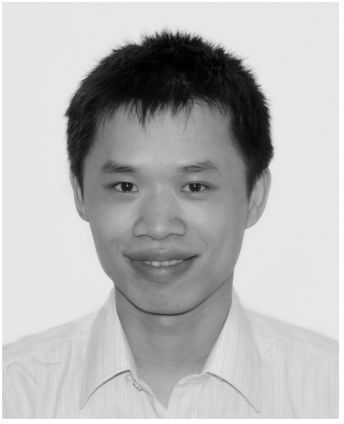

Jie-Peng Zhang was born in Guangdong, China, in 1977. He obtained his B.Sc. in 2000 and Ph.D. in 2005 under the supervision of Prof. X.-M. Chen at Sun Yat-Sen (Zhongshan) University (SYSU). He was a JSPS postdoc at Kyoto University under the supervision of Prof. S. Kitagawa from 2005 to 2007 and then joined SYSU in 2007. His current research interest is in the design, synthesis, function, and sorption mechanism of porous coordination polymers.

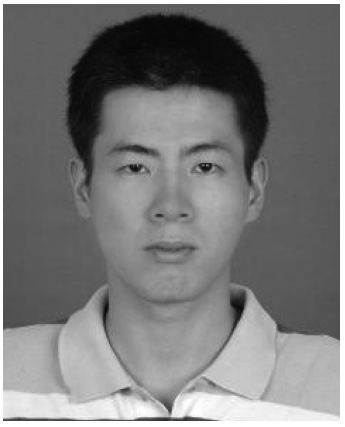

Yue-Biao Zhang was born in Guangdong, China, in 1984. He received his B.Sc. in 2006 from SYSU. After then, he joined Professor X.-M. Chen's group as a graduate student. He focuses his research on the crystal engineering of porous coordination polymers.

Jian-Bin Lin was born in Guangdong, China, in 1983. He received his B.Sc. in chemistry in 2006 from SYSU and then joined Prof. X.-M. Chen's group for his Ph.D. study, working in the synthesis, structures, and property studies of porous coordination polymers.

Xiao-Ming Chen was born in Guangdong, China. He obtained his B.Sc. in 1983 and M.Sc. in 1986 from SYSU under the supervision of Prof. H.-F. Fan and his Ph.D. under the supervision of Prof. T. C. W. Mak at the Chinese University of Hong Kong in 1992. He then joined SYSU and became Professor in 1995. His current research interest is in the synthesis and crystal engineering of functional metal complexes and coordination polymers, as well as in situ metal/ligand reactions. He has authored or coauthored more than 300 papers and 5 book chapters and received several awards, including the National Nature Science Prize of China.

ACKNOWLEDGMENT

This work was supported by the 973 project (Grants 2007CB-815302 and 2012CB821706) and the National Natural Science Foundation of China (Grants 20821001, 90922031, and 21001120).

REFERENCES

(1) Batten, S. R.; Neville, S. M.; Turner, D. R. *Coordination Polymers: Design, Analysis and Application*; RSC Publishing: Cambridge, U.K., 2009.

(2) Bailar, J. C. *Preparative Inorganic Reaction*; Interscience: New York, 1964.

(3) (a) Hoskins, B. F.; Robson, R. *J. Am. Chem. Soc.* **1989**, *111*, 5962. (b) Hoskins, B. F.; Robson, R. *J. Am. Chem. Soc.* **1990**, *112*, 1546.
(4) Kitagawa, S.; Kitaura, R.; Noro, S. *Angew. Chem., Int. Ed.* **2004**, *43*, 2334.
(5) (a) Janiak, C. *Dalton Trans.* **2003**, 2781. (b) Janiak, C.; Vieth, J. K. *New J. Chem.* **2010**, *34*, 2366. (c) Li, H.; Eddaoudi, M.; O'Keeffe, M.; Yaghi, O. M. *Nature* **1999**, *402*, 276. (d) Tranchemontagne, D. J.; Mendoza-Cortes, J. L.; O'Keeffe, M.; Yaghi, O. M. *Chem. Soc. Rev.* **2009**, *38*, 1257.
(6) (a) Wells, A. F. *Three-Dimensional Nets and Polyhedra*; Wiley-Interscience: New York, 1977. (b) Wells, A. F. *Further Studies of Three-Dimensional Nets*; American Crystallographic Association: Knoxville, TN, 1979. (c) Wells, A. F. *Structural Inorganic Chemistry*; Oxford University Press: Oxford, U.K., 1984.
(7) (a) IZA Structure Commission. http://izasc.ethz.ch/fmi/xsl/IZA-SC/ft.xsl. (b) O'Keeffe, M.; Peskov, M. A.; Ramsden, S. J.; Yaghi, O. M. *Acc. Chem. Res.* **2008**, *41*, 1782. Reticular Chemistry Structure Resource (RCSR). http://rcsr.anu.edu.au/. (c) Ramsden, S. J.; Robins, V.; Hyde, S. T.; Hungerford, S. Euclidean Patterns in Non-Euclidean Tilings (EPINET). http://epinet.anu.edu.au/ (accessed September 13, 2011).
(8) Blatov, V. A.; O'Keeffe, M.; Proserpio, D. M. *CrystEngComm* **2010**, *12*, 44.
(9) Blatov, V. A.; Shevchenko, A. P.; Proserpio, D. M. TOPOS 4.0, 2010. http://www.topos.ssu.samara.ru (accessed September 13, 2011).
(10) (a) Robson, R. *Dalton Trans.* **2000**, 3735. (b) Robson, R. *Dalton Trans.* **2008**, 5113.
(11) Yaghi, O. M.; O'Keeffe, M.; Ockwig, N. W.; Chae, H. K.; Eddaoudi, M.; Kim, J. *Nature* **2003**, *423*, 705.
(12) Kondo, M.; Okubo, T.; Asami, A.; Noro, S.; Yoshitomi, T.; Kitagawa, S.; Ishii, T.; Matsuzaka, H.; Seki, K. *Angew. Chem., Int. Ed.* **1999**, *38*, 140.
(13) Natarajan, S.; Mahata, P. *Curr. Opin. Solid State Mater. Sci.* **2009**, *13*, 46.
(14) (a) Zhang, X.-M.; Zheng, Y.-Z.; Li, C.-R.; Zhang, W.-X.; Chen, X.-M. *Cryst. Growth Des.* **2007**, *7*, 980. (b) Jia, J.; Lin, X.; Wilson, C.; Blake, A. J.; Champness, N. R.; Hubberstey, P.; Walker, G.; Cussen, E. J.; Schroder, M. *Chem. Commun.* **2007**, 840. (c) Zhang, Y.-B.; Zhang, W.-X.; Feng, F.-Y.; Zhang, J.-P.; Chen, X.-M. *Angew. Chem., Int. Ed.* **2009**, *48*, 5287. (d) Gu, X.; Lu, Z.-H.; Xu, Q. *Chem. Commun.* **2010**, *46*, 7400. (e) Chen, B.; Xiang, S.; Qian, G. *Acc. Chem. Res.* **2010**, *43*, 1115. (f) Chun, H. *J. Am. Chem. Soc.* **2007**, *130*, 800. (g) Li, J.-R.; Timmons, D. J.; Zhou, H.-C. *J. Am. Chem. Soc.* **2009**, *131*, 6368.
(15) (a) Masciocchi, N.; Galli, S.; Sironi, A. *Comments Inorg. Chem.* **2005**, *26*, 1. (b) Zhang, J.-P.; Chen, X.-M. *Chem. Commun.* **2006**, 1689. (c) Klingele, J.; Dechert, S.; Meyer, F. *Coord. Chem. Rev.* **2009**, *253*, 2698. (d) Phan, A.; Doonan, C. J.; Uribe-Romo, F. J.; Knobler, C. B.; O'Keeffe, M.; Yaghi, O. M. *Acc. Chem. Res.* **2010**, *43*, 58. (e) Pettinari, C.; Masciocchi, N.; Pandolfo, L.; Pucci, D. *Chem.—Eur. J.* **2010**, *16*, 1106. (f) Mohamed, A. A. *Coord. Chem. Rev.* **2010**, *254*, 1918. (g) Olguin, J.; Brooker, S. *Coord. Chem. Rev.* **2011**, *255*, 203. (h) Ouellette, W.; Jones, S.; Zubieta, J. *CrystEngComm* **2011**, *13*, 4457. (i) Aromí, G.; Barrios, L. A.; Roubeau, O.; Gamez, P. *Coord. Chem. Rev.* **2011**, *255*, 485.
(16) Hernandez, M. P.; Fernandez-Bertran, J. F.; Farias, M. H.; Diaz, J. A. *Surf. Interface Anal.* **2007**, *39*, 434.
(17) Ohtsu, H.; Shimazaki, Y.; Odani, A.; Yamauchi, O.; Mori, W.; Itoh, S.; Fukuzumi, S. *J. Am. Chem. Soc.* **2000**, *122*, 5733.
(18) (a) Müller-Buschbaum, K.; Mokaddem, Y. *Solid State Sci.* **2008**, *10*, 416. (b) Müller-Buschbaum, K.; Gomez-Torres, S.; Larsen, P.; Wickleder, C. *Chem. Mater.* **2007**, *19*, 655. (c) Zurawski, A.; Mai, M.; Baumann, D.; Feldmann, C.; Muller-Buschbaum, K. *Chem. Commun.* **2011**, *47*, 496.
(19) Zhang, J.-P.; Qi, X.-L.; Liu, Z.-J.; Zhu, A.-X.; Chen, Y.; Wang, J.; Chen, X.-M. *Cryst. Growth Des.* **2011**, *11*, 796.
(20) Chen, X.-M.; Tong, M.-L. *Acc. Chem. Res.* **2007**, *40*, 162.
(21) Rowsell, J. L. C.; Spencer, E. C.; Eckert, J.; Howard, J. A. K.; Yaghi, O. M. *Science* **2005**, *309*, 1350.
(22) (a) Moulton, B.; Zaworotko, M. J. *Chem. Rev.* **2001**, *101*, 1629. (b) Zhang, J.-P.; Huang, X.-C.; Chen, X.-M. *Chem. Soc. Rev.* **2009**, *38*, 2385.
(23) (a) Tian, Y. Q.; Xu, H. J.; Weng, L. H.; Chen, Z. X.; Zhao, D. Y.; You, X. Z. *Eur. J. Inorg. Chem.* **2004**, 1813. (b) Huang, X. C.; Zhang, J. P.; Chen, X. M. *Cryst. Growth Des.* **2006**, *6*, 1194.
(24) (a) Masciocchi, N.; Moret, M.; Cairati, P.; Sironi, A.; Ardizzoia, G. A.; La Monica, G. *Dalton Trans.* **1995**, 1671. (b) Liu, X. Y.; Zhu, H. L. *Synth. React. Inorg. Met.-Org. Nano-Met. Chem.* **2005**, *35*, 155.
(25) (a) Huang, X. C.; Zhang, J. P.; Chen, X. M. *J. Am. Chem. Soc.* **2004**, *126*, 13218. (b) Huang, X. C.; Li, D.; Chen, X. M. *CrystEngComm* **2006**, *8*, 351.
(26) Huang, X. C.; Zhang, J. P.; Lin, Y. Y.; Chen, X. M. *Chem. Commun.* **2005**, 2232.
(27) Zhang, J.-P.; Qi, X.-L.; He, C.-T.; Wang, Y.; Chen, X.-M. *Chem. Commun.* **2011**, *47*, 4156.
(28) (a) Cui, Y.; Lee, S. J.; Lin, W. *J. Am. Chem. Soc.* **2003**, *125*, 6014. (b) Byrne, P.; Lloyd, G. O.; Anderson, K. M.; Clarke, N.; Steed, J. W. *Chem. Commun.* **2008**, 3720.
(29) Martií-Rujas, J.; Islam, N.; Hashizume, D.; Izumi, F.; Fujita, M.; Kawano, M. *J. Am. Chem. Soc.* **2011**, *133*, 5853.
(30) (a) Kepert, C. J.; Prior, T. J.; Rosseinsky, M. J. *J. Am. Chem. Soc.* **2000**, *122*, 5158. (b) Zhang, J.-P.; Lin, Y.-Y.; Zhang, W.-X.; Chen, X.-M. *J. Am. Chem. Soc.* **2005**, *127*, 14162.
(31) (a) Ardizzoia, G. A.; Brenna, S.; Castelli, F.; Galli, S.; Masciocchi, N.; Maspero, A. *Inorg. Chem. Commun.* **2008**, *11*, 502. (b) Wu, T.; Li, D.; Ng, S. W. *CrystEngComm* **2005**, *7*, 514. (c) Huang, X.-C.; Luo, W.; Shen, Y.-F.; Ng, S. W. *Acta Crystallogr., Sect. E* **2007**, *63*, m2041.
(32) Sturm, M.; Brandl, F.; Engel, D.; Hoppe, W. *Acta Crystallogr., Sect. B* **1975**, *31*, 2369.
(33) Lehnert, R.; Seel, F. *Z. Anorg. Allg. Chem.* **1980**, *464*, 187.
(34) Spek, A. L.; Duisenberg, A. J. M.; Feiters, M. C. *Acta Crystallogr., Sect. C* **1983**, *39*, 1212.
(35) Sanchez, V.; Storr, A.; Thompson, R. C. *Can. J. Chem.* **2002**, *80*, 133.
(36) Tian, Y. Q.; Cai, C. X.; Ji, Y.; You, X. Z.; Peng, S. M.; Lee, G. H. *Angew. Chem., Int. Ed.* **2002**, *41*, 1384.
(37) (a) Tian, Y. Q.; Cai, C. X.; Ren, X. M.; Duan, C. Y.; Xu, Y.; Gao, S.; You, X. Z. *Chem.—Eur. J.* **2003**, *9*, 5673. (b) Tian, Y.-Q.; Chen, Z.-X.; Weng, L.-H.; Guo, H.-B.; Gao, S.; Zhao, D. Y. *Inorg. Chem.* **2004**, *43*, 4631.
(38) Huang, X. C.; Zhang, J. P.; Chen, X. M. *Chin. Sci. Bull.* **2003**, *48*, 1531.
(39) Park, K. S.; Ni, Z.; Cote, A. P.; Choi, J. Y.; Huang, R. D.; Uribe-Romo, F. J.; Chae, H. K.; O'Keeffe, M.; Yaghi, O. M. *Proc. Natl. Acad. Sci. U.S.A.* **2006**, *103*, 10186.
(40) (a) Li, Y. S.; Liang, F. Y.; Bux, H.; Feldhoff, A.; Yang, W. S.; Caro, J. *Angew. Chem., Int. Ed.* **2010**, *49*, 548. (b) Li, Y. S.; Liang, F. Y.; Bux, H. G.; Yang, W. S.; Caro, J. *J. Membr. Sci.* **2010**, *354*, 48. (c) Li, Y. S.; Bux, H.; Feldhoff, A.; Li, G. L.; Yang, W. S.; Caro, J. *Adv. Mater.* **2010**, *22*, 3322. (d) McCarthy, M. C.; Varela-Guerrero, V.; Barnett, G. V.; Jeong, H. K. *Langmuir* **2010**, *26*, 14636. (e) Aguado, S.; Canivet, J.; Farrusseng, D. *Chem. Commun.* **2010**, *46*, 7999.
(41) (a) Gucuyener, C.; van den Bergh, J.; Gascon, J.; Kapteijn, F. *J. Am. Chem. Soc.* **2010**, *132*, 17704. (b) Aguado, S.; Bergeret, G.; Titus, M. P.; Moizan, V.; Nieto-Draghi, C.; Bats, N.; Farrusseng, D. *New J. Chem.* **2011**, *35*, 546.
(42) (a) Huang, X.-C. Ph.D. Thesis, Sun Yat-Sen University, Guangzhou, China, 2004. (b) Huang, X. C.; Lin, Y. Y.; Zhang, J. P.; Chen, X. M. *Angew. Chem., Int. Ed.* **2006**, *45*, 1557.
(43) Sigama-Aldrich Co. http://www.sigmaaldrich.com/catalog/search/TablePage/20471712 (accessed September 13, 2011).
(44) (a) Wu, H.; Zhou, W.; Yildirim, T. *J. Am. Chem. Soc.* **2007**, *129*, 5314. (b) Fischer, M.; Hoffmann, F.; Froba, M. *ChemPhysChem* **2009**, *10*, 2647. (c) Zhou, M.; Wang, Q.; Zhang, L.; Liu, Y. C.; Kang, Y. *J. Phys. Chem. B* **2009**, *113*, 11049. (d) Han, S. S.; Choi, S. H.; Goddard, W. A. *J. Phys. Chem. C* **2010**, *114*, 12039. (e) Wu, H.; Zhou, W.; Yildirim, T. *J. Phys. Chem. C* **2009**, *113*, 3029. (f) Guo, H. C.; Shi, F.; Ma, Z. F.; Liu, X. Q. *J. Phys. Chem. C* **2010**, *114*, 12158.
(45) (a) Cravillon, J.; Munzer, S.; Lohmeier, S. J.; Feldhoff, A.; Huber, K.; Wiebcke, M. *Chem. Mater.* **2009**, *21*, 1410. (b) Nune, S. K.;

Thallapally, P. K.; Dohnalkova, A.; Wang, C. M.; Liu, J.; Exarhos, G. J. *Chem. Commun.* **2010**, *46*, 4878. (c) Pan, Y.; Liu, Y.; Zeng, G.; Zhao, L.; Lai, Z. *Chem. Commun.* **2011**, *47*, 2071.

(46) (a) Demessence, A.; Boissiere, C.; Grosso, D.; Horcajada, P.; Serre, C.; Férey, G.; Soler-Illia, G.; Sanchez, C. *J. Mater. Chem.* **2010**, *20*, 7676. (b) Lu, G.; Hupp, J. T. *J. Am. Chem. Soc.* **2010**, *132*, 7832.

(47) Shi, Q.; Chen, Z. F.; Song, Z. W.; Li, J. P.; Dong, J. X. *Angew. Chem., Int. Ed.* **2011**, *50*, 672.

(48) Zhang, J.-P.; Zhu, A.-X.; Lin, R.-B.; Qi, X.-L.; Chen, X.-M. *Adv. Mater.* **2011**, *23*, 1268.

(49) Beldon, P. J.; Fábián, L.; Stein, R. S.; Thirumurugan, A.; Cheetham, A. K.; Friščić, T. *Angew. Chem., Int. Ed.* **2010**, *49*, 9640.

(50) Lin, J.-B.; Lin, R.-B.; Cheng, X.-N.; Zhang, J.-P.; Chen, X.-M. *Chem. Commun.* **2011**, *47*, 9185.

(51) Low, J. J.; Benin, A. I.; Jakubczak, P.; Abrahamian, J. F.; Faheem, S. A.; Willis, R. R. *J. Am. Chem. Soc.* **2009**, *131*, 15834.

(52) Cychosz, K. A.; Matzger, A. J. *Langmuir* **2010**, *26*, 17198.

(53) Kusgens, P.; Rose, M.; Senkovska, I.; Frode, H.; Henschel, A.; Siegle, S.; Kaskel, S. *Microporous Mesoporous Mater.* **2009**, *120*, 325.

(54) Krishna, R.; van Baten, J. M. *J. Membr. Sci.* **2010**, *360*, 323.

(55) (a) Bux, H.; Liang, F. Y.; Li, Y. S.; Cravillon, J.; Wiebcke, M.; Caro, J. *J. Am. Chem. Soc.* **2009**, *131*, 16000. (b) Bux, H.; Chmelik, C.; van Baten, J. M.; Krishna, R.; Caro, J. *Adv. Mater.* **2010**, *22*, 4741.

(56) Venna, S. R.; Carreon, M. A. *J. Am. Chem. Soc.* **2010**, *132*, 76.

(57) (a) Ordonez, M. J. C.; Balkus, K. J.; Ferraris, J. P.; Musselman, I. H. *J. Membr. Sci.* **2010**, *361*, 28. (b) Diaz, K.; Garrido, L.; Lopez-Gonzalez, M.; del Castillo, L. F.; Riande, E. *Macromolecules* **2010**, *43*, 316. (c) Basu, S.; Maes, M.; Cano-Odena, A.; Alaerts, L.; De Vos, D. E.; Vankelecom, I. F. J. *J. Membr. Sci.* **2009**, *344*, 190.

(58) Ostermann, R.; Cravillon, J.; Weidmann, C.; Wiebcke, M.; Smarsly, B. M. *Chem. Commun.* **2011**, *47*, 442.

(59) Chang, N.; Gu, Z. Y.; Yan, X. P. *J. Am. Chem. Soc.* **2010**, *132*, 13645.

(60) Luebbers, M. T.; Wu, T. J.; Shen, L. J.; Masel, R. I. *Langmuir* **2010**, *26*, 15625.

(61) Li, K. H.; Olson, D. H.; Seidel, J.; Emge, T. J.; Gong, H. W.; Zeng, H. P.; Li, J. *J. Am. Chem. Soc.* **2009**, *131*, 10368.

(62) (a) Chizallet, C.; Lazare, S.; Bazer-Bachi, D.; Bonnier, F.; Lecocq, V.; Soyer, E.; Quoineaud, A. A.; Bats, N. *J. Am. Chem. Soc.* **2010**, *132*, 12365. (b) Chizallet, C.; Bats, N. *J. Phys. Chem. Lett.* **2010**, *1*, 349.

(63) (a) Jiang, H. L.; Liu, B.; Akita, T.; Haruta, M.; Sakurai, H.; Xu, Q. *J. Am. Chem. Soc.* **2009**, *131*, 11302. (b) Esken, D.; Turner, S.; Lebedev, O. I.; Van Tendeloo, G.; Fischer, R. A. *Chem. Mater.* **2010**, *22*, 6393.

(64) Isimjan, T. T.; Kazemian, H.; Rohani, S.; Ray, A. K. *J. Mater. Chem.* **2010**, *20*, 10241.

(65) Moggach, S. A.; Bennett, T. D.; Cheetham, A. K. *Angew. Chem., Int. Ed.* **2009**, *48*, 7087.

(66) Chapman, K. W.; Halder, G. J.; Chupas, P. J. *J. Am. Chem. Soc.* **2009**, *131*, 17546.

(67) Tian, Y. Q.; Zhao, Y. M.; Chen, Z. X.; Zhang, G. N.; Weng, L. H.; Zhao, D. Y. *Chem.—Eur. J.* **2007**, *13*, 4146.

(68) Lewis, D. W.; Ruiz-Salvador, A. R.; Gomez, A.; Rodriguez-Albelo, L. M.; Coudert, F. X.; Slater, B.; Cheetham, A. K.; Mellot-Draznieks, C. *CrystEngComm* **2009**, *11*, 2272.

(69) Hayashi, H.; Cote, A. P.; Furukawa, H.; O'Keeffe, M.; Yaghi, O. M. *Nat. Mater.* **2007**, *6*, 501.

(70) Wang, B.; Cote, A. P.; Furukawa, H.; O'Keeffe, M.; Yaghi, O. M. *Nature* **2008**, *453*, 207.

(71) Banerjee, R.; Phan, A.; Wang, B.; Knobler, C.; Furukawa, H.; O'Keeffe, M.; Yaghi, O. M. *Science* **2008**, *319*, 939.

(72) Banerjee, R.; Furukawa, H.; Britt, D.; Knobler, C.; O'Keeffe, M.; Yaghi, O. M. *J. Am. Chem. Soc.* **2009**, *131*, 3875.

(73) Morris, W.; Leung, B.; Furukawa, H.; Yaghi, O. K.; He, N.; Hayashi, H.; Houndonougbo, Y.; Asta, M.; Laird, B. B.; Yaghi, O. M. *J. Am. Chem. Soc.* **2010**, *132*, 11006.

(74) Baburin, I. A.; Leoni, S.; Seifert, G. *J. Phys. Chem. B* **2008**, *112*, 9437.

(75) Morris, W.; Doonan, C. J.; Furukawa, H.; Banerjee, R.; Yaghi, O. M. *J. Am. Chem. Soc.* **2008**, *130*, 12626.

(76) (a) Masciocchi, N.; Attilio Ardizzoia, G.; Brenna, S.; Castelli, F.; Galli, S.; Maspero, A.; Sironi, A. *Chem. Commun.* **2003**, 2018. (b) Tian, Y. Q.; Xu, L.; Cai, C. X.; Wei, J. C.; Li, Y. Z.; You, X. Z. *Eur. J. Inorg. Chem.* **2004**, 1039.

(77) Tian, Y. Q.; Yao, S. Y.; Gu, D.; Cui, K. H.; Guo, D. W.; Zhang, G.; Chen, Z. X.; Zhao, D. Y. *Chem.—Eur. J.* **2010**, *16*, 1137.

(78) (a) Wu, T.; Bu, X. H.; Liu, R.; Lin, Z. E.; Zhang, J.; Feng, P. Y. *Chem.—Eur. J.* **2008**, *14*, 7771. (b) Wu, T.; Bu, X. H.; Zhang, J.; Feng, P. Y. *Chem. Mater.* **2008**, *20*, 7377.

(79) (a) Zhang, J.; Wu, T.; Zhou, C.; Chen, S. M.; Feng, P. Y.; Bu, X. H. *Angew. Chem., Int. Ed.* **2009**, *48*, 2542. (b) Wu, T.; Zhang, J.; Bu, X. H.; Feng, P. Y. *Chem. Mater.* **2009**, *21*, 3830. (c) Wu, T.; Zhang, J.; Zhou, C.; Wang, L.; Bu, X.; Feng, P. *J. Am. Chem. Soc.* **2009**, *131*, 6111.

(80) (a) Liu, Y.; Kravtsov, V. C.; Larsen, R.; Eddaoudi, M. *Chem. Commun.* **2006**, 1488. (b) Alkordi, M. H.; Brant, J. A.; Wojtas, L.; Kravtsov, V. C.; Cairns, A. J.; Eddaoudi, M. *J. Am. Chem. Soc.* **2009**, *131*, 17753. (c) Wang, S.; Zhao, T.; Li, G.; Wojtas, L.; Huo, Q.; Eddaoudi, M.; Liu, Y. *J. Am. Chem. Soc.* **2010**, *132*, 18038.

(81) Debatin, F.; Thomas, A.; Kelling, A.; Hedin, N.; Bacsik, Z.; Senkovska, I.; Kaskel, S.; Junginger, M.; Muller, H.; Schilde, U.; Jager, C.; Friedrich, A.; Holdt, H. J. *Angew. Chem., Int. Ed.* **2010**, *49*, 1258.

(82) Yang, Q. F.; Cui, X. B.; Yu, J. H.; Lu, J.; Yu, X. Y.; Zhang, X.; Xu, J. Q.; Hou, Q.; Wang, T. G. *CrystEngComm* **2008**, *10*, 1531.

(83) Masciocchi, N.; Castelli, F.; Forster, P. M.; Tafoya, M. M.; Cheetham, A. K. *Inorg. Chem.* **2003**, *42*, 6147.

(84) Jarvis, J. A. J.; Wells, A. F. *Acta Crystallogr.* **1960**, *13*, 1027.

(85) Masciocchi, N.; Bruni, S.; Cariati, E.; Cariati, F.; Galli, S.; Sironi, A. *Inorg. Chem.* **2001**, *40*, 5897.

(86) Huang, X. C.; Zhang, J. P.; Lin, Y. Y.; Yu, X. L.; Chen, X. M. *Chem. Commun.* **2004**, 1100.

(87) Tian, Y. Q.; Xu, H. J.; Li, Y. Z.; You, X. Z. *Z. Anorg. Allg. Chem.* **2004**, *630*, 1371.

(88) Schubert, D. M.; Visi, M. Z.; Knobler, C. B. *Main Group Chem.* **2008**, *7*, 311.

(89) Zhang, L. R.; Qu, X. J.; Bi, M. H.; Wang, S.; Gong, S. Z.; Huo, Q. S.; Liu, Y. L. *Microporous Mesoporous Mater.* **2009**, *119*, 344.

(90) Li, X.-P.; Zhang, J.-Y.; Pan, M.; Zheng, S.-R.; Liu, Y.; Su, C.-Y. *Inorg. Chem.* **2007**, *46*, 4617.

(91) Chen, S. S.; Chen, M.; Takamizawa, S.; Chen, M. S.; Su, Z.; Sun, W. Y. *Chem. Commun.* **2011**, *47*, 752.

(92) Chen, S.-S.; Chen, M.; Takamizawa, S.; Wang, P.; Lv, G.-C.; Sun, W.-Y. *Chem. Commun.* **2011**, *47*, 4902.

(93) (a) Bovio, B.; Bonati, F.; Banditelli, G. *Inorg. Chim. Acta* **1984**, *87*, 25. (b) Murray, H. H.; Raptis, R. G.; Fackler, J. P. *Inorg. Chem.* **1988**, *27*, 26. (c) Raptis, R. G.; Fackler, J. P. *Inorg. Chem.* **1988**, *27*, 4179. (d) Ehlert, M. K.; Rettig, S. J.; Storr, A.; Thompson, R. C.; Trotter, J. *Can. J. Chem.* **1990**, *68*, 1444. (e) Ardizzoia, G. A.; Cenini, S.; La Monica, G.; Masciocchi, N.; Maspero, A.; Moret, M. *Inorg. Chem.* **1998**, *37*, 4284. (f) Kim, S. J.; Kang, S. H.; Park, K.-M.; Kim, H.; Zin, W.-C.; Choi, M.-G.; Kim, K. *Chem. Mater.* **1998**, *10*, 1889. (g) Dias, H. V. R.; Polach, S. A.; Wang, Z. Y. *J. Fluorine Chem.* **2000**, *103*, 163. (h) Yang, G.; Raptis, R. G. *Inorg. Chem.* **2003**, *42*, 261. (i) Fujisawa, K.; Ishikawa, Y.; Miyashita, Y.; Okamoto, K.-i. *Chem. Lett.* **2004**, *33*, 66. (j) Torralba, M. C.; Ovejero, P.; Mayoral, M. J.; Cano, M.; Campo, J. A.; Heras, J. V.; Pinilla, E.; Torres, M. R. *Helv. Chim. Acta* **2004**, *87*, 250. (k) Dias, H. V. R.; Diyabalanage, H. V. K.; Eldabaja, M. G.; Elbjeirami, O.; Rawashdeh-Omary, M. A.; Omary, M. A. *J. Am. Chem. Soc.* **2005**, *127*, 7489. (l) Omary, M. A.; Rawashdeh-Omary, M. A.; Gonser, M. W. A.; Elbjeirami, O.; Grimes, T.; Cundari, T. R. *Inorg. Chem.* **2005**, *44*, 8200. (m) Dodge, M. W.; Wacholtz, W. F.; Mague, J. T. *J. Chem. Crystallogr.* **2005**, *35*, 5. (n) Dias, H. V. R.; Diyabalanage, H. V. K. *Polyhedron* **2006**, *25*, 1655. (o) Dias, H. V. R.; Gamage, C. S. P. *Angew. Chem., Int. Ed.* **2007**, *46*, 2192. (p) Dias, H. V. R.; Gamage, C. S. P.; Keltner, J.; Diyabalanage, H. V. K.; Omari, I.; Eyobo, Y.; Dias, N. R.; Roehr, N.; McKinney, L.; Poth, T. *Inorg. Chem.* **2007**, *46*, 2979. (q) Yang, G.; Martínez, J. R.; Raptis, R. G. *Inorg. Chim. Acta* **2009**, *362*, 1546. (r) Omary, M. A.; Elbjeirami, O.;

Gamage, C. S. P.; Sherman, K. M.; Dias, H. V. R. *Inorg. Chem.* **2009**, *48*, 1784.
(94) (a) Ardizzoia, G. A.; Cenini, S.; La Monica, G.; Masciocchi, N.; Moret, M. *Inorg. Chem.* **1994**, *33*, 1458. (b) Maspero, A. *J. Organomet. Chem.* **2003**, *672*, 123. (c) Yang, G.; Raptis, R. G. *Inorg. Chim. Acta* **2003**, *352*, 98. (d) Yang, G.; Raptis, R. G. *Inorg. Chim. Acta* **2007**, *360*, 2503.
(95) Masciocchi, N.; Moret, M.; Cairati, P.; Sironi, A.; Ardizzoia, G. A.; La Monica, G. *J. Am. Chem. Soc.* **1994**, *116*, 7668.
(96) (a) Ehlert, M. K.; Rettig, S. J.; Storr, A.; Thompson, R. C.; Trotter, J. *Can. J. Chem.* **1989**, *67*, 1970. (b) Ehlert, M. K.; Storr, A.; Thompson, R. C.; Einstein, F. W. B.; Batchelor, R. J. *Can. J. Chem.* **1993**, *71*, 331. (c) Masciocchi, N.; Ardizzoia, G. A.; Maspero, A.; LaMonica, G.; Sironi, A. *Inorg. Chem.* **1999**, *38*, 3657. (d) Mascocchi, N.; Ardizzoia, G. A.; Brenna, S.; LaMonica, G.; Maspero, A.; Galli, S.; Sironi, A. *Inorg. Chem.* **2002**, *41*, 6080. (e) Cingolani, A.; Galli, S.; Masciocchi, N.; Pandolfo, L.; Pettinari, C.; Sironi, A. *J. Am. Chem. Soc.* **2005**, *127*, 6144. (f) Quitmann, C. C.; Müller-Buschbaum, K. *Z. Anorg. Allg. Chem.* **2005**, *631*, 1191.
(97) (a) Burger, W.; Strähle, J. *Z. Anorg. Allg. Chem.* **1985**, *529*, 111. (b) Umakoshi, K.; Yamauchi, Y.; Nakamiya, K.; Kojima, T.; Yamasaki, M.; Kawano, H.; Onishi, M. *Inorg. Chem.* **2003**, *42*, 3907.
(98) Ehlert, M. K.; Rettig, S. J.; Storr, A.; Thompson, R. C.; Trotter, J. *Acta Crystallogr. ,Sect. C* **1994**, *50*, 1023.
(99) Xu, J. Y.; Qiao, X.; Song, H. B.; Yan, S. P.; Liao, D. Z.; Gao, S.; Journaux, Y.; Cano, J. *Chem. Commun.* **2008**, 6414.
(100) (a) Ardizzoia, G. A.; Angaroni, M. A.; La Monica, G.; Cariati, F.; Moret, M.; Masciocchi, N. *Chem. Commun.* **1990**, 1021. (b) Mezei, G.; Baran, P.; Raptis, R. G. *Angew. Chem., Int. Ed.* **2004**, *43*, 574.
(101) (a) Rusanov, E. B.; Ponomarova, V. V.; Komarchuk, V. V.; Stoeckli-Evans, H.; Fernandez-Ibañez, E.; Stoeckli, F.; Sieler, J.; Domasevitch, K. V. *Angew. Chem.* **2003**, *115*, 2603. (b) Domasevitch, K. V.; Boldog, I.; Rusanov, E. B.; Hunger, J.; Blaurock, S.; Schröder, M.; Sieler, J. *Z. Anorg. Allg. Chem.* **2005**, *631*, 1095.
(102) He, J.; Yin, Y. G.; Wu, T.; Li, D.; Huang, X. C. *Chem. Commun.* **2006**, 2845.
(103) Zhang, J. P.; Horike, S.; Kitagawa, S. *Angew. Chem., Int. Ed.* **2007**, *46*, 889.
(104) Zhang, J. P.; Kitagawa, S. *J. Am. Chem. Soc.* **2008**, *130*, 907.
(105) Choi, H. J.; Dinca, M.; Long, J. R. *J. Am. Chem. Soc.* **2008**, *130*, 7848.
(106) Choi, H. J.; Dinca, M.; Dailly, A.; Long, J. R. *Energy Environ. Sci.* **2010**, *3*, 117.
(107) Galli, S.; Masciocchi, N.; Colombo, V.; Maspero, A.; Palmisano, G.; Lopez-Garzon, F. J.; Domingo-Garcia, M.; Fernandez-Morales, I.; Barea, E.; Navarro, J. A. R. *Chem. Mater.* **2010**, *22*, 1664.
(108) Salles, F.; Maurin, G.; Serre, C.; Llewellyn, P. L.; Knofel, C.; Choi, H. J.; Filinchuk, Y.; Oliviero, L.; Vimont, A.; Long, J. R.; Férey, G. *J. Am. Chem. Soc.* **2010**, *132*, 13782.
(109) Hou, L.; Lin, Y. Y.; Chen, X. M. *Inorg. Chem.* **2008**, *47*, 1346.
(110) Tonigold, M.; Lu, Y.; Bredenkotter, B.; Rieger, B.; Bahnmuller, S.; Hitzbleck, J.; Langstein, G.; Volkmer, D. *Angew. Chem., Int. Ed.* **2009**, *48*, 7546.
(111) Masciocchi, N.; Galli, S.; Colombo, V.; Maspero, A.; Palmisano, G.; Seyyedi, B.; Lamberti, C.; Bordiga, S. *J. Am. Chem. Soc.* **2010**, *132*, 7902.
(112) Haasnoot, J. G. *Coord. Chem. Rev.* **2000**, *200−202*, 131.
(113) Potts, K. T. *Chem. Rev.* **1961**, *61*, 87.
(114) Zhang, J.-P.; Zheng, S.-L.; Huang, X.-C.; Chen, X.-M. *Angew. Chem., Int. Ed.* **2004**, *43*, 206.
(115) Eddaoudi, M.; Kim, J.; O'Keeffe, M.; Yaghi, O. M. *J. Am. Chem. Soc.* **2002**, *124*, 376.
(116) Zhang, R. B.; Zhang, J.; Li, Z. J.; Cheng, J. K.; Qin, Y. Y.; Yao, Y. G. *Cryst. Growth Des.* **2008**, *8*, 3735.
(117) Zhang, J. P.; Lin, Y. Y.; Huang, X. C.; Chen, X. M. *J. Am. Chem. Soc.* **2005**, *127*, 5495.
(118) Zhai, Q. G.; Hu, M. C.; Li, S. N.; Jiang, Y. C. *Inorg. Chim. Acta* **2009**, *362*, 1355.
(119) Zhang, J.-P.; Chen, X.-M. *J. Am. Chem. Soc.* **2008**, *130*, 6010.
(120) Zhang, J.-P.; Chen, X.-M. *J. Am. Chem. Soc.* **2009**, *131*, 5516.
(121) Matsuda, R.; Kitaura, R.; Kitagawa, S.; Kubota, Y.; Belosludov, R. V.; Kobayashi, T. C.; Sakamoto, H.; Chiba, T.; Takata, M.; Kawazoe, Y.; Mita, Y. *Nature* **2005**, *436*, 238.
(122) Chen, D.; Liu, Y.-J.; Lin, Y.-Y.; Zhang, J.-P.; Chen, X.-M. *CrystEngComm* **2011**, *13*, 3827.
(123) Yang, C.; Wang, X. P.; Omary, M. A. *J. Am. Chem. Soc.* **2007**, *129*, 15454.
(124) Yang, C.; Wang, X. P.; Omary, M. A. *Angew. Chem., Int. Ed.* **2009**, *48*, 2500.
(125) Yang, G.; Zhang, P.-P.; Liu, L.-L.; Kou, J.-F.; Hou, H.-W.; Fan, Y.-T. *CrystEngComm* **2009**, *11*, 663.
(126) Ouellette, W.; Hudson, B. S.; Zubieta, J. *Inorg. Chem.* **2007**, *46*, 4887.
(127) Zhang, J.-P.; Lin, Y.-Y.; Huang, X.-C.; Chen, X.-M. *Chem. Commun.* **2005**, 1258.
(128) Zhang, J.-P.; Lin, Y.-Y.; Huang, X.-C.; Chen, X.-M. *Cryst. Growth Des.* **2006**, *6*, 519.
(129) Lin, J.-B.; Zhang, J.-P.; Zhang, W.-X.; Xue, W.; Xue, D.-X.; Chen, X.-M. *Inorg. Chem.* **2009**, *48*, 6652.
(130) Fu, A.-Y.; Jiang, Y.-L.; Wang, Y.-Y.; Gao, X.-N.; Yang, G.-P.; Hou, L.; Shi, Q.-Z. *Inorg. Chem.* **2010**, *49*, 5495.
(131) (a) Bao, X.; Liu, J.-L.; Leng, J.-D.; Lin, Z.; Tong, M.-L.; Nihei, M.; Oshio, H. *Chem.—Eur. J.* **2010**, *16*, 7973. (b) Bao, X.; Guo, P.-H.; Liu, J.-L.; Leng, J.-D.; Tong, M.-L. *Chem.—Eur. J.* **2011**, *17*, 2335.
(132) Liu, D.; Li, M.; Li, D. *Chem. Commun.* **2009**, 6943.
(133) Lin, J.-B.; Xue, W.; Zhang, J.-P.; Chen, X.-M. *Chem. Commun.* **2011**, *47*, 926.
(134) Lin, J.-B.; Zhang, J.-P.; Chen, X.-M. *J. Am. Chem. Soc.* **2010**, *132*, 6654.
(135) Zhang, J. J.; Yang, N. F.; Zhang, C. H.; Li, B. H. *Chin. J. Inorg. Chem.* **2010**, *26*, 533.
(136) Chen, X.-D.; Wu, H.-F.; Du, M. *Chem. Commun.* **2008**, 1296.
(137) Yang, G.; Raptis, R. G. *Chem. Commun.* **2004**, 2058.
(138) Ouellette, W.; Prosvirin, A. V.; Chieffo, V.; Dunbar, K. R.; Hudson, B.; Zubieta, J. *Inorg. Chem.* **2006**, *45*, 9346.
(139) (a) Zhai, Q. G.; Wu, X. Y.; Chen, S. M.; Zhao, Z. G.; Lu, C. Z. *Inorg. Chem.* **2007**, *46*, 5046. (b) Zhai, Q. G.; Lu, C. Z.; Zhang, Q. Z.; Wu, X. Y.; Xu, X. J.; Chen, S. M.; Chen, L. J. *Inorg. Chim. Acta* **2006**, *359*, 3875. (c) Kuang, X.; Wu, X.-Y.; Zhang, J.; Lu, C.-Z. *Chem. Commun.* **2011**, *47*, 4150.
(140) Kuang, X. F.; Wu, X. Y.; Yu, R. M.; Donahue, J. P.; Huang, J. S.; Lu, C. Z. *Nat. Chem.* **2010**, *2*, 461.
(141) (a) Ouellette, W.; Yu, M. H.; O'Connor, C. J.; Hagrman, D.; Zubieta, J. *Angew. Chem., Int. Ed.* **2006**, *45*, 3497. (b) Ouellette, W.; Liu, H. X.; O'Connor, C. J.; Zubieta, J. *Inorg. Chem.* **2009**, *48*, 4655.
(142) (a) Ding, B.; Yi, L.; Cheng, P.; Liao, D.-Z.; Yan, S.-P. *Inorg. Chem.* **2006**, *45*, 5799. (b) Zhai, Q. G.; Lu, C. Z.; Chen, S. M.; Xu, X. J.; Yang, W. B. *Cryst. Growth Des.* **2006**, *6*, 1393.
(143) Su, C. Y.; Goforth, A. M.; Smith, M. D.; Pellechia, P. J.; zur Loye, H. C. *J. Am. Chem. Soc.* **2004**, *126*, 3576.
(144) Goforth, A. M.; Su, C. Y.; Hipp, R.; Macquart, R. B.; Smith, M. D.; zur Loye, H. C. *J. Solid State Chem.* **2005**, *178*, 2511.
(145) Zhu, A.-X.; Lin, J.-B.; Zhang, J.-P.; Chen, X.-M. *Inorg. Chem.* **2009**, *48*, 3882.
(146) Wei, G.; Shen, Y. F.; Li, Y. R.; Huang, X. C. *Inorg. Chem.* **2010**, *49*, 9191.
(147) (a) Park, H.; Britten, J. F.; Mueller, U.; Lee, J.; Li, J.; Parise, J. B. *Chem. Mater.* **2007**, *19*, 1302. (b) Vaidhyanathan, R.; Iremonger, S. S.; Dawson, K. W.; Shimizu, G. K. H. *Chem. Commun.* **2009**, 5230. (c) Park, H.; Moureau, D. M.; Parise, J. B. *Chem. Mater.* **2005**, *18*, 525. (d) Lin, Y.-Y.; Zhang, Y.-B.; Zhang, J.-P.; Chen, X.-M. *Cryst. Growth Des.* **2008**, *8*, 3673. (e) Ren, H.; Song, T. Y.; Xu, J. N.; Jing, S. B.; Yu, Y.; Zhang, P.; Zhang, L. R. *Cryst. Growth Des.* **2009**, *9*, 105.
(148) Vaidhyanathan, R.; Iremonger, S. S.; Shimizu, G. K. H.; Boyd, P. G.; Alavi, S.; Woo, T. K. *Science* **2010**, *330*, 650.
(149) (a) Zhai, Q. G.; Wu, X. Y.; Chen, S. M.; Lu, C. Z.; Yang, W. B. *Cryst. Growth Des.* **2006**, *6*, 2126. (b) Zhou, W. W.; Bing, L.; Chen,

W. T.; Zheng, F. K.; Chen, J. T.; Guo, G. C.; Huang, J. S. *Chin. J. Struct. Chem.* **2007**, *26*, 703. (c) Chen, S.; Sun, S.; Gao, S. *J. Solid State Chem.* **2008**, *181*, 3308. (d) Li, D. P.; Zhou, X. H.; Liang, X. Q.; Li, C. H.; Chen, C.; Liu, J.; You, X. Z. *Cryst. Growth Des.* **2010**, *10*, 2136. (e) Song, Z.; Gao, H.; Li, G.; Yu, Y.; Shi, Z.; Feng, S. *CrystEngComm* **2009**, *11*, 1579.

(150) (a) Mulyana, Y.; Kepert, C. J.; Lindoy, L. F.; Parkin, A.; Turner, P. *Dalton Trans.* **2005**, 1598. (b) Wang, F.; Yu, R.; Zhang, Q.-S.; Zhao, Z.-G.; Wu, X.-Y.; Xie, Y.-M.; Qin, L.; Chen, S.-C.; Lu, C.-Z. *J. Solid State Chem.* **2009**, *182*, 2555.

(151) Chuang, J.; Ouellette, W.; Zubieta, J. *Inorg. Chim. Acta* **2008**, *361*, 2357.

(152) Rajeswaran, M.; Blanton, T. N.; Giesen, D. J.; Whitcomb, D. R.; Zumbulyadis, N.; Antalek, B. J.; Neumann, M. M.; Misture, S. T. *J. Solid State Chem.* **2006**, *179*, 1053.

(153) (a) Bai, Y. L.; Tao, J.; Huang, R. B.; Zheng, L. S. *Angew. Chem., Int. Ed.* **2008**, *47*, 5344. (b) Wang, X.-L.; Qin, C.; Wu, S.-X.; Shao, K.-Z.; Lan, Y.-Q.; Wang, S.; Zhu, D.-X.; Su, Z.-M.; Wang, E.-B. *Angew. Chem., Int. Ed.* **2009**, *48*, 5291. (c) Zhang, Z. J.; Xiang, S. C.; Chen, Y. S.; Ma, S. Q.; Lee, Y.; Phely-Bobin, T.; Chen, B. L. *Inorg. Chem.* **2010**, *49*, 8444.

(154) Biswas, S.; Tonigold, M.; Speldrich, M.; Kögerler, P.; Volkmer, D. *Eur. J. Inorg. Chem.* **2009**, *2009*, 3094.

(155) Zhou, X.-H.; Peng, Y.-H.; Du, X.-D.; Zuo, J.-L.; You, X.-Z. *CrystEngComm* **2009**, *11*, 1964.

(156) Søtofte, I.; Nielsen, K. *Acta Chem. Scand., A* **1981**, *35*, 739.

(157) Shao, K.-Z.; Zhao, Y.-H.; Xing, Y.; Lan, Y.-Q.; Wang, X.-L.; Su, Z.-M.; Wang, R.-S. *Cryst. Growth Des.* **2008**, *8*, 2986.

(158) (a) Hu, R.-F.; Zhang, J.; Kang, Y.; Yao, Y.-G. *Inorg. Chem. Commun.* **2005**, *8*, 828. (b) Lu, J.; Zhao, K.; Fang, Q.-R.; Xu, J.-Q.; Yu, J.-H.; Zhang, X.; Bie, H.-Y.; Wang, T.-G. *Cryst. Growth Des.* **2005**, *5*, 1091.

(159) Biswas, S.; Grzywa, M.; Nayek, H. P.; Dehnen, S.; Senkovska, I.; Kaskel, S.; Volkmer, D. *Dalton Trans.* **2009**, 6487.

(160) Denysenko, D.; Grzywa, M.; Tonigold, M.; Streppel, B.; Krkljus, I.; Hirscher, M.; Mugnaioli, E.; Kolb, U.; Hanss, J.; Volkmer, D. *Chem.—Eur. J.* **2011**, *17*, 1837.

(161) Kolb, H. C.; Finn, M. G.; Sharpless, K. B. *Angew. Chem., Int. Ed.* **2001**, *40*, 2004.

(162) Yue, Y.-F.; Wang, B.-W.; Gao, E.-Q.; Fang, C.-J.; He, C.; Yan, C.-H. *Chem. Commun.* **2007**, 2034.

(163) (a) Demessence, A.; D'Alessandro, D. M.; Foo, M. L.; Long, J. R. *J. Am. Chem. Soc.* **2009**, *131*, 8784. (b) Sumida, K.; Foo, M. L.; Horike, S.; Long, J. R. *Eur. J. Inorg. Chem.* **2010**, 3739. (c) Demessence, A.; Long, J. R. *Chem.—Eur. J.* **2010**, *16*, 5902.

(164) Mautner, F. A.; Gspan, C.; Gatterer, K.; Goher, M. A. S.; Abu-Youssef, M. A. M.; Bucher, E.; Sitte, W. *Polyhedron* **2004**, *23*, 1217.

(165) Demko, Z. P.; Sharpless, K. B. *J. Org. Chem.* **2001**, *66*, 7945.

(166) Zhao, H.; Qu, Z. R.; Ye, H. Y.; Xiong, R. G. *Chem. Soc. Rev.* **2008**, *37*, 84.

(167) Carlucci, L.; Ciani, G.; Proserpio, D. M. *Angew. Chem., Int. Ed.* **1999**, *38*, 3488.

(168) Wu, T.; Yi, B. H.; Li, D. *Inorg. Chem.* **2005**, *44*, 4130.

(169) Wu, T.; Zhou, R.; Li, D. *Inorg. Chem. Commun.* **2006**, *9*, 341.

(170) Zhang, X.-M.; Zhao, Y.-F.; Wu, H.-S.; Batten, S. R.; Weng, N. S. *Dalton Trans.* **2006**, 3170.

(171) Wu, T.; Chen, M.; Li, D. *Eur. J. Inorg. Chem.* **2006**, 2132.

(172) Wang, X. S.; Tang, Y. Z.; Huang, X. F.; Qu, Z. R.; Che, C. M.; Chan, P. W. H.; Xiong, R. G. *Inorg. Chem.* **2005**, *44*, 5278.

(173) Tong, X.-L.; Liu, H.; Yu, Q.; Li, J.-R. *Acta Crystallogr., Sect. E* **2008**, *64*, m132.

(174) Panda, T.; Pachfule, P.; Chen, Y.; Jiang, J.; Banerjee, R. *Chem. Commun.* **2011**, *47*, 2011.

(175) Wang, X. W.; Chen, J.-Z.; Liu, J.-H. *Cryst. Growth Des.* **2007**, *7*, 1227.

(176) (a) He, X.; Lu, C. Z.; Yuan, D. Q. *Inorg. Chem.* **2006**, *45*, 5760. (b) Liu, D. S.; Huang, G. S.; Huang, C. C.; Huang, X. H.; Chen, J. Z.; You, X. Z. *Cryst. Growth Des.* **2009**, *9*, 5117. (c) Zhong, D. C.; Lin, J. B.; Lu, W. G.; Jiang, L.; Lu, T. B. *Inorg. Chem.* **2009**, *48*, 8656. (d) Zhong, D. C.; Lu, W. G.; Jiang, L.; Feng, X. L.; Lu, T. B. *Cryst. Growth Des.* **2010**, *10*, 739.

(177) Lin, H. M.; Chang, T. Y. *Cryst. Growth Des.* **2009**, *9*, 2988.

(178) Qiu, Y.; Deng, H.; Mou, J.; Yang, S.; Zeller, M.; Batten, S. R.; Wu, H.; Li, J. *Chem. Commun.* **2009**, 5415.

(179) Tao, J.; Ma, Z. J.; Huang, R. B.; Zheng, L. S. *Inorg. Chem.* **2004**, *43*, 6133.

(180) Dinca, M.; Yu, A. F.; Long, J. R. *J. Am. Chem. Soc.* **2006**, *128*, 8904.

(181) (a) Xie, L.; Liu, S.; Gao, C.; Cao, R.; Cao, J.; Sun, C.; Su, Z. *Inorg. Chem.* **2007**, *46*, 7782. (b) Ma, S.; Wang, X.-S.; Yuan, D.; Zhou, H.-C. *Angew. Chem., Int. Ed.* **2008**, *47*, 4130. (c) Ouellette, W.; Liu, H. X.; Whitenack, K.; O'Connor, C. J.; Zubieta, J. *Cryst. Growth Des.* **2009**, *9*, 4258. (d) Ma, S.; Yuan, D.; Wang, X.-S.; Zhou, H.-C. *Inorg. Chem.* **2009**, *48*, 2072. (e) Ma, S.; Yuan, D.; Chang, J.-S.; Zhou, H.-C. *Inorg. Chem.* **2009**, *48*, 5398. (f) Das, S.; Kim, H.; Kim, K. *J. Am. Chem. Soc.* **2009**, *131*, 3814. (g) Zhang, X.-M.; Lv, J.; Ji, F.; Wu, H.-S.; Jiao, H.; Schleyer, P. v. R. *J. Am. Chem. Soc.* **2011**, *133*, 4788.

(182) Dinca, M.; Dailly, A.; Liu, Y.; Brown, C. M.; Neumann, D. A.; Long, J. R. *J. Am. Chem. Soc.* **2006**, *128*, 16876.

(183) Horike, S.; Dinca, M.; Tamaki, K.; Long, J. R. *J. Am. Chem. Soc.* **2008**, *130*, 5854.

(184) Dinca, M.; Long, J. R. *J. Am. Chem. Soc.* **2007**, *129*, 11172.

(185) (a) Dinca, M.; Han, W. S.; Liu, Y.; Dailly, A.; Brown, C. M.; Long, J. R. *Angew. Chem., Int. Ed.* **2007**, *46*, 1419. (b) Sumida, K.; Horike, S.; Kaye, S. S.; Herm, Z. R.; Queen, W. L.; Brown, C. M.; Grandjean, F.; Long, G. J.; Dailly, A.; Long, J. R. *Chem. Sci.* **2010**, *1*, 184.

(186) Dinca, M.; Dailly, A.; Tsay, C.; Long, J. R. *Inorg. Chem.* **2008**, *47*, 11.

(187) Dinca, M.; Dailly, A.; Long, J. R. *Chem.—Eur. J.* **2008**, *14*, 10280.

(188) Ouellette, W.; Prosvirin, A. V.; Whitenack, K.; Dunbar, K. R.; Zubieta, J. *Angew. Chem., Int. Ed.* **2009**, *48*, 2140.

(189) Li, J. R.; Tao, Y.; Yu, Q.; Bu, X. H.; Sakamoto, H.; Kitagawa, S. *Chem.—Eur. J.* **2008**, *14*, 2771.

(190) Tong, X. L.; Wang, D. Z.; Hu, T. L.; Song, W. C.; Tao, Y.; Bu, X. H. *Cryst. Growth Des.* **2009**, *9*, 2280.

(191) Maspero, A.; Galli, S.; Colombo, V.; Peli, G.; Masciocchi, N.; Stagni, S.; Barea, E.; Navarro, J. A. R. *Inorg. Chim. Acta* **2009**, *362*, 4340.